NASA CR-134823

7N-20
40149

"THRUST CHAMBER LIFE PREDICTION"

VOLUME III - FATIGUE LIFE PARAMETRIC STUDY

CONTRACT NAS3-17838

MAY 1975

PREPARED BY

BOEING AEROSPACE COMPANY
(A DIVISION OF THE BOEING COMPANY)
RESEARCH AND ENGINEERING
SEATTLE, WASHINGTON

PREPARED FOR

NATIONAL AERONAUTICS AND SPACE ADMINISTRATION
LEWIS RESEARCH CENTER
CLEVELAND, OHIO

MICROFILMED 10-9-75

D180-18673-3

1. Report No.	2. Government Accession No.	3. Recipient's Catalog No.
NASA CR-134823		

4. Title and Subtitle	5. Report Date
"Thrust Chamber Life Prediction" Volume III - Fatigue Life Parametric Study	MAY 1975
	6. Performing Organization Code D180-18673-3
7. Author(s) William H. Armstrong and Elliott W. Brogren	8. Performing Organization Report No
9. Performing Organization Name and Address Boeing Aerospace Company (A Division of The Boeing Company) P. O. Box 3999 Seattle, Washington 98124	10. Work Unit No.
	11. Contract or Grant No. NAS3-17838
12. Sponsoring Agency Name and Address National Aeronautics and Space Administration Lewis Research Center	13. Type of Report and Period Covered Task III - Final Report
	14. Sponsoring Agency Code

15. Supplementary Notes

R. J. Quentmeyer, NASA Technical Monitor

16. Abstract

A parametric study was conducted to analytically determine the cyclic thermomechanical behavior of various configurations of the outer cylinder of a plug type thrust chamber model developed by the NASA/LeRC. This thrust chamber represents the current trend in nozzle design calling for high performance coupled with weight and volume limitations as well as extended life for reusability.

The objective was to identify material properties which significantly affect the inelastic behavior of the cylinder under a specified thrust chamber operating cycle consisting of a hot phase (engine burn), a cold phase (engine shutdown with cylinder coolant flowing) and transients connecting the two phases. The study involved heat flow and structural analyses of variations of a basic configuration of the cylinder. The basic cylinder was modeled from typical physical and mechanical properties of a copper alloy called Amzirc. Material properties such as thermal conductivity and yield strength were varied, one at a time, to evaluate the effects on thermomechanical response of the cylinder to the thrust chamber operating cycle.

Results are presented which show plots of continuous temperature histories and diagrams of continuous isotherms at selected times during the thrust chamber operating cycle. Computed structural data show critical regions for low-cycle fatigue, cyclic histories of strain, isograms of effective strain at critical times during the cycle, and variations in maximum effective strain with each material parameter.

17. Key Words (Suggested by Author(s))	18. Distribution Statement
Thrust Chamber, Low-Cycle Fatigue, Amzirc, Copper Alloy, Heat Transfer, Thermal Analysis, Inelastic, Viscoplastic, Finite-Element Analysis	Unclassified - Unlimited

19. Security Classif. (of this report)	20. Security Classif. (of this page)	21. No. of Pages	22. Price*
Unclassified	Unclassified		

* For sale by the National Technical Information Service, Springfield, Virginia 22151

NASA-C-168 (Rev. 6-71)

FOREWORD

This report was prepared by the Boeing Aerospace Company, Seattle, Washington, for the Lewis Research Center (LeRC) of the National Aeronautics and Space Administration (NASA). An analytical study was conducted to predict thermomechanical response of the outer cylinder of a plug type thrust chamber to a specified operating cycle and variations in basic material properties such as thermal conductivity and yield strength. Heat flow and structural analyses were conducted in accordance with Task III requirements of Contract NAS3-17838 "Thrust Chamber Life Prediction". The study was under the cognizance of R. J. Quentmeyer of NASA/LeRC.

The analyses and documentation of results were conducted by E. W. Brogren and W. H. Armstrong. The program manager was J. W. Straayer.

TABLE OF CONTENTS

SECTION		PAGE
	FOREWORD	ii
	CONTENTS	iii
	LIST OF FIGURES	iv
	LIST OF TABLES	ix
1.0	SUMMARY	1-1
2.0	INTRODUCTION	2-1
3.0	PLUG NOZZLE THRUST CHAMBER	3-1
3.1	BASELINE MATERIAL PROPERTIES	
3.2	OPERATING CONDITIONS	
4.0	PLUG NOZZLE THRUST CHAMBER MODELS	4-1
4.1	THERMAL ANALYSIS MODEL	
4.2	STRUCTURAL ANALYSIS MODEL	
5.0	HEAT TRANSFER ANALYSIS	5-1
5.1	THERMAL ANALYSIS RESULTS	
6.0	STRUCTURAL ANALYSIS	6-1
6.1	STRUCTURAL ANALYSIS RESULTS	
6.1.1	Strain and Temperature Histories	
6.1.2	Variation in Strain with Change in Parameters	
7.0	CONCLUDING REMARKS	7-1
8.0	REFERENCES	8-1

LIST OF FIGURES

FIGURE		PAGE
3.0-1	CROSS SECTION OF PLUG NOZZLE THRUST CHAMBER THROAT	3-3
3.1-1	EFFECT OF TEMPERATURE ON THERMAL CONDUCTIVITY OF AMZIRC	3-5
3.1-2	EFFECT OF TEMPERATURE ON SPECIFIC HEAT OF AMZIRC	3-5
3.1-3	EFFECT OF TEMPERATURE ON DENSITY OF AMZIRC	3-6
3.1-4	ESTIMATED CREEP BEHAVIOR OF 1/2 HARD AMZIRC	3-6
3.1-5	THERMAL EXPANSION OF AMZIRC	3-7
3.1-6	EFFECT OF TEMPERATURE ON PROPORTIONAL LIMIT OF AMZIRC	3-7
3.1-7	EFFECT OF TEMPERATURE ON ELASTIC MODULUS OF AMZIRC	3-8
3.1-8	TYPICAL STRESS-STRAIN CURVES FOR 1/2 HARD AMZIRC	3-8
3.2-1	BOUNDARY CONDITIONS FOR THERMAL ANALYSES	3-9
4.1-1	PLUG NOZZLE CYLINDER THERMAL MODEL	4-3
4.2-1	PLUG NOZZLE OUTER CYLINDER FINITE ELEMENT MODEL SHOWING ELEMENT IDENTIFICATION NUMBER	4-4
5.1-1	REPRESENTATIVE TEMPERATURES FOR TYPICAL HEATING-COOLING CYCLE FOR CONFIGURATION P.0	5-3
5.1-2	REPRESENTATIVE TEMPERATURES FOR TYPICAL HEATING-COOLING CYCLE FOR CONFIGURATION P.1	5-4
5.1-3	REPRESENTATIVE TEMPERATURES FOR TYPICAL HEATING-COOLING CYCLE FOR CONFIGURATION P.2	5-5

LIST OF FIGURES (Continued)

FIGURE		PAGE
5.1-4	OUTER CYLINDER ISOTHERMS TASK III BASELINE (CASE P.0) TIME = 0.50 SECOND	5-6
5.1-5	OUTER CYLINDER ISOTHERMS TASK III HIGH CONDUCTIVITY (CASE P.1) TIME = 0.50 SECOND	5-7
5.1-6	OUTER CYLINDER ISOTHERMS TASK III LOW CONDUCTIVITY (CASE P.2) TIME = 0.50 SECOND	5-8
6.1-1	STRAIN VS. TIME, ELEMENT #131, CONFIGURATION P.0	6-11
6.1-2	EFFECTIVE STRAIN VS. TIME, ELEMENT #131, CONFIGURATION P.0	6-12
6.1-3	TEMPERATURE VS. TIME, ELEMENT #131, CONFIGURATION P.0	6-13
6.1-4	TYPICAL LOW CYCLE FATIGUE LIFE OF AMZIRC	6-14
6.1-5	REGION OF MAXIMUM EFFECTIVE STRAIN RANGE IN CONFIGURATION P.0	6-15
6.1-6	VARIATION IN EFFECTIVE STRAIN RANGE IN REGION OF MAXIMUM STRAIN IN CONFIGURATION P.0	6-16
6.1-7	EFFECTIVE CREEP STRAIN, ELEMENT #131, CONFIGURATION P.0	6-17
6.1-8	STRAIN VS. TIME, ELEMENT #131, CONFIGURATION P.1	6-18
6.1-9	EFFECTIVE STRAIN VS. TIME, ELEMENT #131, CONFIGURATION P.1	6-19
6.1-10	TEMPERATURE VS. TIME, ELEMENT #131, CONFIGURATION P.1	6-20
6.1-11	STRAIN VS. TIME, ELEMENT #10, CONFIGURATION P.2	6-21

LIST OF FIGURES (Continued)

FIGURE		PAGE
6.1-12	EFFECTIVE STRAIN VS. TIME, ELEMENT #10, CONFIGURATION P.2	6-22
6.1-13	TEMPERATURE VS. TIME, ELEMENT #10, CONFIGURATION P.2	6-23
6.1-14	STRAIN VS. TIME, ELEMENT #131, CONFIGURATION P.2	6-24
6.1-15	EFFECTIVE STRAIN VS. TIME, ELEMENT #131, CONFIGURATION P.2	6-25
6.1-16	TEMPERATURE VS. TIME, ELEMENT #131, CONFIGURATION P.2	6-26
6.1-17	STRAIN VS. TIME, ELEMENT #133, CONFIGURATION P.3	6-27
6.1-18	EFFECTIVE STRAIN VS. TIME, ELEMENT #131, CONFIGURATION P.3	6-28
6.1-19	TEMPERATURE VS. TIME, ELEMENT #133, CONFIGURATION P.3	6-29
6.1-20	STRAIN VS. TIME, ELEMENT #131, CONFIGURATION P.3	6-30
6.1-21	EFFECTIVE STRAIN VS. TIME, ELEMENT #131, CONFIGURATION P.3	6-31
6.1-22	STRAIN VS. TIME, ELEMENT #10, CONFIGURATION P.4	6-32
6.1-23	EFFECTIVE STRAIN VS. TIME, ELEMENT #10, CONFIGURATION P.4	6-33
6.1-24	TEMPERATURE VS. TIME, ELEMENT #10, CONFIGURATION P.4	6-34
6.1-25	STRAIN VS. TIME, ELEMENT #131, CONFIGURATION P.4	6-35
6.1-26	EFFECTIVE STRAIN VS. TIME, ELEMENT #131, CONFIGURATION P.4	6-36
6.1-27	STRAIN VS. TIME, ELEMENT #131, CONFIGURATION P.5	6-37

LIST OF FIGURES (Continued)

FIGURE		PAGE
6.1-28	EFFECTIVE STRAIN VS. TIME, ELEMENT #131, CONFIGURATION P.5	6-38
6.1-29	STRAIN VS. TIME, ELEMENT #131, CONFIGURATION P.6	6-39
6.1-30	EFFECTIVE STRAIN VS. TIME, ELEMENT #131, CONFIGURATION P.6	6-40
6.1-31	STRAIN VS. TIME, ELEMENT #131, CONFIGURATION P.7	6-41
6.1-32	EFFECTIVE STRAIN VS. TIME, ELEMENT #131, CONFIGURATION P.7	6-42
6.1-33	STRAIN VS. TIME, ELEMENT #131, CONFIGURATION P.8	6-43
6.1-34	EFFECTIVE STRAIN VS. TIME, ELEMENT #131, CONFIGURATION P.8	6-44
6.1-35	STRAIN VS. TIME, ELEMENT #131, CONFIGURATION P.9	6-45
6.1-36	EFFECTIVE STRAIN VS. TIME, ELEMENT #131, CONFIGURATION P.9	6-46
6.1-37	STRAIN VS. TIME, ELEMENT #131, CONFIGURATION P.10	6-47
6.1-38	EFFECTIVE STRAIN VS. TIME, ELEMENT #131, CONFIGURATION P.10	6-48
6.1-39	VARIATION OF MAXIMUM EFFECTIVE STRAIN WITH THERMAL CONDUCTIVITY	6-50
6.1-40	VARIATION OF MAXIMUM EFFECTIVE STRAIN WITH COEFFICIENT OF THERMAL EXPANSION	6-51

LIST OF FIGURES (Continued)

FIGURE		PAGE
6.1-41	VARIATION OF MAXIMUM EFFECTIVE STRAIN WITH MODULUS OF ELASTICITY	6-51
6.1-42	VARIATION OF MAXIMUM EFFECTIVE STRAIN WITH POISSON'S RATIO	6-52
6.1-43	VARIATION OF MAXIMUM EFFECTIVE STRAIN WITH YIELD STRENGTH	6-52
6.1-44	ISOGRAMS OF EFFECTIVE STRAIN AT TIME = 1.85 SECONDS, PARAMETRIC STUDY OF **THERMAL PROPERTIES**	6-53
6.1-45	ISOGRAMS OF EFFECTIVE STRAIN AT TIME = 3.50 SECONDS, PARAMETRIC STUDY OF **THERMAL PROPERTIES**	6-54
6.1-46	ISOGRAMS OF EFFECTIVE STRAIN AT TIME = 1.85 SECONDS, PARAMETRIC STUDY OF MECHANICAL PROPERTIES	6-55
6.1-47	ISOGRAMS OF EFFECTIVE STRAIN AT TIME = 3.50 SECONDS, PARAMETRIC STUDY OF MECHANICAL PROPERTIES	6-56

LIST OF TABLES

TABLE		PAGE
3.0-I	PLUG NOZZLE CYLINDER CONFIGURATIONS	3-4
6.0-I	SUMMARY OF MAXIMUM EFFECTIVE STRAINS IN FINITE-ELEMENT MODEL OF OUTER CYLINDER	6-10
6.1-I	SUMMARY OF PARAMETRIC EFFECTS ON MAXIMUM EFFECTIVE STRAIN RANGE	6-49

1.0 SUMMARY

A parametric study was conducted to analytically determine the cyclic thermomechanical behavior of various configurations of the outer cylinder of a plug type thrust chamber developed by the NASA/LeRC. The cylinder conforms to a test model which was developed to evaluate candidate materials as thrust chamber liners in an engine designed for high performance and extended low-cycle fatigue life for reusability.

The objective was to identify material properties which significantly affect the inelastic behavior of the cylinder under a specified thrust chamber operating cycle consisting of a hot phase (engine burn), a cold phase (engine shutdown with cylinder coolant flowing) and transients connecting the two phases. The study involved heat flow and structural analyses of variations of a basic configuration of the cylinder. The basic cylinder was modeled from typical physical and mechanical properties of a copper alloy called Amzirc. Material properties such as thermal conductivity and yield strength were varied, one at a time, to evaluate the effects on thermomechanical response of the cylinder to the thrust chamber operating cycle.

The cyclic heat flow analysis was performed with the Boeing Engineering Thermal Analyzer (BETA) program. BETA is a large capacity finite difference digital computer program for computing transient or steady state heat flow in two or three dimensions.

Structural response to the applied pressure/temperature cycle was determined with the Boeing Plastic Analysis Capability for Engines (BOPACE) program. BOPACE is a finite-element digital computer program which provides two or three dimensional incremental analysis of problems in viscoplasticity.

Results are presented which show plots of continuous temperature histories and diagrams of continuous isotherms at selected times during the thrust chamber operating cycle. Computed structural data show critical regions for low-cycle fatigue, cyclic histories of strain, isograms

1.0 (Continued)

of effective strain at critical times during the cycle, and variations in maximum effective strain with each material parameter. Results show that inelastic strains in Amzirc are reduced most effectively by decreasing thermal expansion and increasing thermal conductivity. A twenty (20) percent reduction in thermal expansion resulted in a fifty-one (51) percent reduction in maximum computed effective strain range. A twenty-two (22) percent increase in the average value of thermal conductivity for the engine burn period resulted in a five (5) percent reduction in the peak temperature and a twenty-six (26) percent reduction in maximum effective strain range.

2.0 INTRODUCTION

The advent of the Space Shuttle has brought a new era in the design and fabrication of rocket nozzles. The requirement of high-performance coupled with weight and volume limitations has resulted in the design of rocket nozzles that operate at chamber pressures in excess of 2000 N/cm^2 (3000 psia). This has elevated the throat heat flux from 3300 W/cm^2 (20 Btu/in^2-sec) for present day high performance rocket nozzles to 16,000 W/cm^2 (100 Btu/in^2-sec) for the Space Shuttle Main Engine. A further requirement for future high performance rocket nozzles is reusability. For example, the nozzle may have the requirement that it be capable of operating for several hundred major thermal cycles.

The combination of high performance and reusability has created major design problems. One of the critical aspects of the nozzle design is low-cycle fatigue life. This has become a major design problem since a portion of the nozzle, particularly the throat section, is subjected to cyclic inelastic strain due to the large temperature gradient between the hot inner wall and the relatively cool outer shell during the engine start-stop transients as well as during the sustained burn period. This has a major impact on nozzle life and creates the need to accurately predict when an engine may fail.

An essential part in development of a reusable rocket nozzle is material selection. Recognizing the need, NASA has initiated programs to identify most suitable materials for engine components and to study material properties which most significantly affect low-cycle fatigue damage. In particular, LeRC is conducting programs to test available copper-base alloys as thrust chamber liners and to perform analytical studies of copper to assess variations in thrust chamber thermomechanical behavior with changes in material variables such as thermal conductivity and yield strength. The results of the tests and analyses may lead to development of new materials with greater resistance to low-cycle fatigue damage.

THIS PAGE LEFT INTENTIONALLY BLANK.

3.0 PLUG NOZZLE THRUST CHAMBER

The structure analyzed during this study is the outer cylinder of a plug type thrust chamber. The region analyzed was near the thrust chamber throat plane and is shown in cross section in Figure 3.0-1. Details of structural arrangement and dimensions of the thrust chamber centerbody as well as the outer cylinder are presented in this figure.

Eleven (11) different configurations of the outer cylinder were analyzed in the parametric study. Dimensions of all configurations were the same; differences consisted only of material properties assigned to the thermal and structural models used in the analyses. For the purpose of identification the configurations were defined by identification numbers P.0 through P.10. P.0 was the baseline, modeled from typical material properties of half-hard Amzirc. The differences in the cylinder configurations are shown in Table 3.0-I.

A review of material conductivity data was carried out in order to establish significant yet realistic extremes of thermal conductivity to use for P.1 and P.2 analyses. The highest conductivity found among all solid materials was that for annealed pure silver. Since the intent was to employ arbitrarily varied properties, which were not necessarily representative of any real material, it was decided to treat the high and low extreme conductivity values as constants, independent of temperature.

The high conductivity case, identified as configuration P.1, used a conductivity of 4.80 watt/cm-K (6.422×10^{-3} Btu/in-sec-°R), which is approximately the value for chemically pure, annealed silver in the temperature range from 367K (200°F) to 1089K (1500°F).

For the low conductivity case, configuration P.2, a value of 1.86 watt/cm-K (2.5×10^{-3} Btu/in-sec-°R) was chosen. This value is approximately one half the room temperature conductivity of Amzirc. This value, which is roughly representative of the conductivities of beryllium copper or certain brasses, was felt to differ sufficiently from the

3.0 (Continued)

baseline value to produce a significant impact on strain results but not fall outside the range of real materials.

3.1 BASELINE MATERIAL PROPERTIES

Baseline material properties used in thermal and structural analyses of the cylinder were developed from data in Reference 1. These properties define the temperature dependent character of thermal conductivity, specific heat, density, thermal expansion, modulus of elasticity, Poisson's ratio, typical stress-strain behavior and creep. The baseline properties are shown in Figures 3.1-1 through 3.1-8.

3.2 OPERATING CONDITIONS

The operating conditions for the thermal and stress-strain analyses were specified by the NASA LeRC Project Manager. The thermal operating conditions were defined in terms of thermal boundary conditions (heat transfer coefficients, nozzle surface adiabatic wall temperatures, and coolant bulk temperatures). Mechanical operating conditions consisted of definitions of pressures on the nozzle surfaces and coolant channel walls. All conditions were specified through a typical operating cycle, consisting of a hot phase (engine burn), a cold phase (engine shut down but coolant flowing), and transients connecting the two phases. All conditions were constant during the two main phases and the transients were all assumed to be linear variations between the appropriate main phase values over specified periods of time. The levels and durations of the operating conditions are shown in Figure 3.2-1.

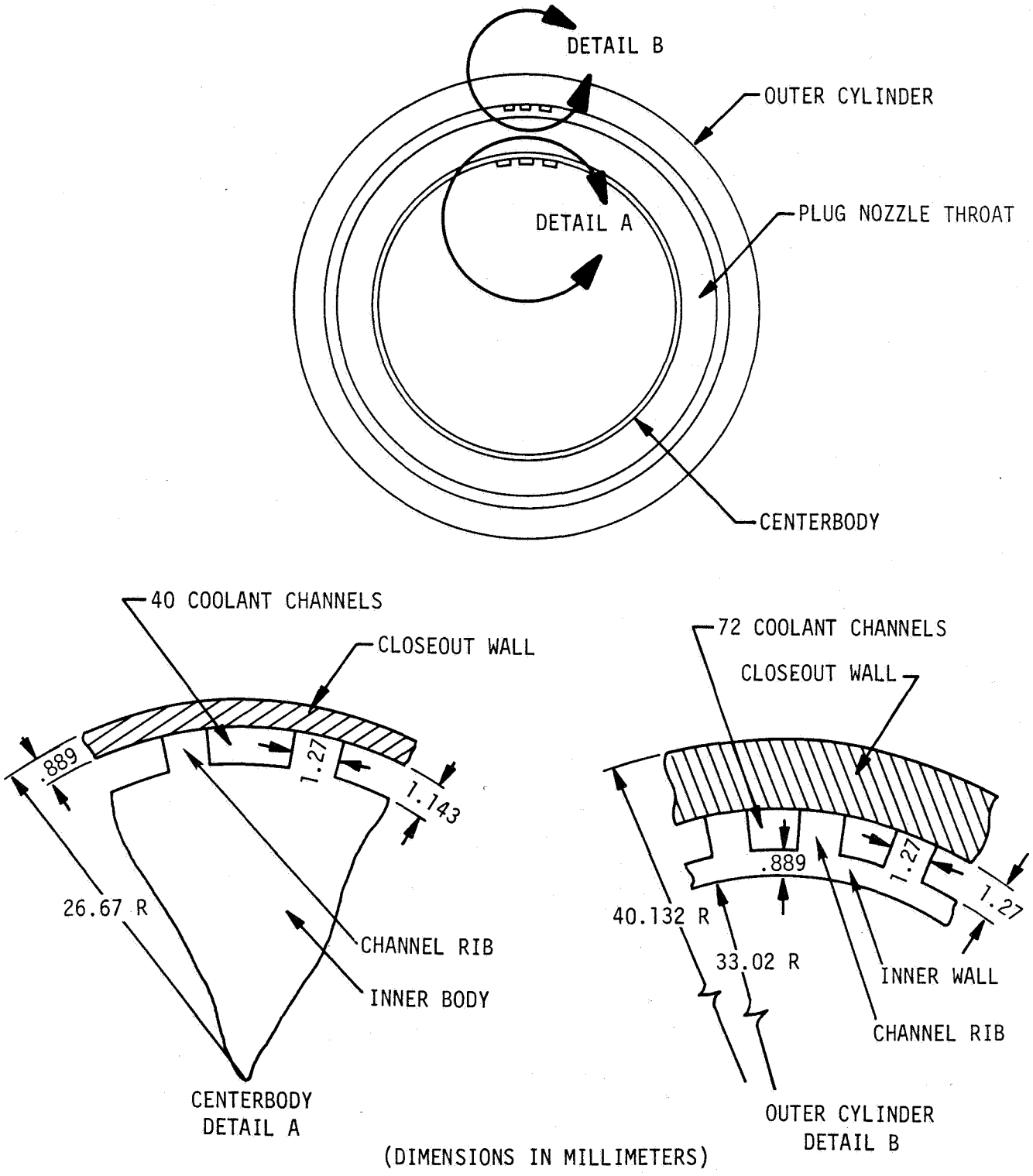

FIGURE 3.0-1 CROSS SECTION OF PLUG NOZZLE THRUST CHAMBER THROAT

TABLE 3.0-I PLUG NOZZLE CYLINDER CONFIGURATIONS

CONFIGURATION	MATERIAL PARAMETER
P.0	BASELINE MATERIAL PROPERTIES
P.1	THERMAL CONDUCTIVITY INCREASED APPROXIMATELY 22% TO A VALUE OF 4.80 watt/cm °K.
P.2	THERMAL CONDUCTIVITY DECREASED APPROXIMATELY 52% TO A VALUE OF 1.87 watt/cm °K.
P.3	THERMAL EXPANSION INCREASED 20%.
P.4	THERMAL EXPANSION DECREASED 20%.
P.5	ELASTIC MODULUS INCREASED 20%.
P.6	ELASTIC MODULUS DECREASED 20%.
P.7	POISSON'S RATIO INCREASED FROM 0.34 TO 0.40.
P.8	POISSON'S RATIO DECREASED FROM 0.34 TO 0.25.
P.9	YIELD STRENGTH INCREASED 25%.
P.10	YIELD STRENGTH DECREASED 25%.

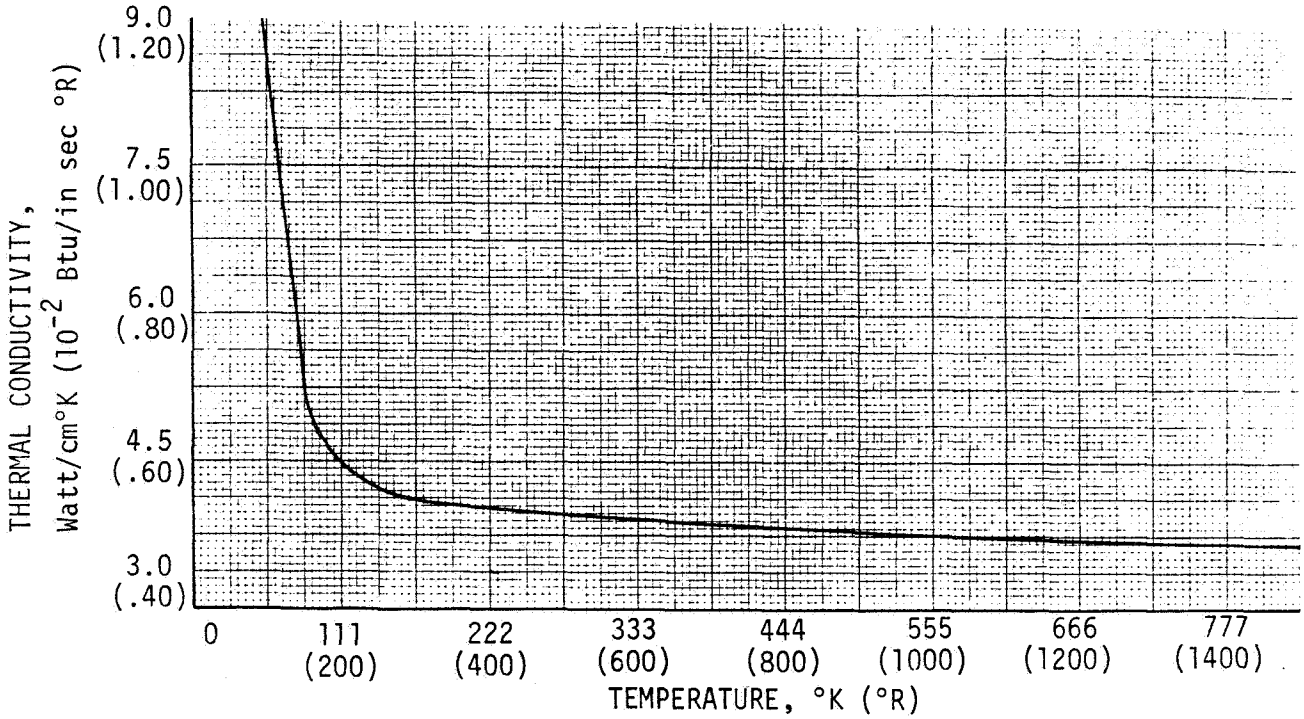

FIGURE 3.1-1 EFFECT OF TEMPERATURE ON THERMAL CONDUCTIVITY OF AMZIRC

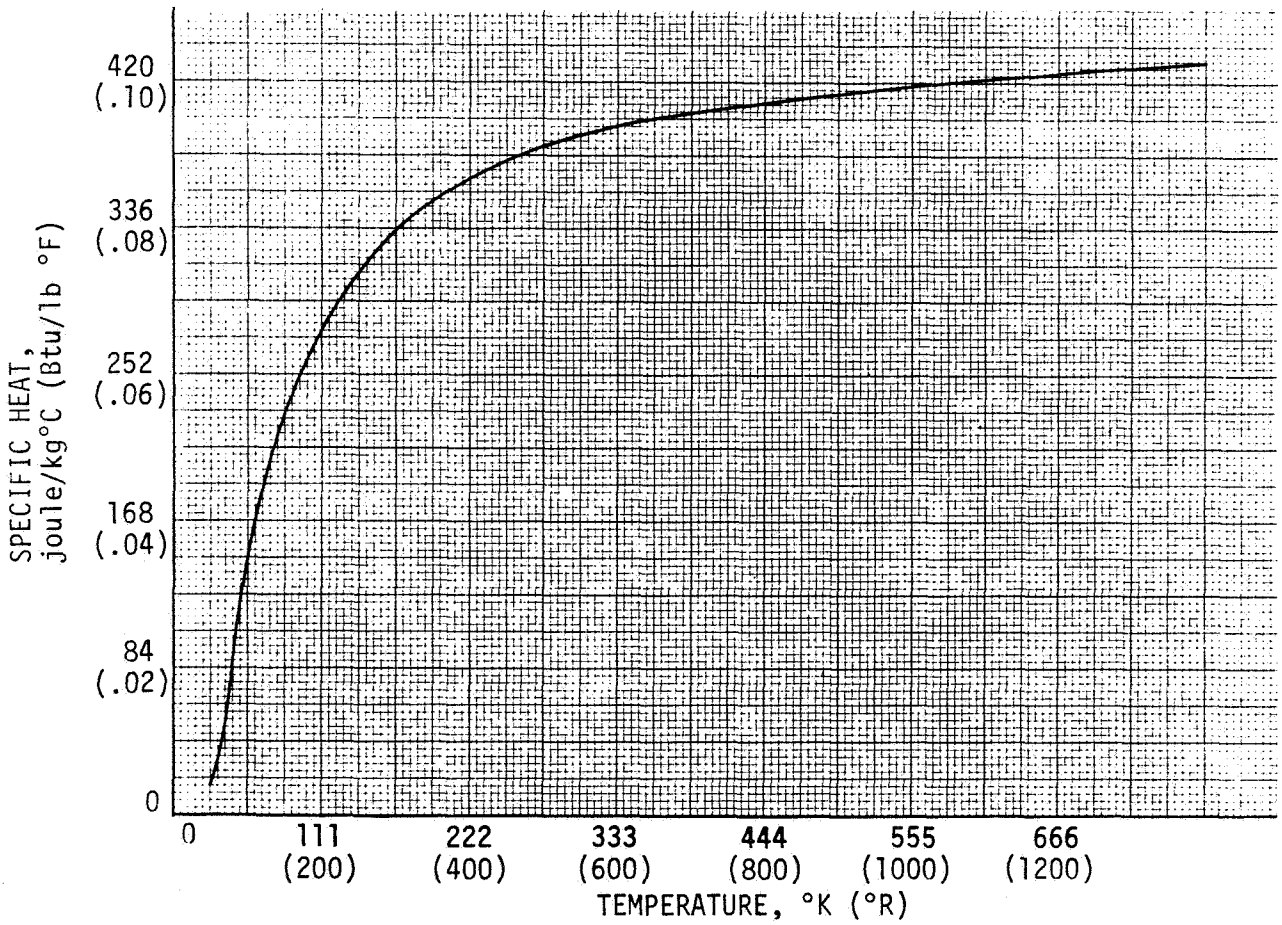

FIGURE 3.1-2 EFFECT OF TEMPERATURE ON SPECIFIC HEAT OF AMZIRC

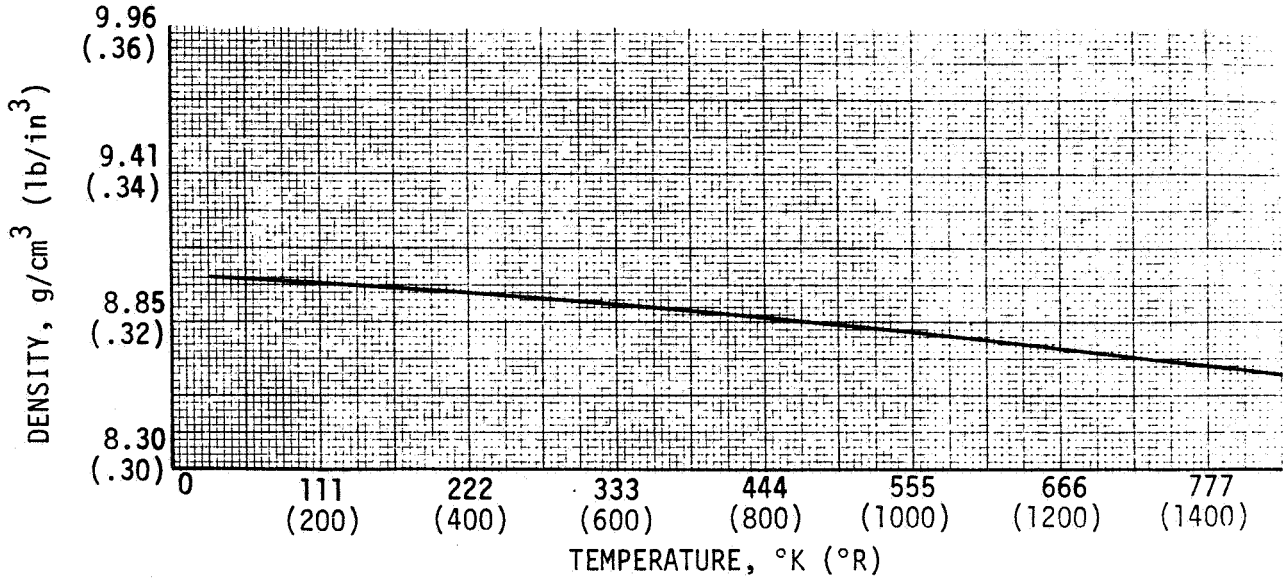

FIGURE 3.1-3 EFFECT OF TEMPERATURE ON DENSITY OF AMZIRC

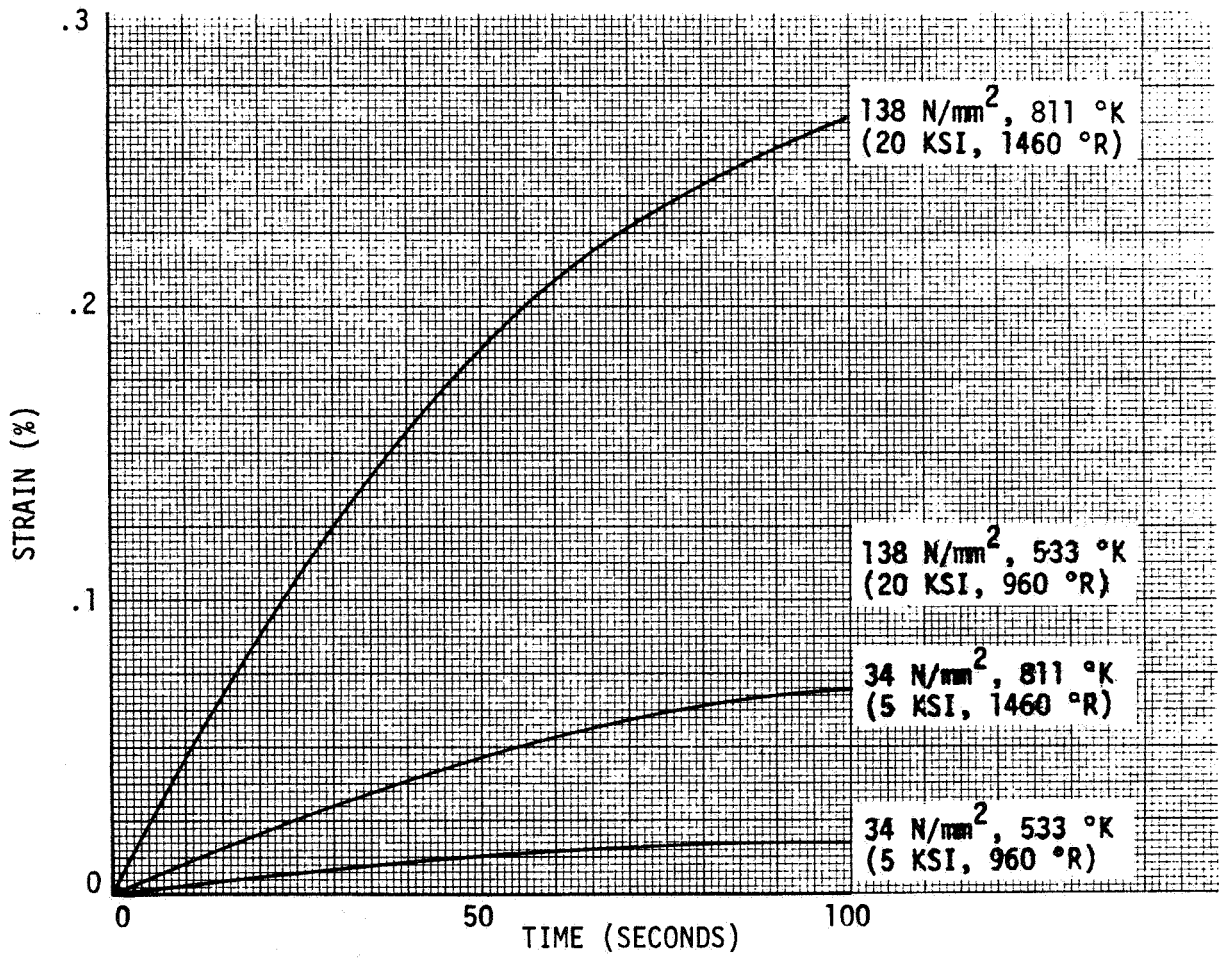

FIGURE 3.1-4 ESTIMATED CREEP BEHAVIOR OF 1/2 HARD AMZIRC

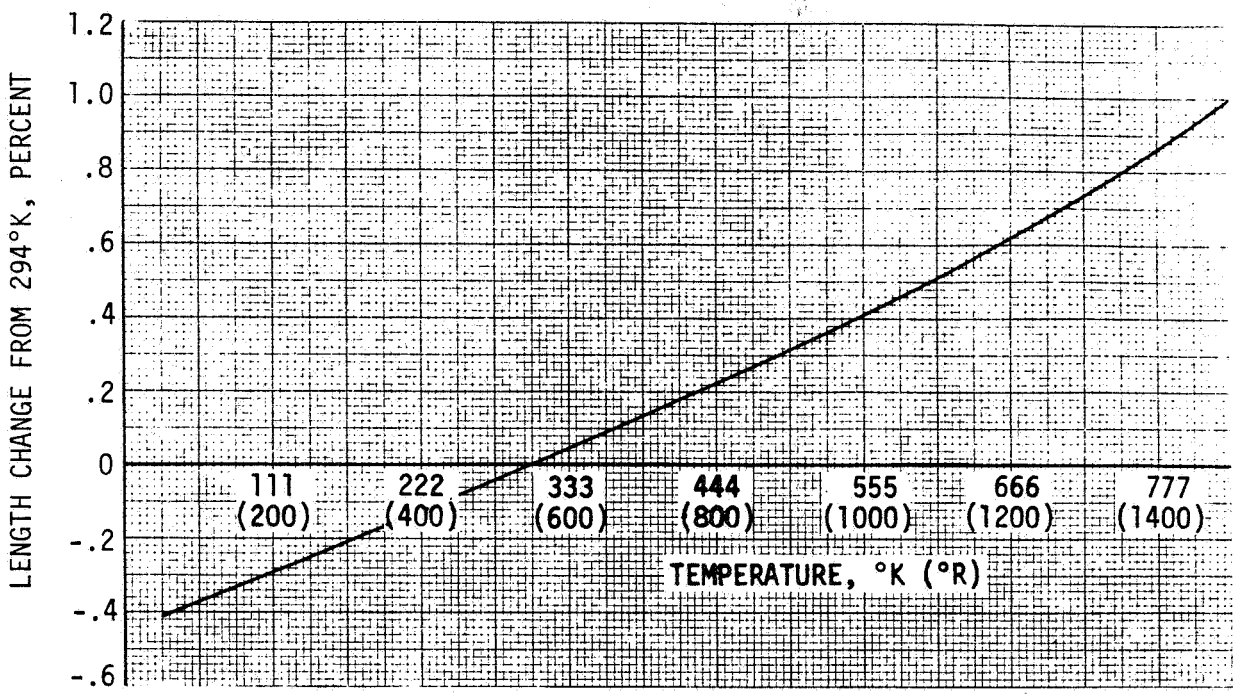

FIGURE 3.1-5 THERMAL EXPANSION OF AMZIRC

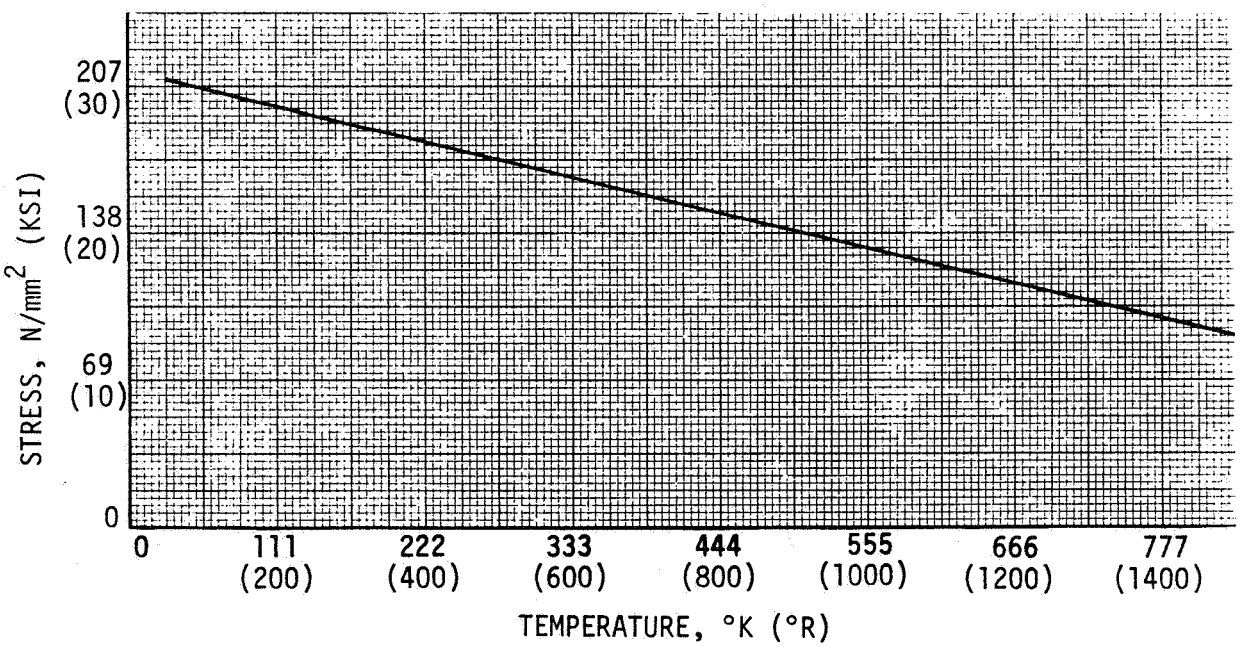

FIGURE 3.1-6 EFFECT OF TEMPERATURE ON PROPORTIONAL LIMIT OF AMZIRC

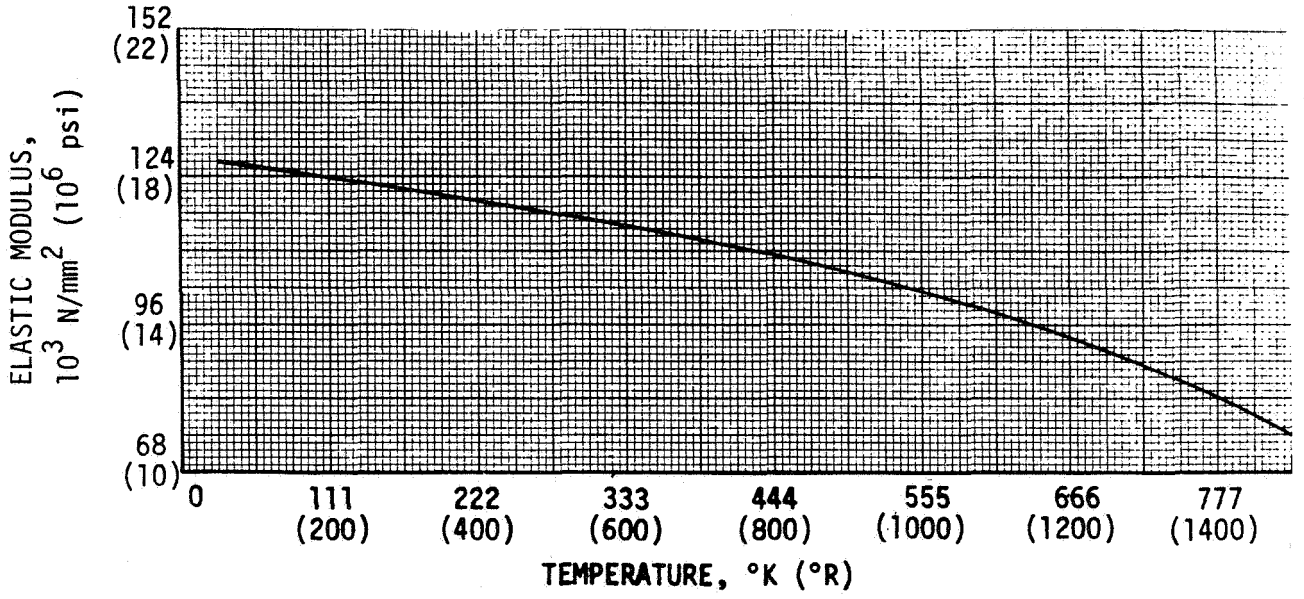

FIGURE 3.1-7 EFFECT OF TEMPERATURE ON ELASTIC MODULUS OF AMZIRC

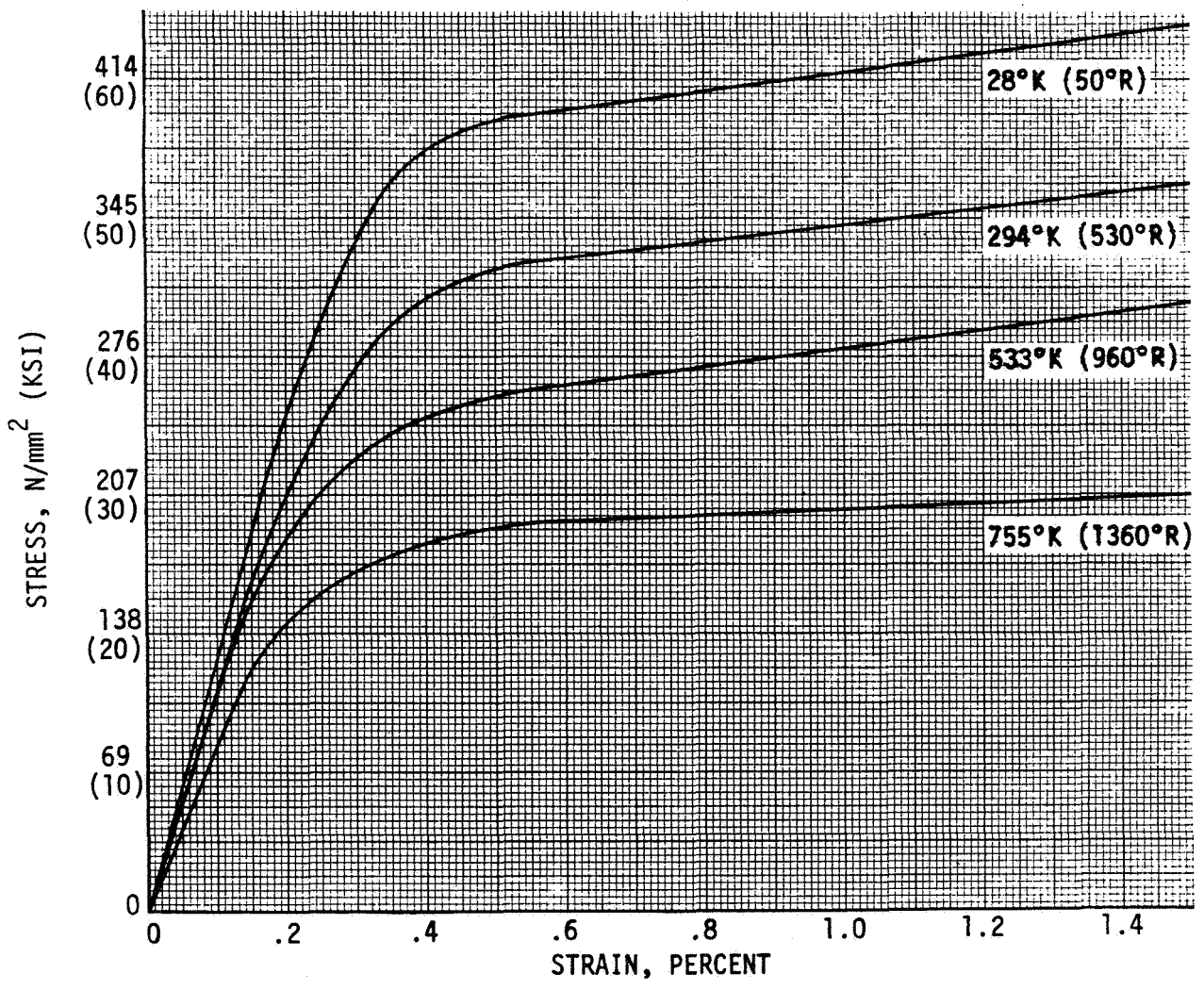

FIGURE 3.1-8 TYPICAL STRESS-STRAIN CURVES FOR 1/2 HARD AMZIRC

CONFIGURATION	P SERIES	
CYCLE PHASE	COLD	HOT
HOT GAS SIDE HEAT TRANSFER COEFFICIENT watt/cm^2-K (Btu/in.^{2}-sec-°R)	0.0	2.02 (.00685)
HOT GAS SIDE ADIABATIC WALL TEMPERATURE K (°R)	278 (500)	3364 (6055)
HOT GAS SIDE WALL PRESSURE kN/m^2 (psia)	96.5 (14.0)	2780 (403)
COOLANT SIDE HEAT TRANSFER COEFFICIENT watt/cm^2-K (Btu/in.^{2}-sec-°R)	10.2 (.0345)	4.83 (.0164)
COOLANT SIDE BULK TEMPERATURE K (°R)	28 (50)	50 (90)
COOLANT SIDE WALL PRESSURE kN/m^2 (psia)	5100 (740)	6550 (950)

TYPICAL CYCLE HISTORY

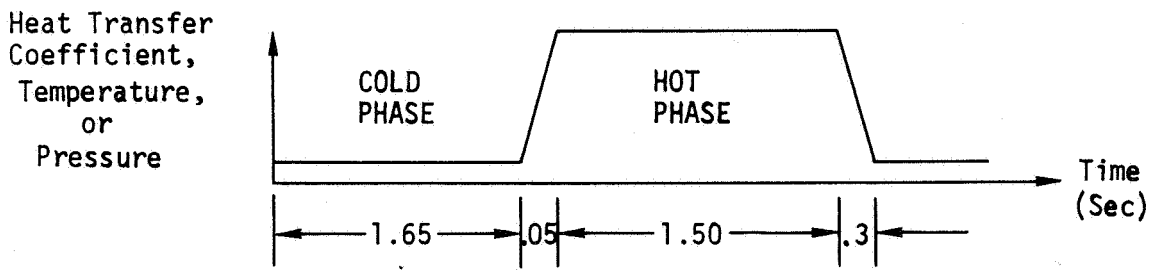

Figure 3.2-1 BOUNDARY CONDITIONS FOR THERMAL ANALYSES

THIS PAGE LEFT INTENTIONALLY BLANK.

4.0 PLUG NOZZLE THRUST CHAMBER MODELS

The models used in analyzing the heat flow and structural behavior of the outer cylinder are presented. Two sets of models were developed; one set was used to perform heat transfer analyses with the BETA program, and the second set was developed to perform the viscoplastic structural analyses with the BOPACE program. Boundaries of the thermal and structural models were identical, but the number of nodes and their locations were different. The mesh size and geometry of each model was determined by accuracy and practical modeling requirements of the two types of analysis.

4.1 THERMAL ANALYSIS MODEL

The BETA program is a large capacity digital program for computing transient or steady state heat flow in two or three dimensions. The program performs numerical solutions of the thermal diffusion equations, accounting for solid conduction, thermal capacitance, radiation interchange, convection, and internally produced or absorbed heat, as required. Variation of material properties with temperature or any other variable may be accounted for and a wide variety of boundary conditions may be accommodated.

The analytical model of the nozzle cylinder is shown in Figure 4.1-1. The properties of symmetry were exploited in order to treat the smallest representative segment of the cylinder, thus maximizing the practical modeling detail and resulting analysis accuracy. The line segment intersections, some of which are numbered on the figure, represent nodes at which mass and material specific heat values were concentrated, thus defining thermal capacitor quantities. The line segments connecting the nodes represent thermal conductors, incorporating material thermal conductivity, conducting length, and conductor cross section area. Output of the analysis consists of temperatures at each of the nodes at any desired times during the cycle.

4.1 (Continued)

Appendix A gives the locations of nodes shown on Figure 4.1-1.

4.2 STRUCTURAL ANALYSIS MODEL

The BOPACE finite-element model used in the structural analyses of the outer cylinder configuration is shown in Figure 4.2-1. The figure shows the finite element identification numbers which correspond to the element data listed in Appendix B. The tabulated element data are comprised of global node numbers which define each finite element in terms of its local node numbers. The nodal coordinate data are also listed in Appendix B.

The BOPACE program provides either the plane-strain or plane-stress constant strain triangles for structural analysis of problems in viscoplasticity. It was assumed that the more appropriate model of the plug nozzle thrust chamber problem would be the plane-strain element.

Because of symmetry of geometry and loading conditions at the nozzle throat plane, it was possible to perform the structural analysis with a model bounded by the inner and outer surfaces and by radial planes through the center of the channel rib and coolant channel; the boundaries of the BOPACE model coincide with the boundaries of the BETA model.

The finite element model of the outer cylinder consisted of 174 nodes with 281 elements. A fine mesh was used to model the area between the heated surface and coolant channel because highly inelastic behavior was anticipated for this region. A relatively coarse mesh was used in the regions which experience little or no inelastic deformation during the operating cycle.

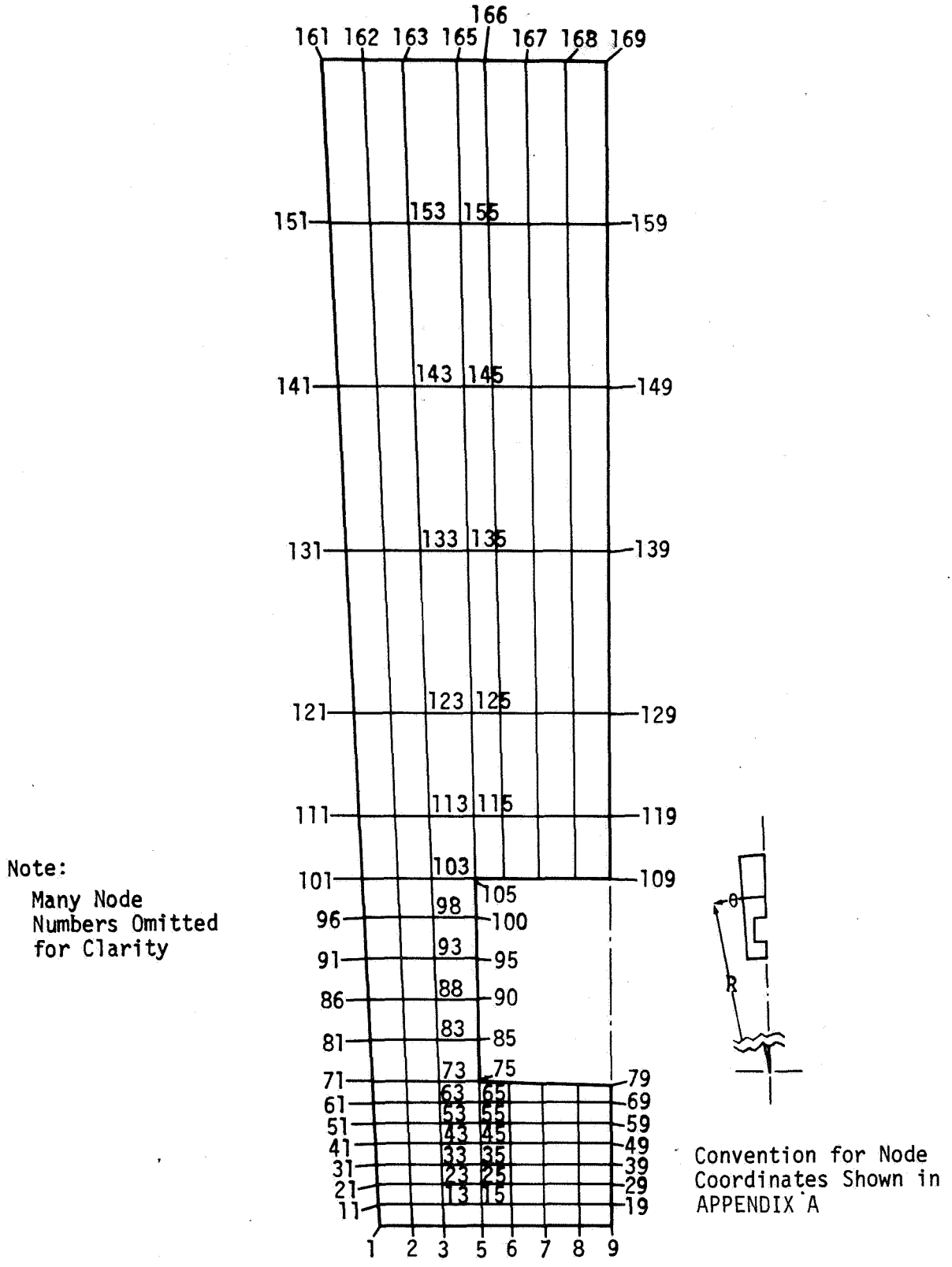

FIGURE 4.1-1 PLUG NOZZLE CYLINDER THERMAL MODEL

FIGURE 4.2-1

PLUG NOZZLE OUTER CYLINDER FINITE ELEMENT
MODEL SHOWING ELEMENT IDENTIFICATION NUMBER

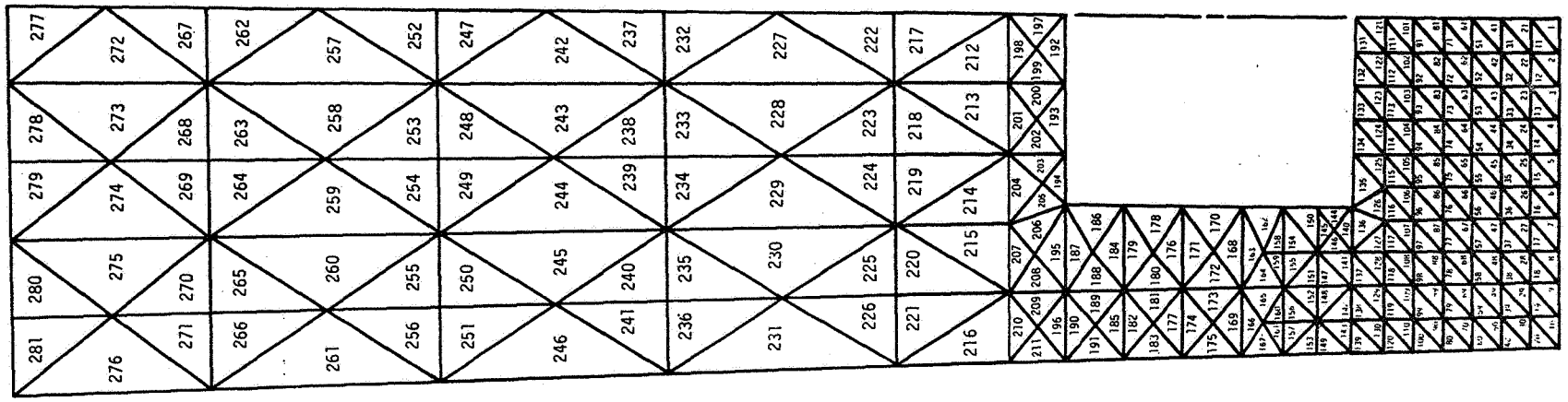

TOTAL NUMBER OF ELEMENTS = 281

TOTAL NUMBER OF NODES = 174

TOTAL NUMBER OF FREEDOMS = 348

5.0 HEAT TRANSFER ANALYSIS

In addition to material properties discussed in Section 3.1, a definition of operating conditions as discussed in Section 3.2, and analytical models discussed in Section 4.1, the execution of the thermal analysis required a description of the initial temperature at each node. For analysis representing the first operating cycle of the engine, some ambient or room temperature value could reasonably be assumed as a uniform initial temperature. On the other hand, after repeated cycles as shown in Figure 3.2-1, some stable periodic temperature variation for each node could be expected to develop.

Thermal analyses of the cold phase were performed with the initial cylinder temperatures assumed as room temperature and results compared with results based on initial temperatures assumed as the computed temperatures at the end of the hot phase. It was found that the effects of the differences in initial temperatures disappeared long before the end of an assumed 1.65 second initial chill-down phase. Furthermore, it was found in each cold phase analysis that all cylinder configurations reached a constant, uniform temperature condition, with temperature equal to the coolant bulk value, before the end of the cold phase. Thus, this temperature was used as the initial temperature existing at the beginning of the cold-hot (engine start) transient. The procedure actually followed for each configuration was to analyze the hot phase first and to use the temperatures computed at the end of the hot phase as the initial temperatures for the cold phase.

Since the length of each cold phase was apparently sufficient to allow an approach to steady-state conditions, it was concluded that the thermal analysis of a single cycle as described simulated with equal accuracy, the first cycle of the engine's operation, or a typical cycle in a chain of many.

5.1 THERMAL ANALYSIS RESULTS

Results of thermal analyses are summarized by means of plots of continuous temperature histories for .ew selected locations for all three cases and a diagram of continuous isotherms at a few selected times during the cycle for each case.

Figures 5.1-1, 5.1-2 and 5.1-3 show temperature histories through a complete heating-cooling cycle for certain selected locations on configurations P.0, P.1, and P.2, respectively. Figures 5.1-4, 5.1-5 and 5.1-6 show isotherms at 25°C intervals for the three cases existing at 0.50 second after the beginning of the heating phase of the cycle. The isotherm plots show clearly the changes in thermal gradients resulting from the changes in thermal conductivity. It is also clear that there is little change in the general shape of the isotherm contours with changes in conductivity.

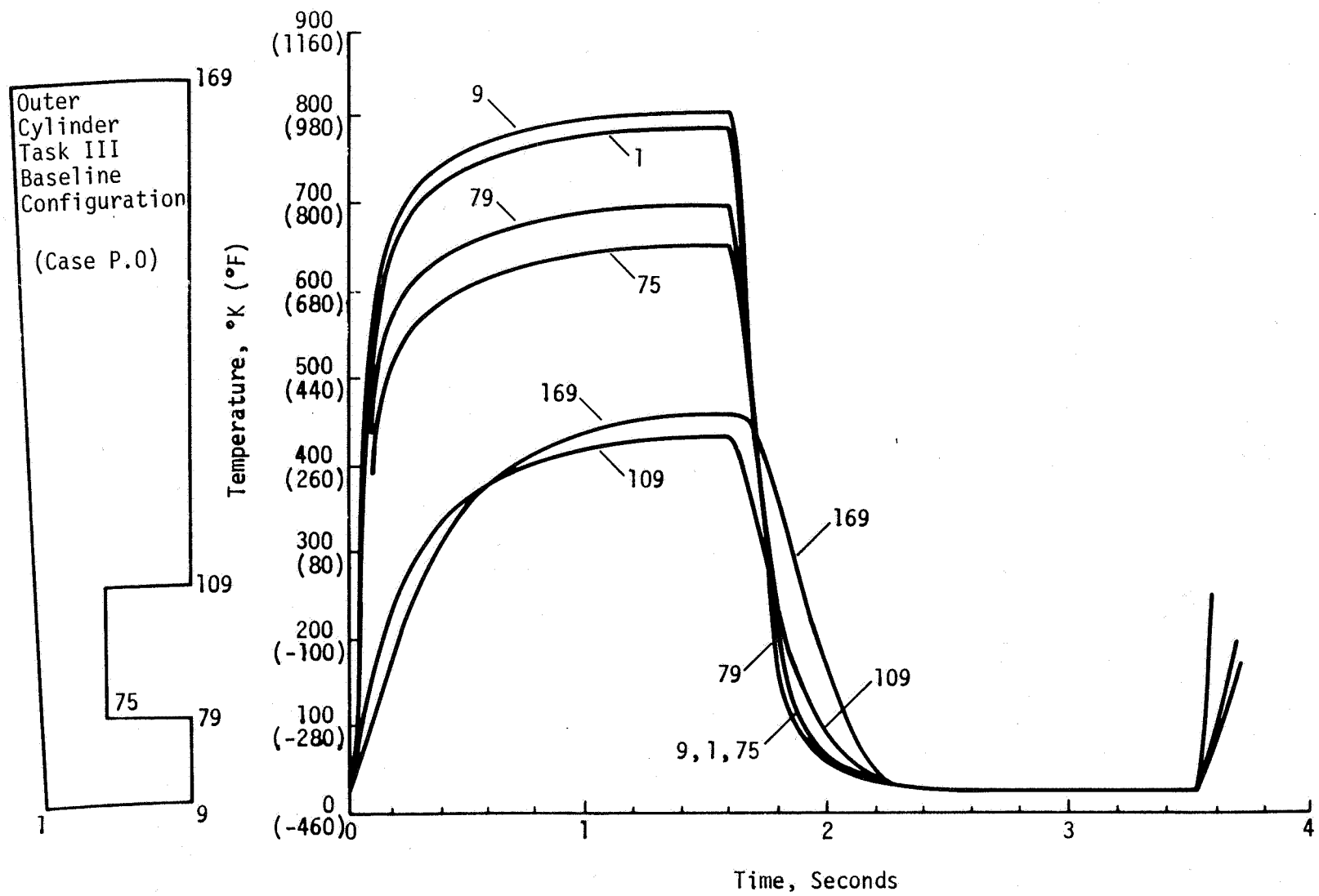

FIGURE 5.1-1 REPRESENTATIVE TEMPERATURES FOR TYPICAL HEATING-COOLING CYCLE FOR CONFIGURATION P.0

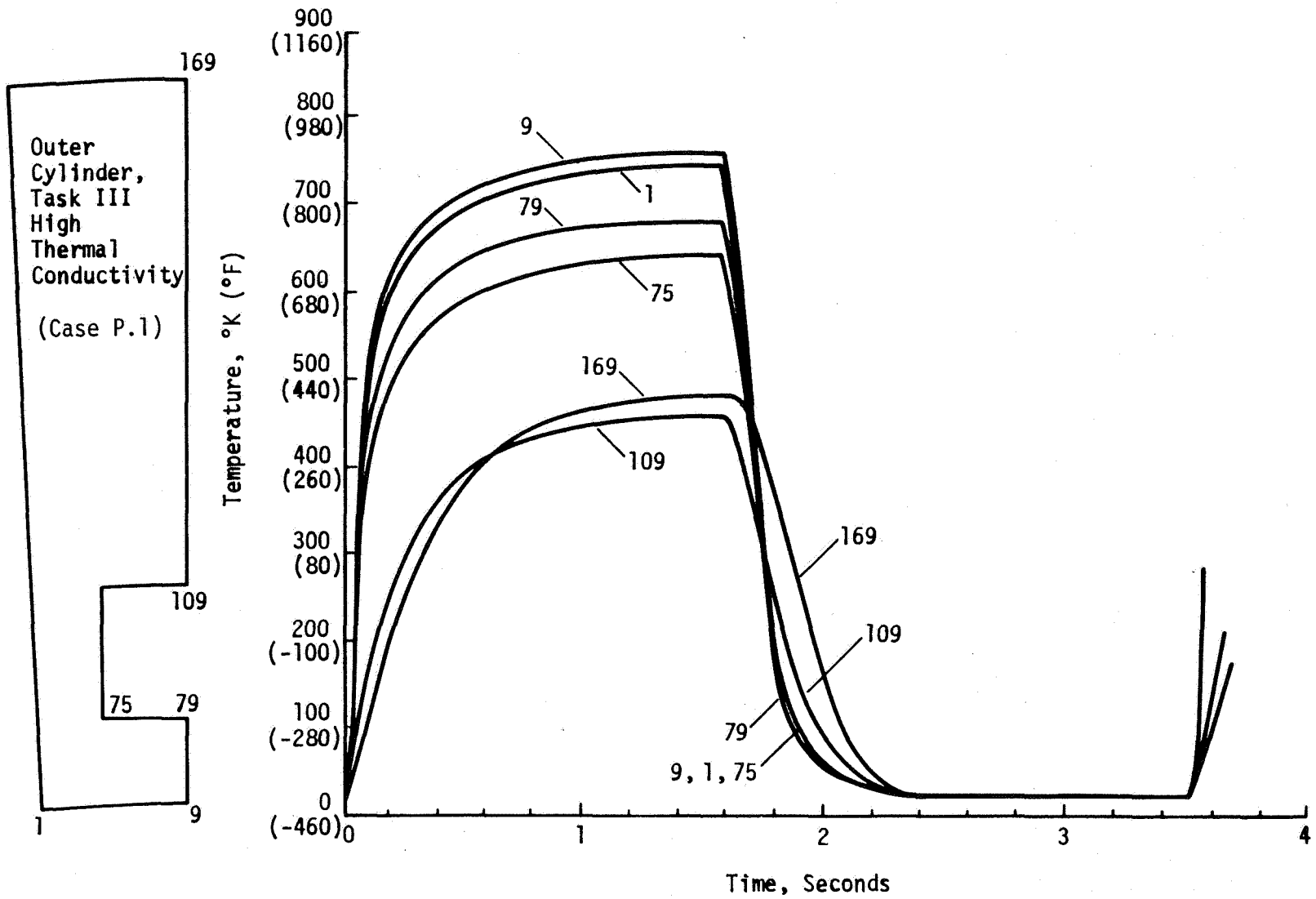

Figure 5.1-2 REPRESENTATIVE TEMPERATURES FOR TYPICAL HEATING-COOLING CYCLE FOR CONFIGURATION P.1

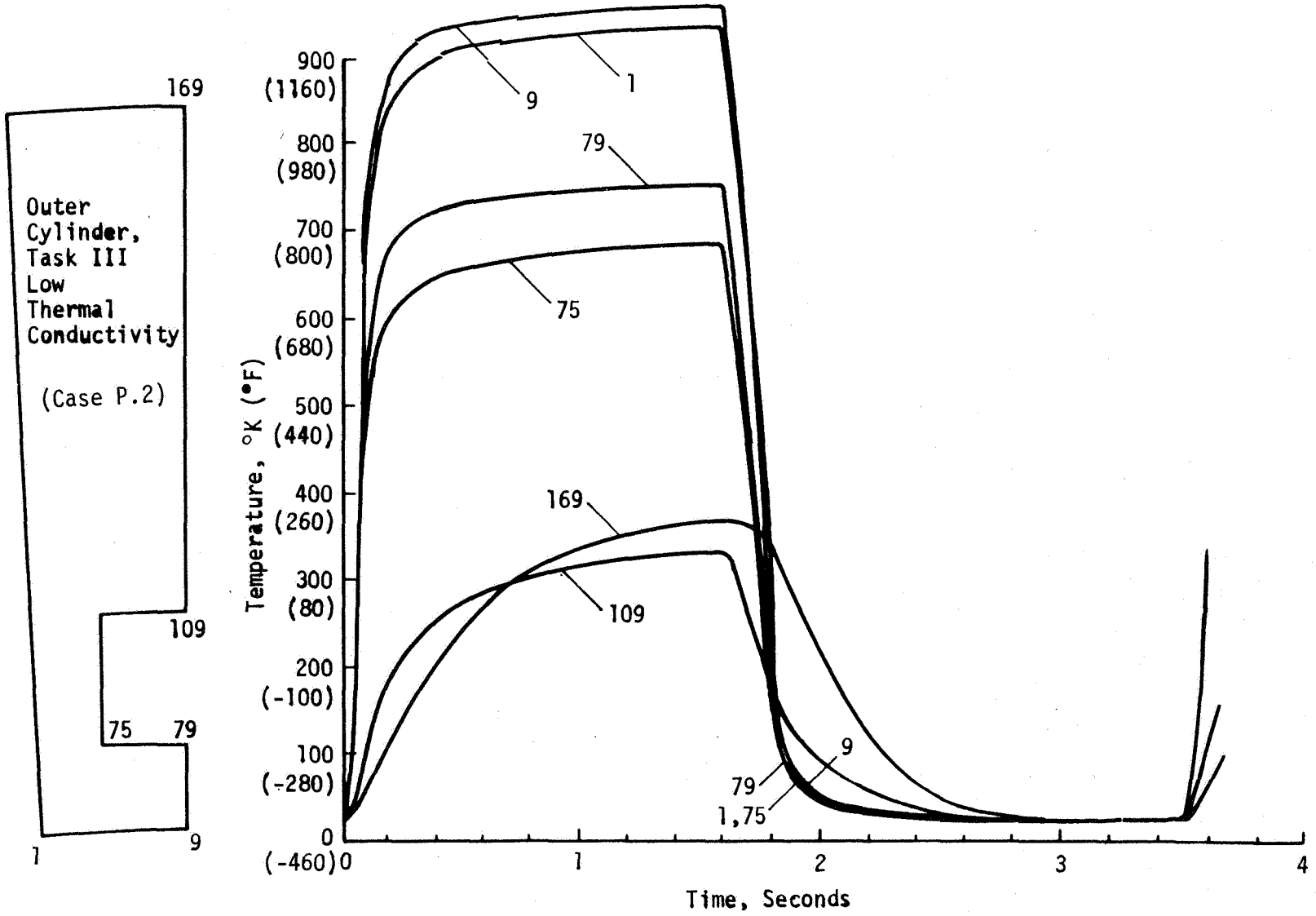

Figure 5.1-3 REPRESENTATIVE TEMPERATURES FOR TYPICAL HEATING-COOLING CYCLE FOR CONFIGURATION P.2

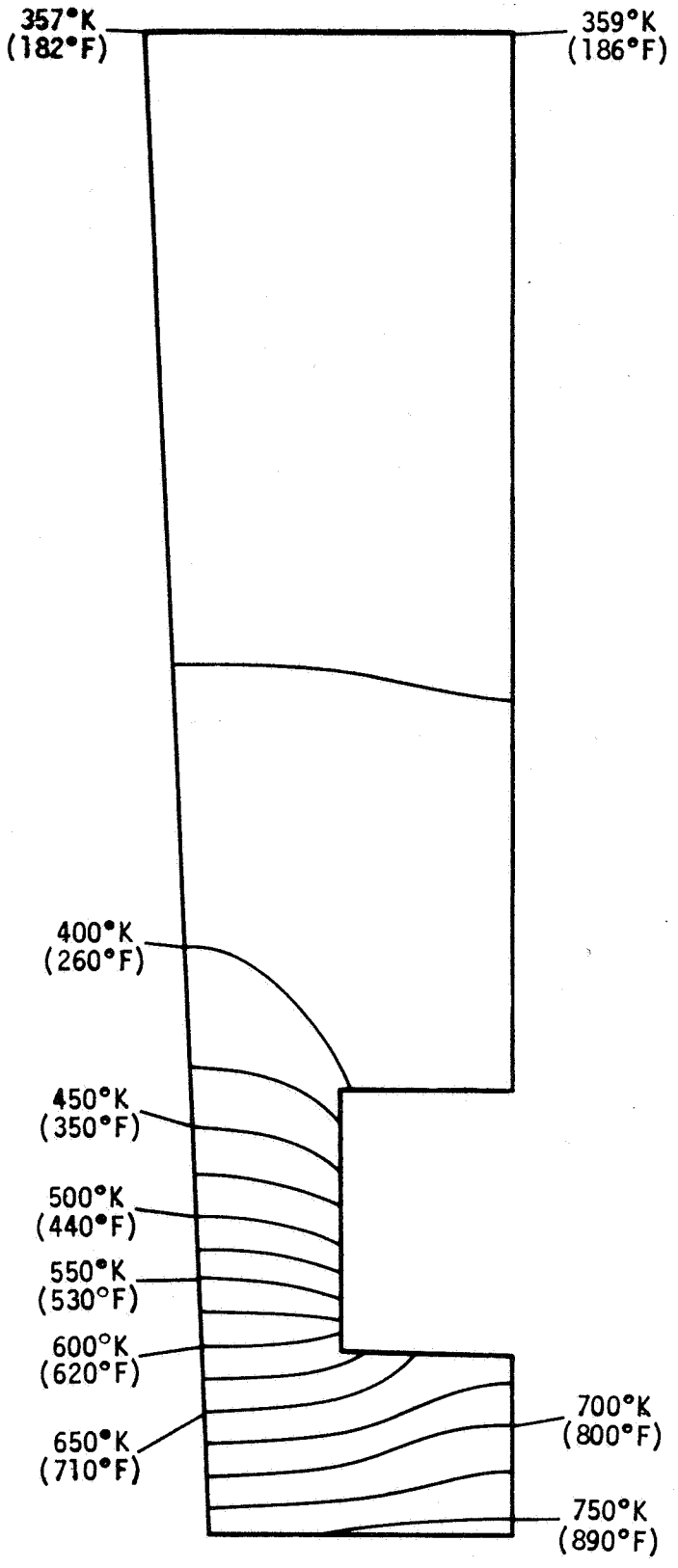

Figure 5.1-4 OUTER CYLINDER ISOTHERMS TASK III BASELINE (CASE P.0)
TIME = 0.50 SECOND

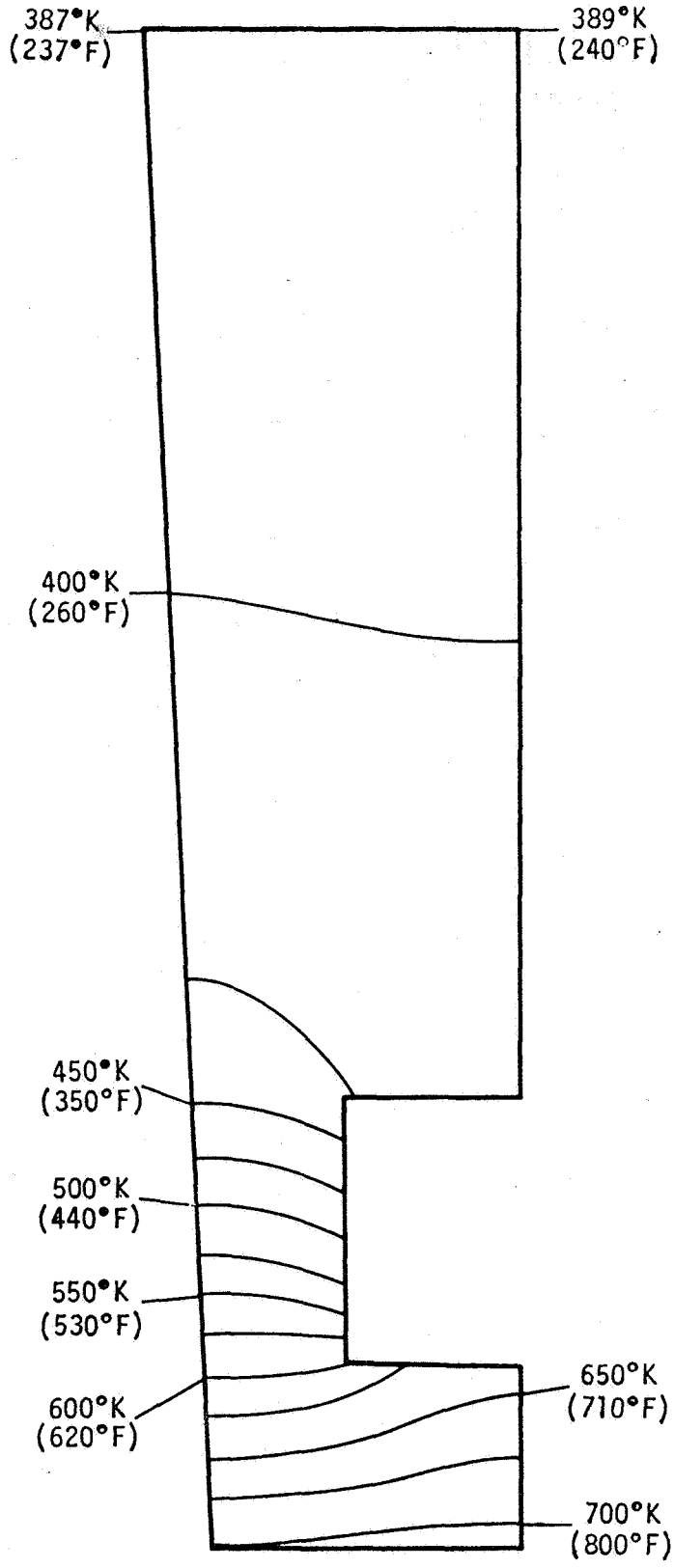

Figure 5.1-5 OUTER CYLINDER ISOTHERMS TASK III HIGH CONDUCTIVITY (CASE P.1)
TIME = 0.50 SECONDS

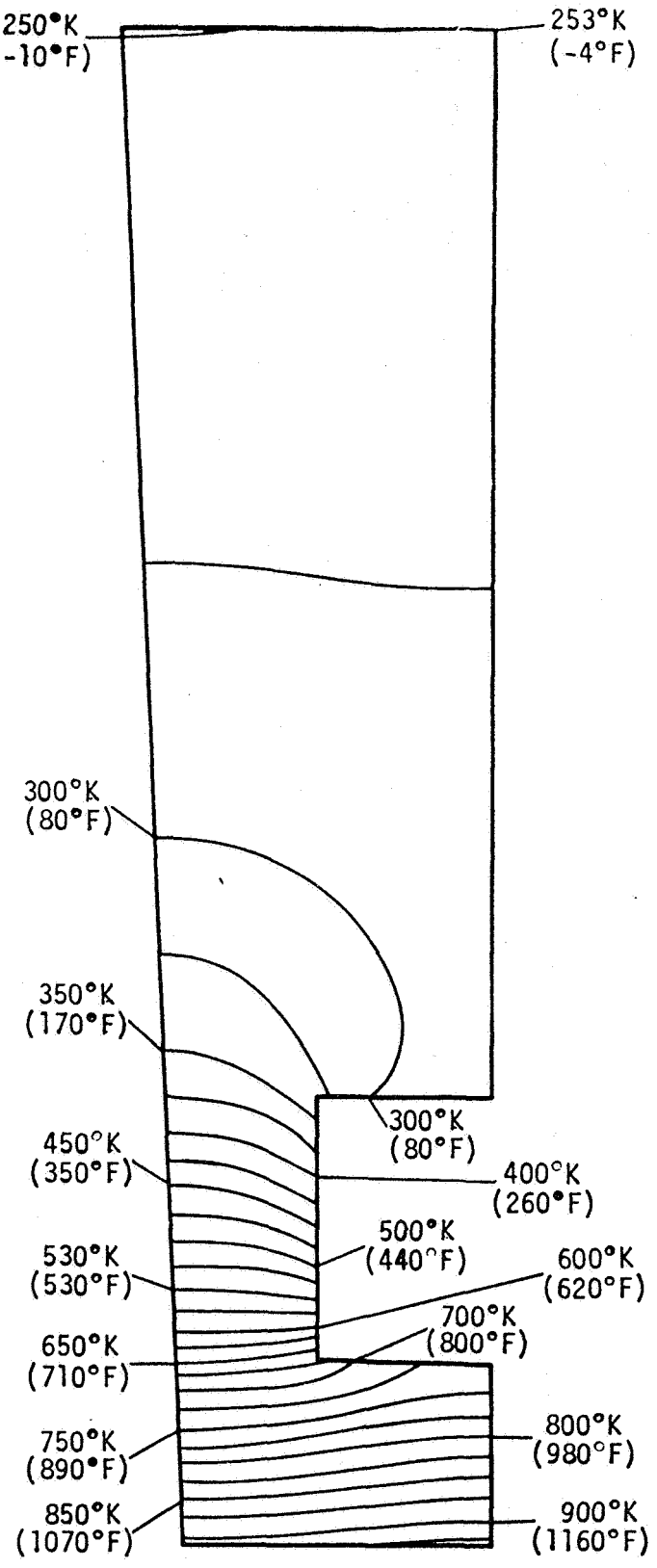

Figure 5.1-6 OUTER CYLINDER ISOTHERMS TASK III LOW CONDUCTIVITY (CASE P.2)
TIME = 0.50 SECONDS

6.0 STRUCTURAL ANALYSIS

The thrust chamber structural analysis was performed with the BOPACE computer program to account for, in an incremental manner, effects of variable amplitude cyclic loads and temperatures. In addition, variations of material properties with temperature, mechanically or thermally induced plasticity, and combinations of creep and stress relaxation are incorporated in the program.

Output from the BOPACE program provided histories of stresses and strains and their multiaxial component parts (elastic, plastic and creep) throughout the finite-element model of Section 4.0. These results were evaluated to define times and locations and magnitudes of maximum strains, strain histories, and isograms of effective strains at critical times during the operating cycle. The critical times (times of occurrence of maximum effective strain) were approximately 1.85 and 3.50 seconds for all cylinder configurations. Thus the critical time period encompassed the engine burn phase and included portions of the start and shutdown transients. During the critical time period, strains generally went through a complete reversal throughout the inner wall region. A summary of maximum effective strains is presented in Table 6.0-I.

6.1 STRUCTURAL ANALYSIS RESULTS

Results of the structural analyses were summarized by means of strain and temperature histories of the critical region in each configuration. The critical region is defined as the finite element exhibiting the maximum effective strain range during the operating cycle. Strain histories for radial, circumferential, and axial components are also shown. Since histories are presented, the times at which maximum strains were observed are also defined for the operating cycle. The critical times which occurred during start and shutdown transients generally coincided with times of maximum temperature gradients in the radial direction.

6.1 (Continued)

The histories of component strains do not present the total strains in that thermal strain is not included. The reason for this method of presentation is that the plotted values were the quantities used in computing the total effective strain (equivalent uniaxial strain) from the equation

$$\varepsilon_{eff} = \sqrt{\frac{2}{3}} \sqrt{(\varepsilon_r{}^t - \varepsilon_\theta{}^t)^2 + (\varepsilon_r{}^t - \varepsilon_z{}^t)^2 + (\varepsilon_\theta{}^t - \varepsilon_z{}^t)^2} \qquad (6.1\text{-}1)$$

where subscripts r, θ, z denote radial, circumferential and axial strains respectively and superscript t denotes total cumulative strain defined by

$$\varepsilon^t = \varepsilon^e + \varepsilon^p + \varepsilon^c + \varepsilon^T. \qquad (6.1\text{-}2)$$

Here superscripts e, p, c, T denote elastic, plastic, creep and thermal strains. Since the materials were assumed isotropic in thermal strain, this quantity cancels from equation (6.1-1). It should be noted that since the total strain in the axial direction must be zero for the plane-strain model, the thermal strain histories are simply the negative values of the histories shown for the axial strain component.

The critical strain and temperature data are shown in Figures 6.1-1 through 6.1-29. The time origin of the histories of strain and temperature is at the beginning of the initial thrust chamber cooldown from 294°K. Since the initial cooldown was used only to carry the thrust chamber cylinder to the beginning of start transient, the same initial temperature-pressure increments were used for all cylinder configurations. These initial cooldown increments provided satisfactory convergence within the BOPACE program; experience has shown that more rapid convergence to the deformed configuration is achieved when temperature increments of $\leq$ 65°C are used in the BOPACE analysis. The total temperature change during initial cooldown of the cylinders was 249°C. Thus, several loading increments for initial cooldown were necessary. Since the behavior during initial cooldown of the cylinder is time independent

6.1 (Continued)

and temperature gradients were not expected to differ significantly from configuration to configuration, the conditions at the end of this period depend only on the model and the convergence criterion required to follow the monotonically decreasing temperature to the beginning of start transient.

A sampling of strain and temperature histories of finite elements within the high strain region of the cylinder configurations is shown in Appendix C. The high strain area within the cylinder model is the inner wall.

6.1.1 Strain and Temperature Histories

The histories of strain in the critical region of baseline configuration P.0 are shown in Figures 6.1-1 and 6.1-2. The critical region is element #131 located at the centerline of the coolant channel on the channel surface. The maximum effective strains shown in Figure 6.1-2 were 1.31 and 2.21 percent at 1.85 and 3.50 seconds respectively. Thus the computed cyclic strain range in element #131 is 3.52 percent.

The temperature history of element #131 is shown in Figure 6.1-3 which shows that the temperature in that region increased from 600°K to 700°K between 1.85 and 3.20 seconds then decreased to 100°K at 3.50 seconds. This temperature history applies to all configurations except P.1 and P.2 since thermal properties were invariant for all but P.1 and P.2.

The critical strain range was applied to the fatigue curve for half-hard Amzirc shown in Figure 6.1-4. The predicted cycles to fracture in element #131 of P.0 is approximately 600 cycles.

Shutdown was the most damaging phase of the cycle for P.0 as evidenced by the magnitude of peak strains and the presence of a region of high strain extending diagonally across the inner wall from element #8 on the heated surface to element #131. This band of high strain is indicated by the shaded region of Figure 6.1-5. The effective

6.1.1 (Continued)

strains within this band are shown in Figure 6.1-6. It was observed that a relatively large gradient in effective strain range (approximately 16 percent per cm) developed in the band extending from element #65 to element #131. Element #131 is expected to be the "point" of initiation of a low-cycle fatigue crack, but because of the large gradient in effective strain range, it is difficult to predict the number of cycles to a through crack condition. This is because the fatigue curve was established from test data for uniaxial specimens with homogeneous strains in the test section. Thus cumulative low-cycle fatigue damage was uniform within the uniaxial specimens. Cumulative damage is not uniform throughout the inner wall of P.0 and through fracture of the inner wall will depend on the rate of crack growth from the small area of element #131. (Note: The area of element #131 is 0.0094 square mm, or approximately 0.7 percent of the area of the inner wall model).

Predicted creep behavior of element #131 is shown in Figure 6.1-7. Element #131 creep data are representative of computed time dependent strains throughout the inner wall region of all cylinder configurations. Since creep strains were three orders in magnitude smaller than total effective strain, creep has a negligible effect on low-cycle fatigue life of the cylinders. Also, creep is expected to remain almost constant after the first cycle because of hardening and the fact that unloading during the cooldown transient happens so rapidly that measurable creep reversal will not occur.

Strain and temperature histories for all other configurations are presented in Figures 6.1-8 through 6.1-38. The results are similar to those computed for P.0. Peak strains occur during start and shut-down transients at times of 1.85 and 3.50 seconds. It was observed that peak strain ranges for all parametric configurations were lower than the computed value for the baseline.

6.1.1 (Continued)

Strain and temperature histories at two different locations are presented for configurations P.2, P.3 and P.4. This was done to show conditions at the critical region which was different than element #131. Strain and temperature histories are also shown for element #131 of these three cylinders for comparison with baseline data. It is seen that shutdown was the most damaging phase of the cycle for all configurations except P.2 and P.4.

6.1.2 Variation in Strain with Change in Parameters

The parametric effects on maximum strain range of the various configurations are summarized in Table 6.1-I. It is seen that all variations of material properties considered in the parametric study resulted in a reduction of the maximum strain range with respect to the baseline case. The reduction ranged from 2 to 51 percent, but this does not mean that all changes in the material variables result in decreased low-cycle fatigue damage and increased cyclic life. For example, the 52 percent decrease in average thermal conductivity for case P.2 resulted in an 8 percent reduction in maximum effective strain. Closer examination showed, however, that temperatures were higher for P.2 and also that strains throughout the inner wall region were significantly higher than in P.0 during start transient. Thus the effective strain range was more uniform as well as higher in the entire inner wall region which means cyclic damage is more extensive in P.2. These results in addition to other parametric effects are reviewed in more detail in the following paragraphs.

Thermal Conductivity Effects

The variation in maximum effective strain with thermal conductivity is shown in Figure 6.1-39. The high thermal conductivity case (P.1) resulted in a decrease of 26 percent in maximum effective strain range with the greatest change occurring during shutdown. In addition, the thermal analyses showed an 8 percent decrease in peak temperatures of

6.1.2 (Continued)

P.1 with respect to P.0 (Appendix C). A comparison of the strain field at the critical times is shown in Figures 6.1-44 and 6.1-45 which present isograms of effective strain. It is seen from the isograms that the P.1 strains are lower than P.0. Thus cyclic damage is less severe for the high conductivity case.

The low conductivity case (P.2) resulted in a decrease of peak strain and also caused a shift in the critical region from element #131 observed in P.0 and P.1 to element #10. Element #10 is located at the centerline of the rib on the heated surface of the cylinder. The computed P.2 data showed only an 8 percent decrease in peak strains while peak temperatures increased by 27% over the baseline case. The isograms show that while the peak strain range decreased by 8 percent, the deformation in P.2 was more uniform in the inner wall region and significantly higher during the start transient. Although the effective strain range was lower in P.2 than the baseline, the low conductivity case appears to be more damaging because overall plastic flow in the inner wall was greater for this condition. Also Figure 6.1-39 indicates that P.0 may not be the maximum point of the strain range curve since the slope is relatively flat between P.2 and P.0.

In summary, the thermal conductivity parametric study indicates that increasing the conductivity of half-hard Amzirc is beneficial to the life of the plug nozzle cylinder. Both temperatures and strains decreased with increasing conductivity. Decreasing conductivity, however, is detrimental to fatigue life of the Amzirc cylinder.

Thermal Expansion Effects

Thermal expansion effects on maximum effective strains are shown in Figure 6.1-40. An increase in the coefficient of thermal expansion by 20 percent (P.3) caused the maximum effective strain to decrease by 14 percent and to cause a slight shift in the critical region. Element #133 was the critical element in P.3. The greatest effect on P.3

strain occurred during shutdown where maximum effective strain decreased 32 percent over the baseline.

A comparison of isograms for P.0 and P.3 in Figures 6.1-46 and 6.1-47 show that inner wall strains are generally larger during start and shutdown in P.3. Thus overall cyclic damage is greater in P.3 and since the peak strain ranges are nearly the same (3.0 percent in P.3 and 3.5 percent in P.0) an increase in the coefficient of thermal expansion appears detrimental to fatigue life.

The most significant effects observed in the parametric study occurred when the coefficient of thermal expansion was reduced 20 percent over the baseline. This configuration (P.4) exhibited a 51 percent decrease in the maximum effective strain range with respect to P.0 under the same operating cycle. Also, the critical element in P.4 was element #10. The greatest effect of P.4 strains occurred during shutdown where the maximum effective strain decreased 80 percent over P.0.

A comparison of the isograms in Figures 6.1-46 and 6.1-47 shows that decreasing the coefficient of thermal expansion is definitely beneficial to fatigue life. Strains throughout the inner wall of P.4 are significantly lower at the critical times.

Modulus of Elasticity Effects

The variation in maximum effective strain with elastic modulus is shown in Figure 6.1-41. The configuration with the increased modulus (P.5) exhibited a peak strain range 14 percent lower than the baseline for the same pressure-temperature loading conditions. The critical region in P.5 was element #131 where the greatest effects occurred during shutdown. Effective strains decreased 23 percent during P.5 shutdown, but there was no variation in strain between P.0 and P.5 during start transient.

6.1.2 (Continued)

A comparison of the P.0 and P.5 isograms shows that their effective strain fields were nearly the same. The principal difference between the two configurations is the region of maximum strain at shutdown.

Configuration P.6 wherein the elastic modulus was decreased by 20 percent over the baseline exhibited a 24 percent decrease in maximum effective strain range. The critical element was #131 where greatest effects were observed for the shutdown transient phase of the cycle.

The P.6 isograms show a general decrease in effective strains at the critical times. Also the strain gradient during shutdown is not as severe as for the baseline. It appears that a decrease in elastic modulus is beneficial to fatigue life and second in order of most effective parameters studied.

Poisson's Ratio Effects

The effects on maximum effective strain caused by varying the elastic value of Poisson's ratio are shown in Figure 6.1-42. An 18 percent increase (P.7) of the baseline value, 0.34, caused the maximum effective strain range to decrease by 10 percent.

A decrease in Poisson's ratio (P.8) of 26 percent caused the maximum effective strain range to decrease by 23 percent. The most significant effect on P.8 occurred during shutdown where element #131 effective strain decreased 36 percent over P.0.

A comparison of isograms for P.0, P.7 and P.8 indicates little difference in the general strain fields. Thus the variation in Poisson's ratio does not appear to have a large effect on computed structural behavior of the cylinder.

6.1.2 (Continued)

Yield Strength Effects

The variation in maximum effective strain with yield strength is shown in Figure 6.1-43. For the purposes of these analyses, yield was defined as the points of deviation from linearity in the stress-strain curves in Section 3.1.

In configuration P.9 the temperature dependent baseline yield strength was increased 25 percent. This change resulted in a 17 percent drop in maximum effective strain range with the greatest effect occurring during shutdown. The decrease in effective strain within the critical region, element #131, was 30 percent for the shutdown phase. A comparison of isograms shows that effective strains are essentially unchanged for the start transient, but there is a significant decrease in effective strain during shutdown. Thus an increase in yield strength reduced plastic flow during the operating cycle.

Configuration P.10 was analyzed for the case with a 25 percent decrease in yield strength. P.10 results were essentially the same as critical strains and strain fields observed in the baseline. Examination of the isograms shows that start transient strains were somewhat lower than the baseline and strains during shutdown were slightly greater within the inner wall region. The effective strain range appears to be approximately the same for P.0 and P.10. It is noted that this behavior was not expected; more extensive damage and plastic flow was anticipated for the P.10 configuration. A possible cause of this result is that although the yield point was reduced 25 percent, the shapes of the temperature dependent stress-strain curves for P.10 were essentially the same as for the baseline case. Thus stiffness of the P.10 and P.0 models was approximately the same. A better choice of material properties for the P.10 parameter would have been the properties of fully-annealed Amzirc. Then the effect of decreasing yield strength would have been clearly demonstrated.

TABLE 6.0-I SUMMARY OF MAXIMUM EFFECTIVE STRAINS IN FINITE-ELEMENT MODEL OF OUTER CYLINDER

CONFIGURATION	CRITICAL ELEMENT I.D. NO.	EFFECTIVE STRAIN (%) TIME = 1.85 SEC.	EFFECTIVE STRAIN (%) TIME = 3.50 SEC.	EFFECTIVE STRAIN RANGE (%)
P.0	131	1.31	2.21	3.52
P.1	131	1.19	1.40	2.59
P.2	10	2.49	0.74	3.23
P.2	131*	1.89	0.58	2.47
P.3	133	1.46	1.52	2.98
P.3	131*	1.52	1.23	2.75
P.4	10	1.25	0.43	1.68
P.4	131*	1.13	0.36	1.49
P.5	131	1.31	1.70	3.01
P.6	131	1.33	1.40	2.73
P.7	131	1.33	1.84	3.17
P.8	131	1.26	1.38	2.64
P.9	131	1.33	1.54	2.87
P.10	131	1.25	2.21	3.46

*THIS ELEMENT INCLUDED FOR COMPARISON WITH BASELINE DATA.

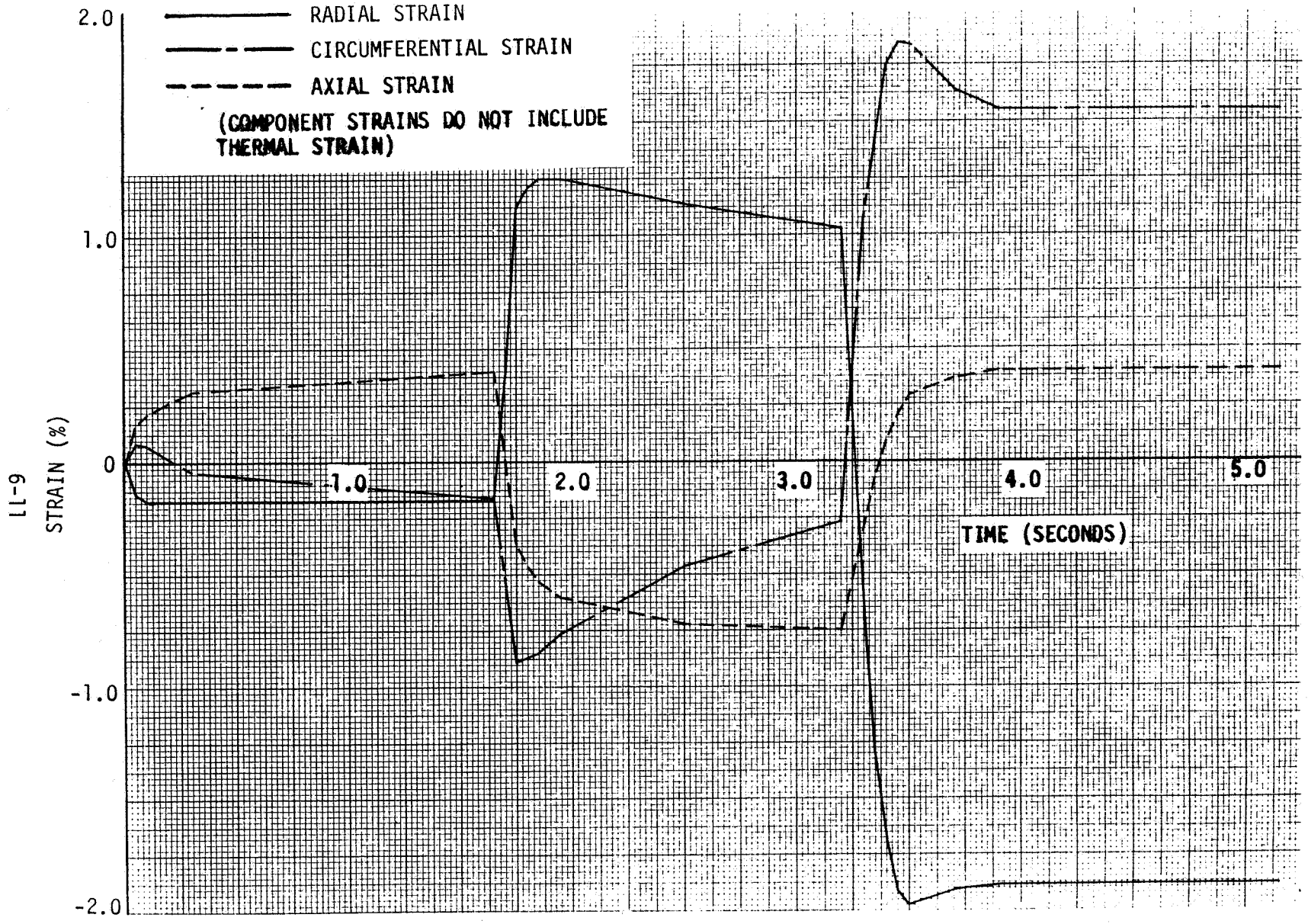

FIGURE 6.1-1 STRAIN VS. TIME, ELEMENT #131, CONFIGURATION P.0

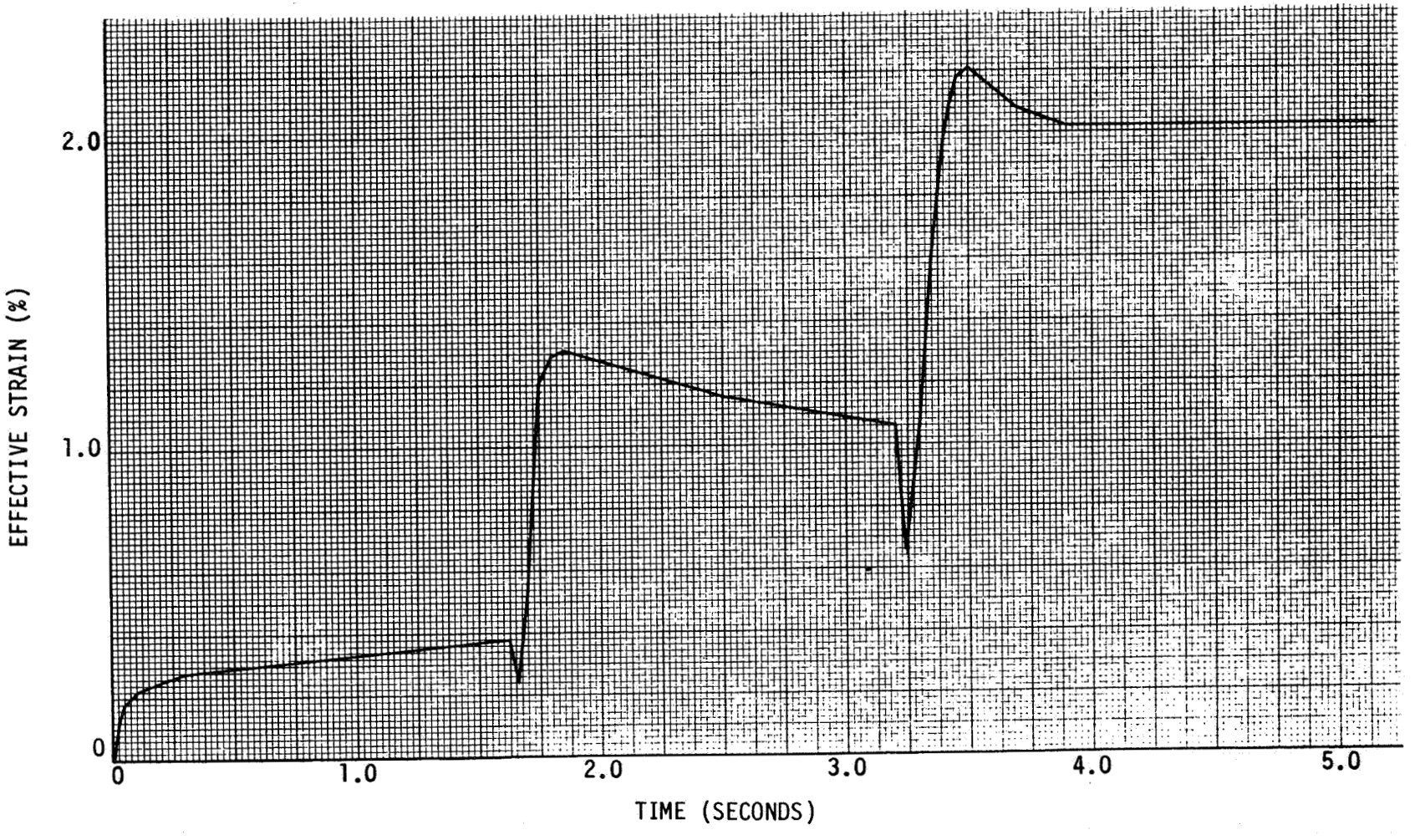

FIGURE 6.1-2 EFFECTIVE STRAIN VS. TIME, ELEMENT #131, CONFIGURATION P.0

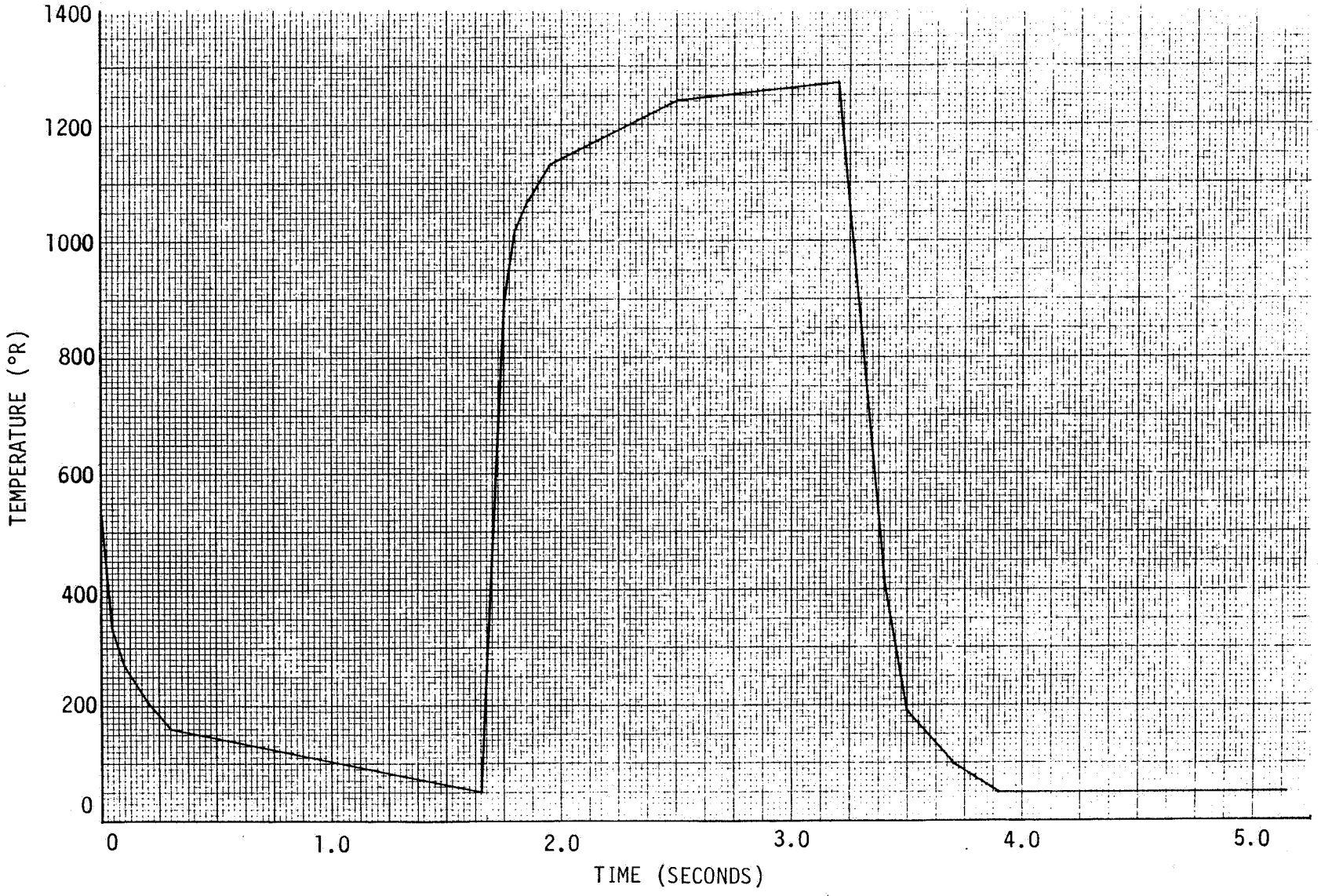

FIGURE 6.1-3 TEMPERATURE VS. TIME, ELEMENT #131, CONFIGURATION P.0

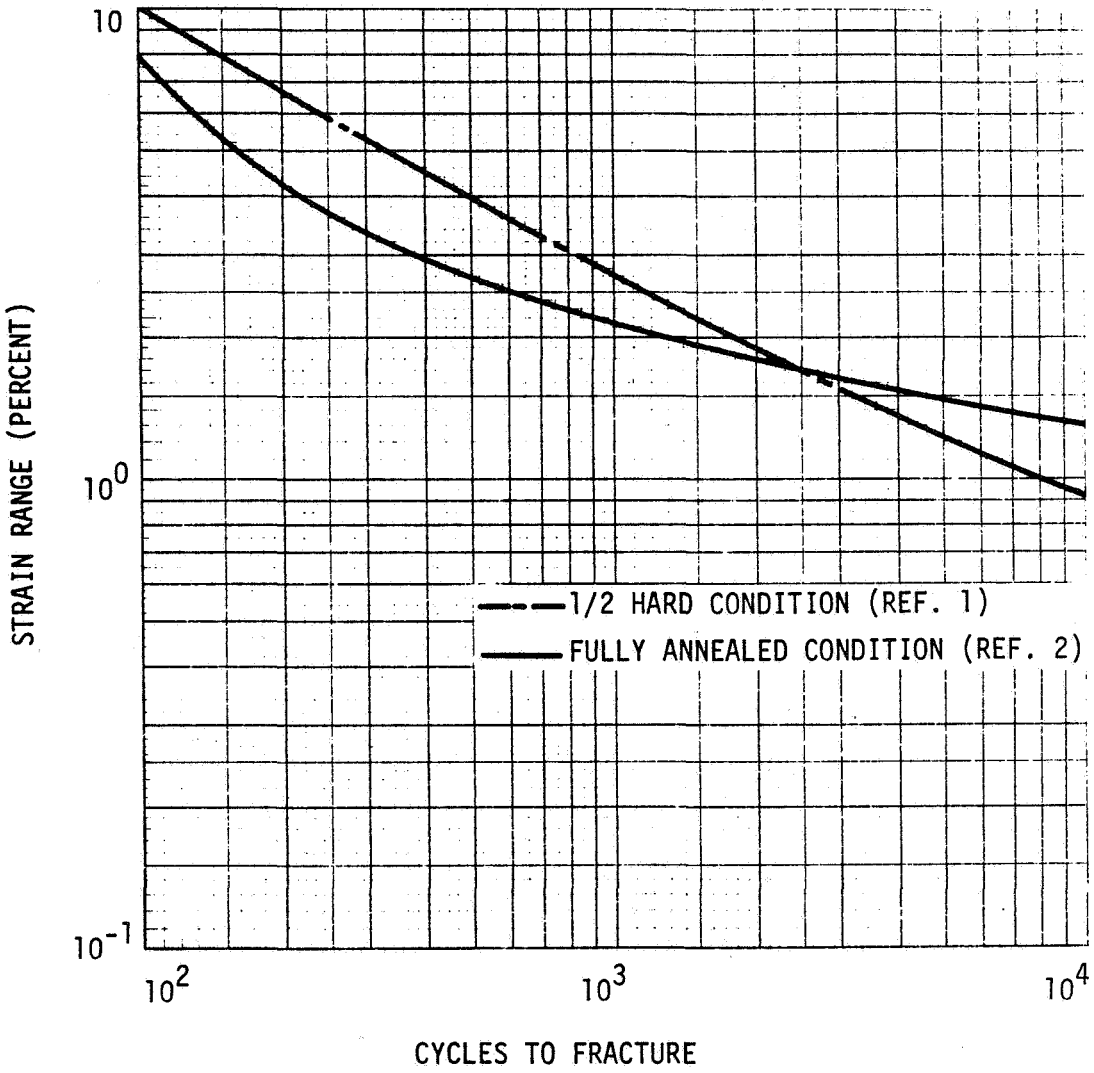

DATA ASSUMED TO APPLY TO:

1. Temperature range of 290 to 810°K.
2. All environments.
3. Effective or uniaxial strain ranges.

FIGURE 6.1-4 TYPICAL LOW CYCLE FATIGUE LIFE OF AMZIRC

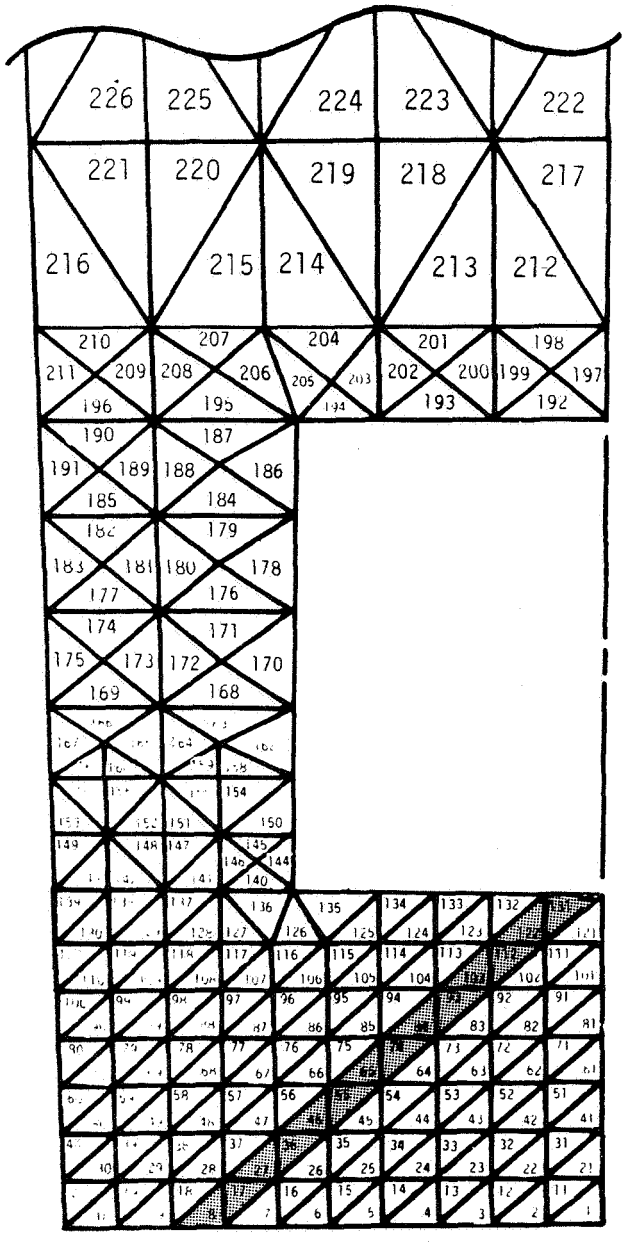

FIGURE 6.1-5 REGION OF MAXIMUM EFFECTIVE STRAIN RANGE IN CONFIGURATION P.0

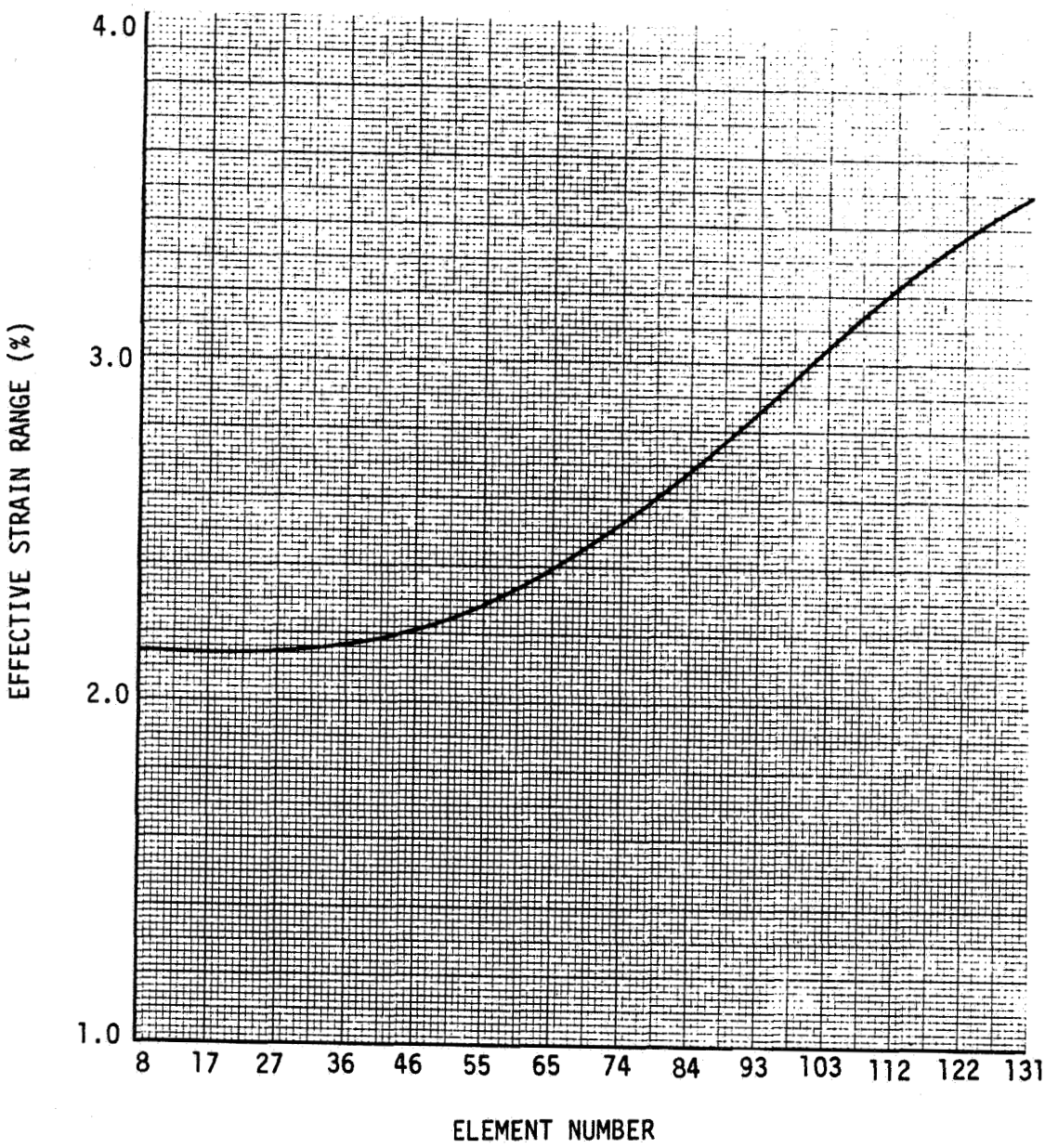

FIGURE 6.1-6 VARIATION IN EFFECTIVE STRAIN RANGE IN REGION OF MAXIMUM STRAIN IN CONFIGURATION P.0

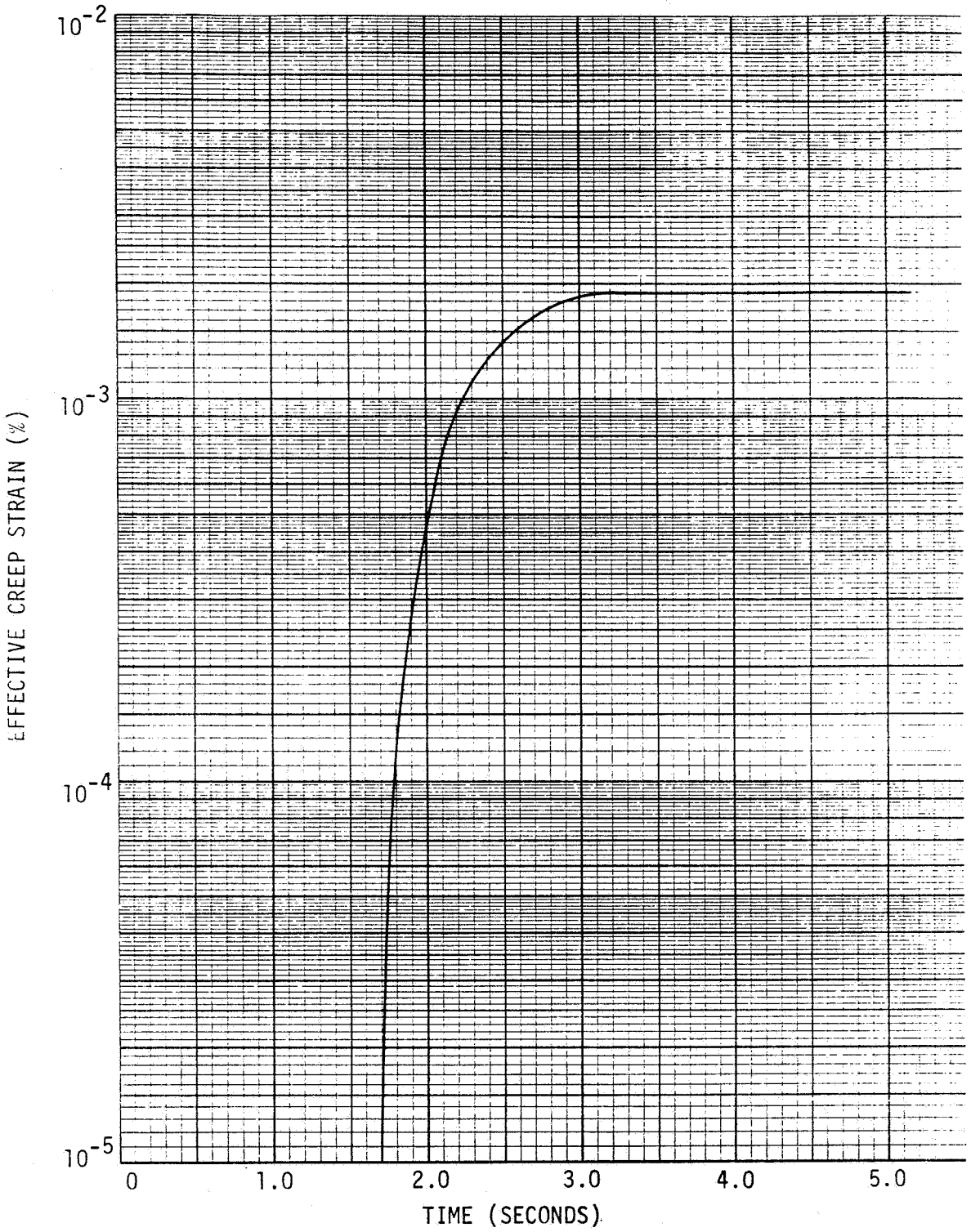

FIGURE 6.1-7 EFFECTIVE CREEP STRAIN, ELEMENT #131, CONFIGURATION B.0

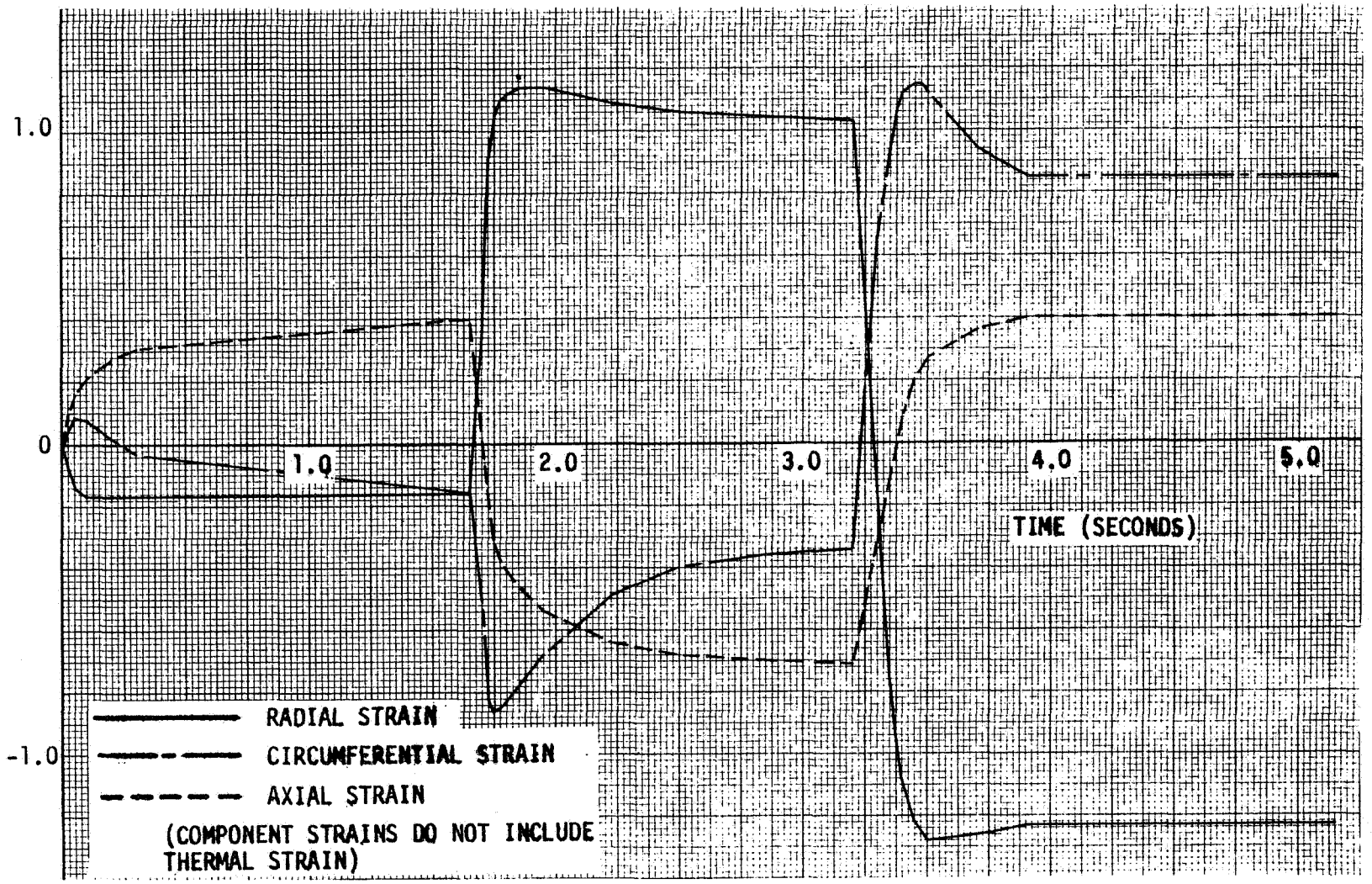

FIGURE 6.1-8 STRAIN VS. TIME, ELEMENT #131, CONFIGURATION P.1

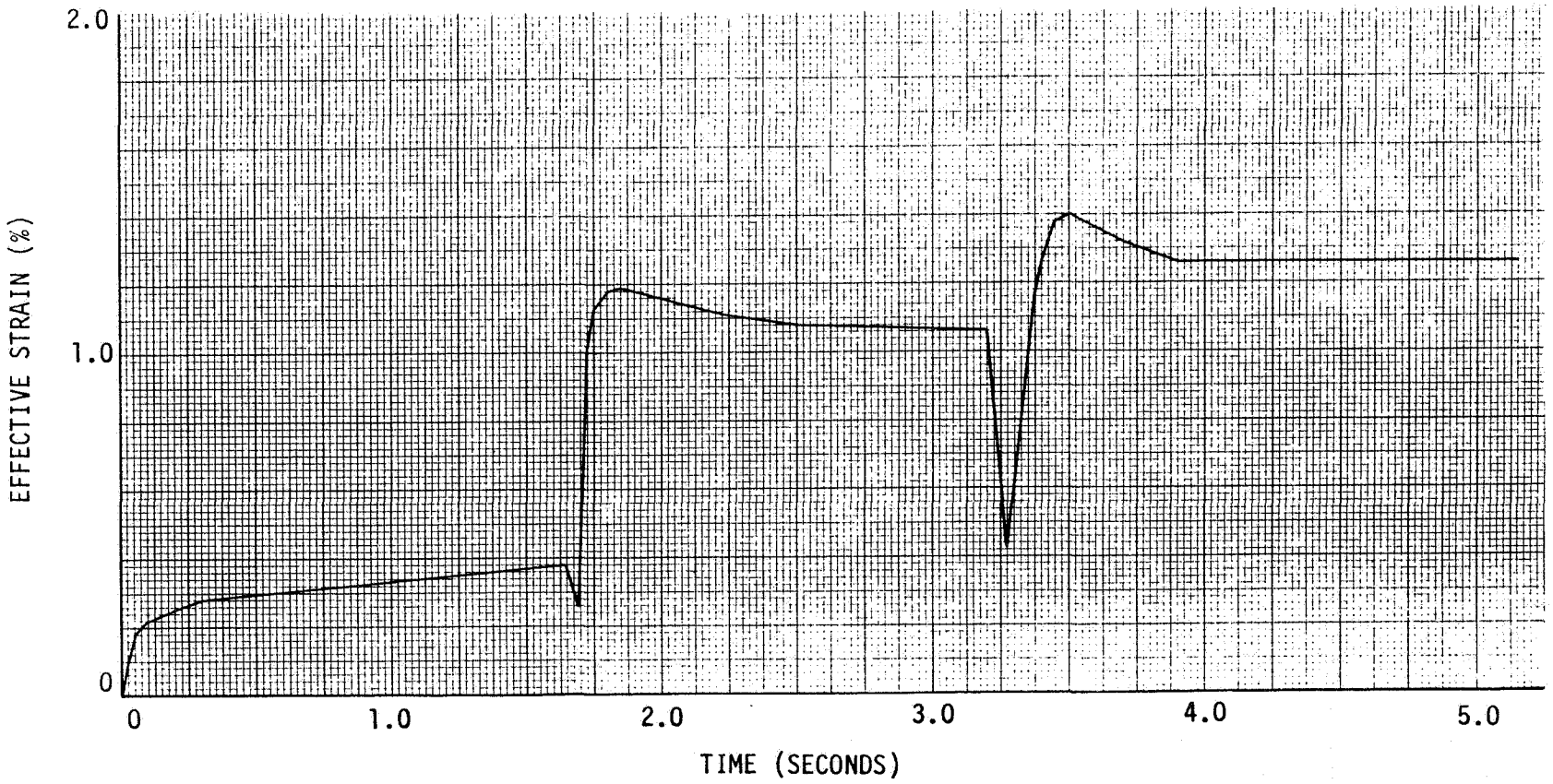

FIGURE 6.1-9 EFFECTIVE STRAIN VS. TIME, ELEMENT #131, CONFIGURATION P.1

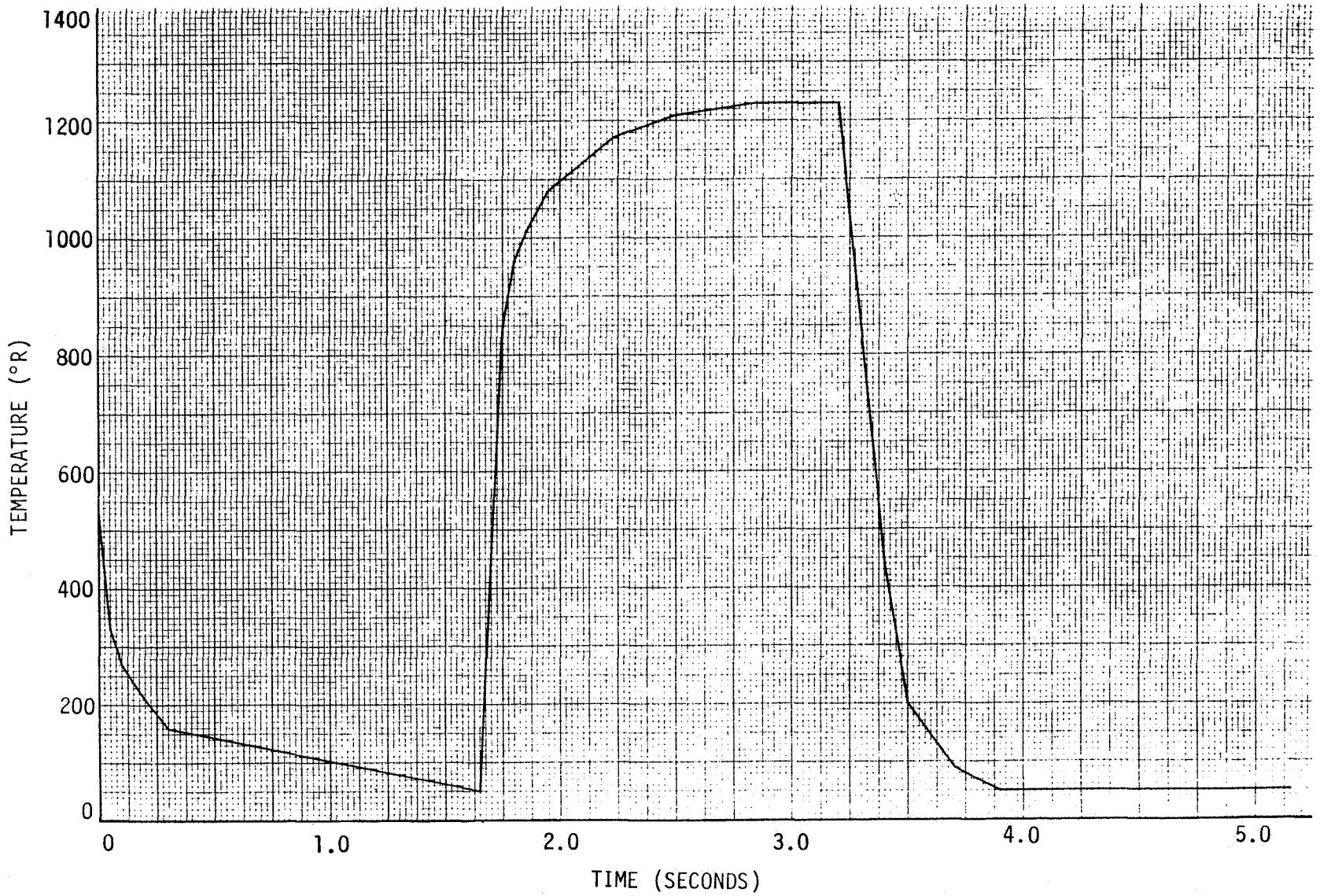

FIGURE 6.1-10 TEMPERATURE VS. TIME, ELEMENT #131, CONFIGURATION P.1

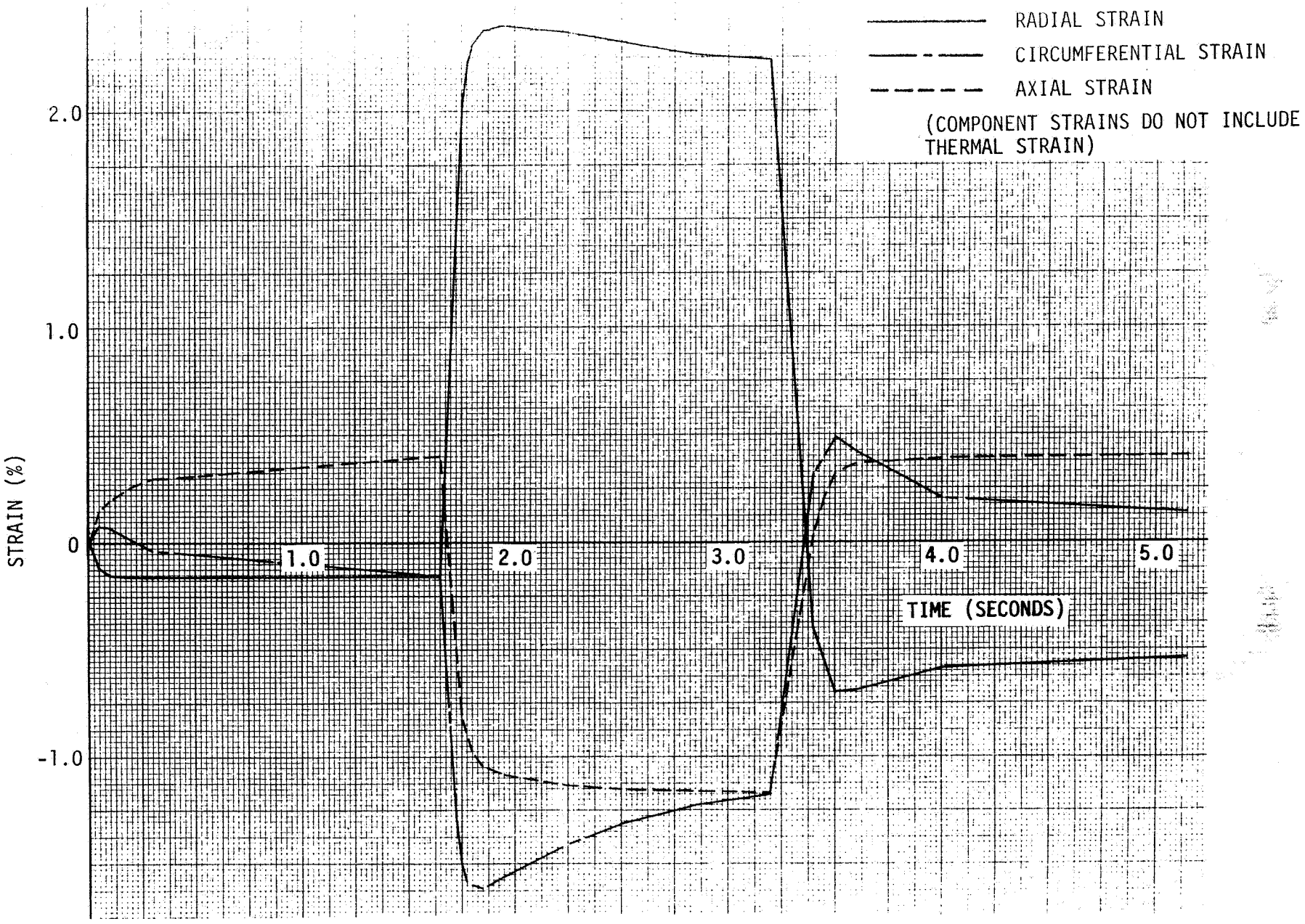

FIGURE 6.1-11 STRAIN VS. TIME, ELEMENT #10, CONFIGURATION P.2

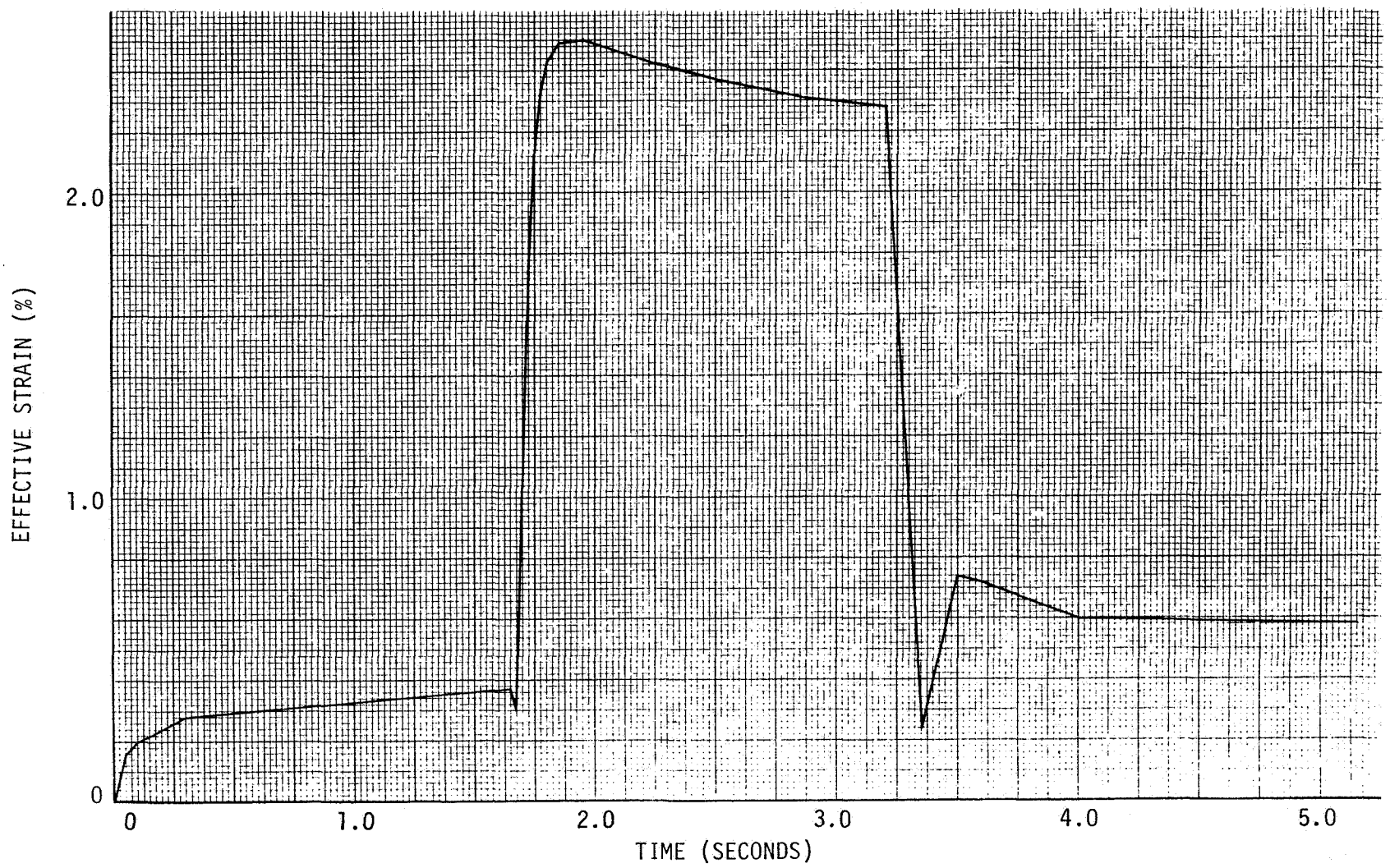

FIGURE 6.1-12 EFFECTIVE STRAIN VS. TIME, ELEMENT #10, CONFIGURATION P.2

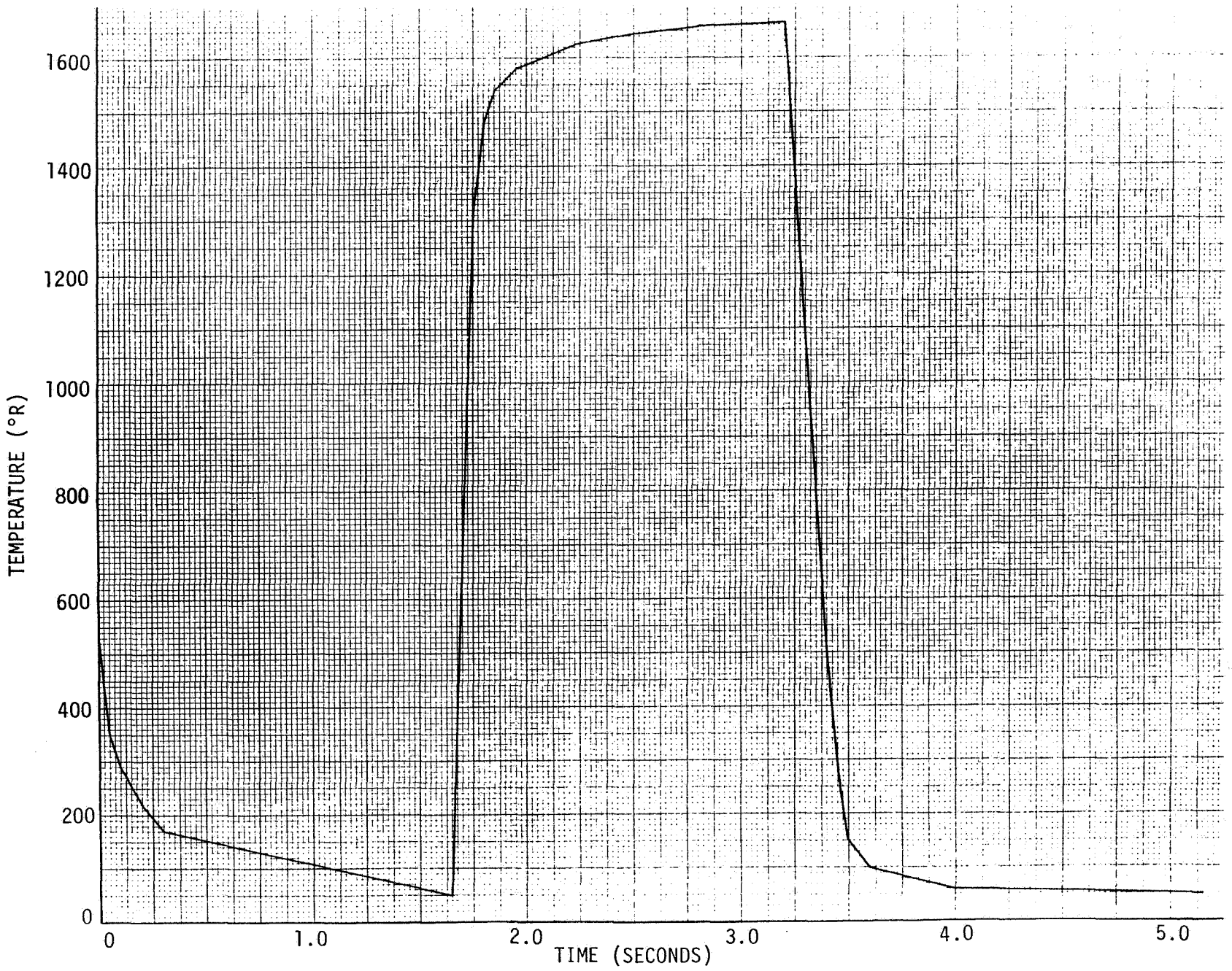

FIGURE 6.1-13 TEMPERATURE VS. TIME, ELEMENT #10, CONFIGURATION P.2

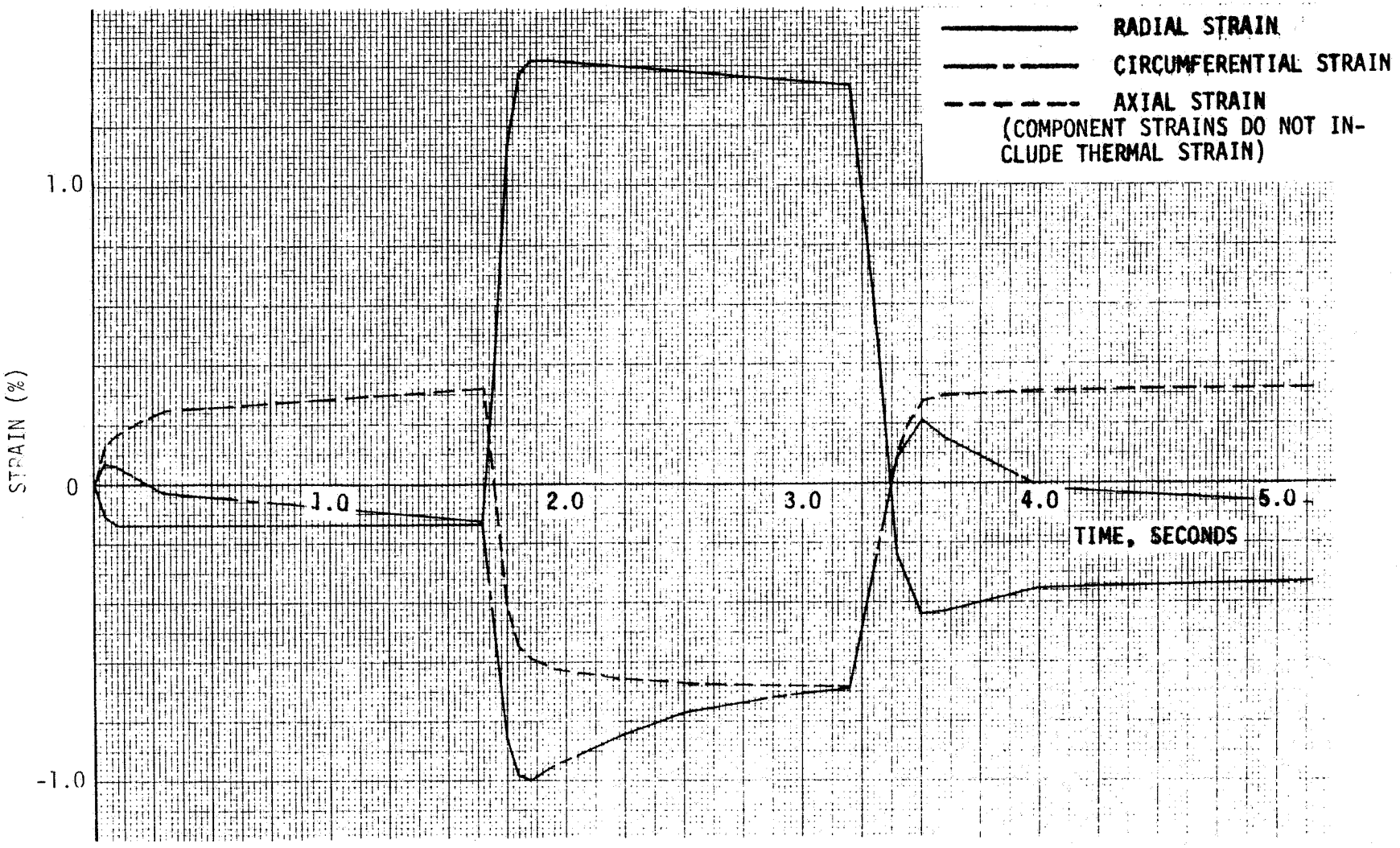

FIGURE 6.1-14 STRAIN VS. TIME, ELEMENT #131, CONFIGURATION P.2

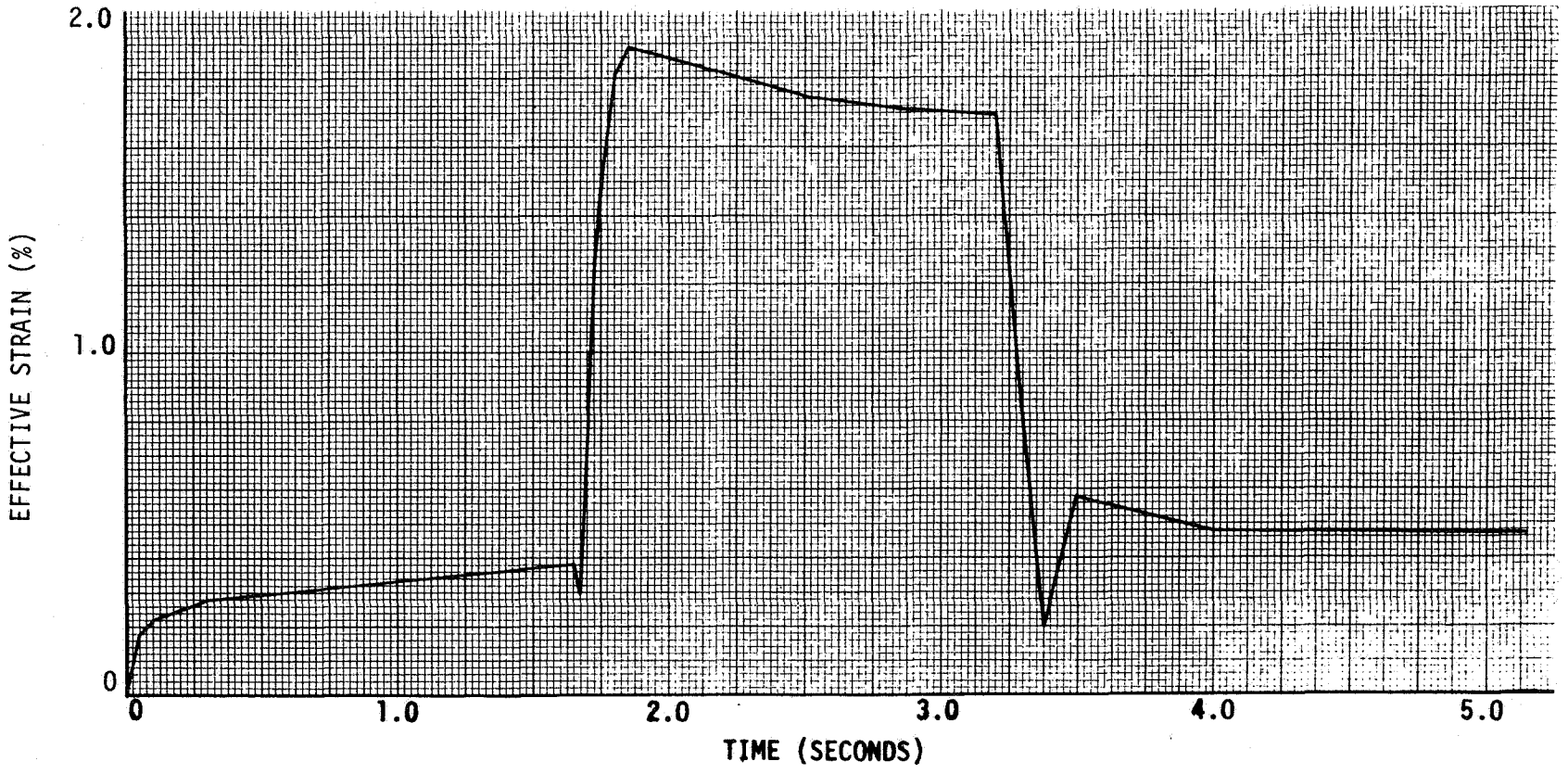

FIGURE 6.1-15 EFFECTIVE STRAIN VS. TIME, ELEMENT #131, CONFIGURATION P.2

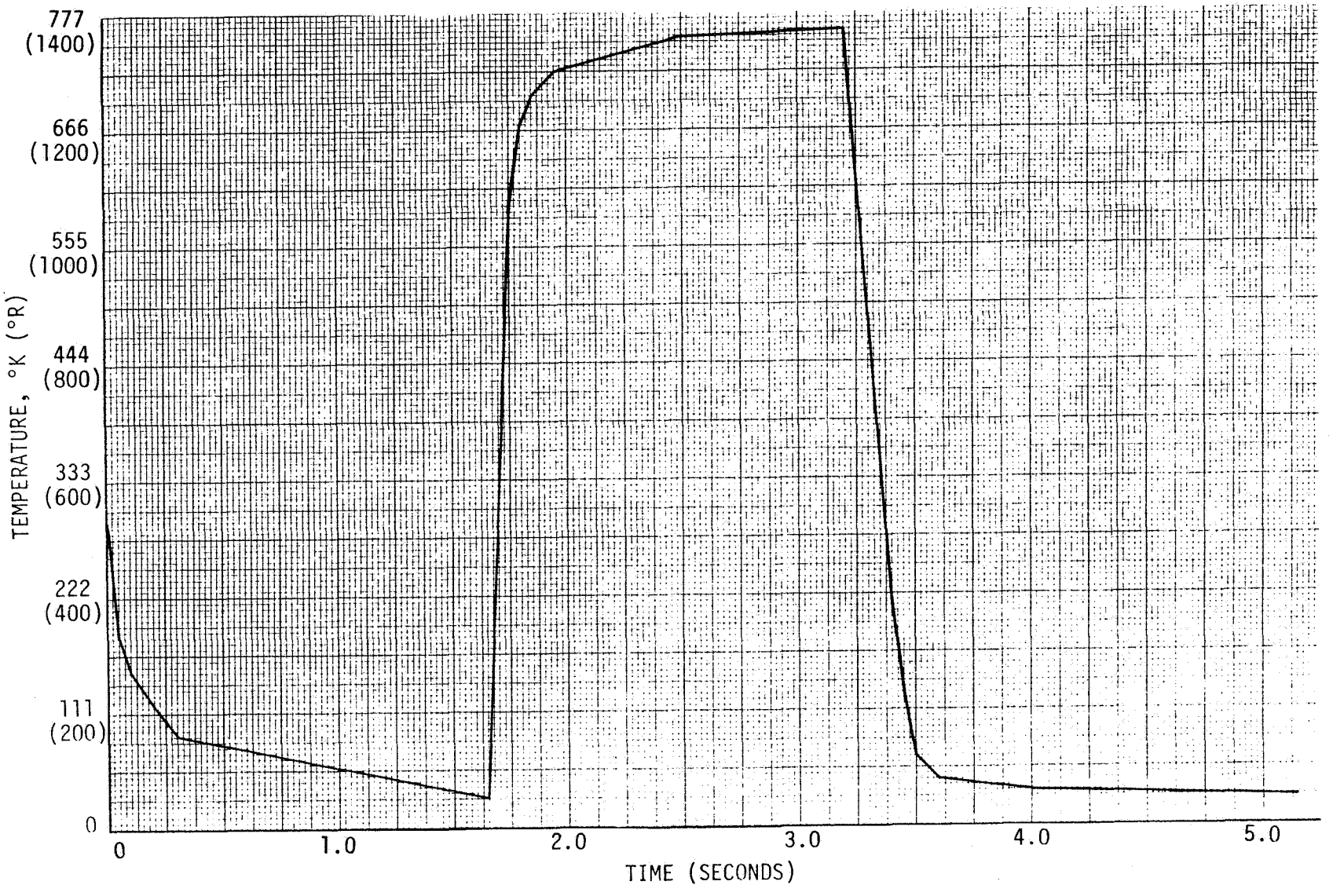

FIGURE 6.1-16 TEMPERATURE VS. TIME, ELEMENT #131, CONFIGURATION P.2

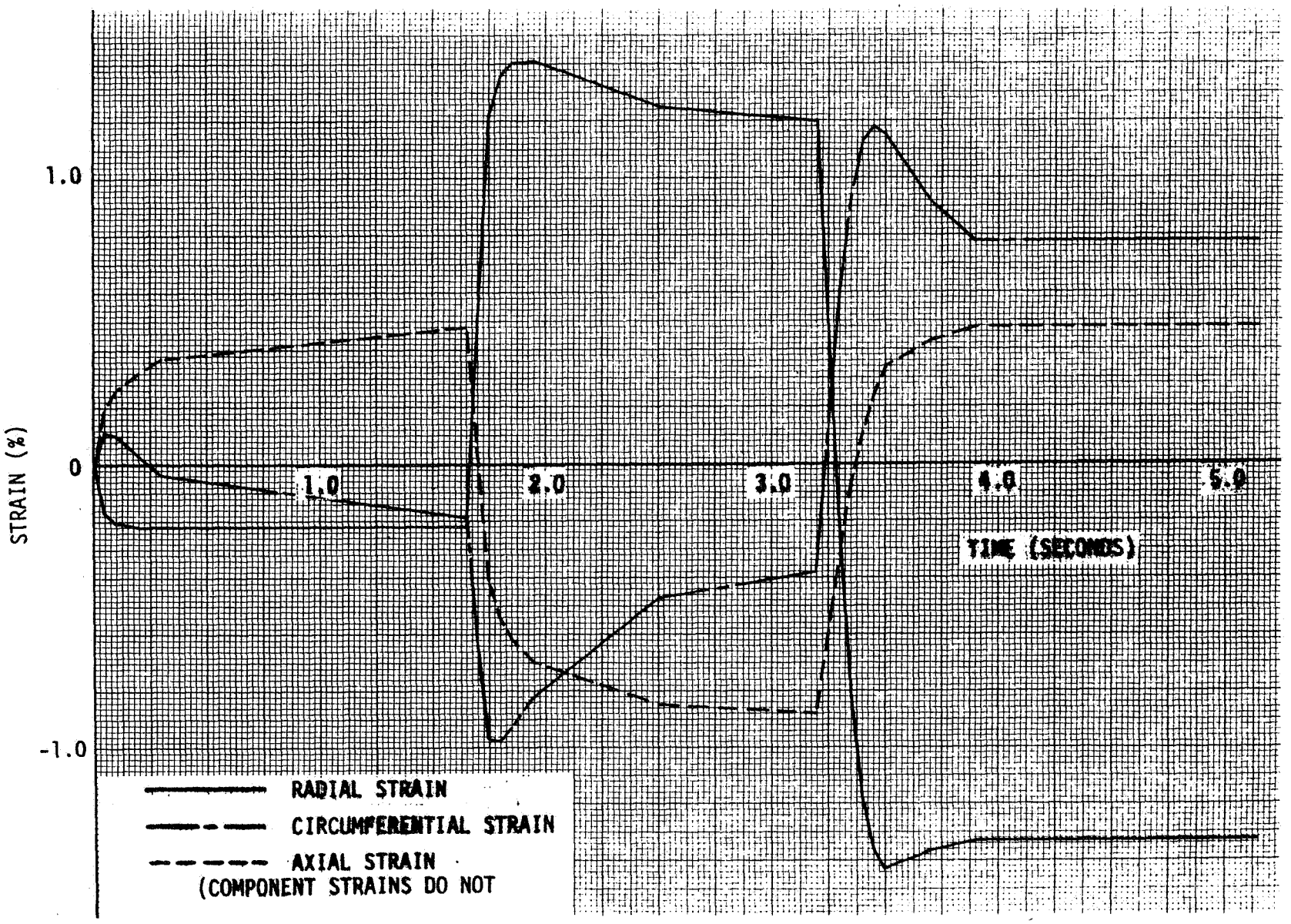

FIGURE 6.1-17 STRAIN VS. TIME, ELEMENT #133, CONFIGURATION P.3

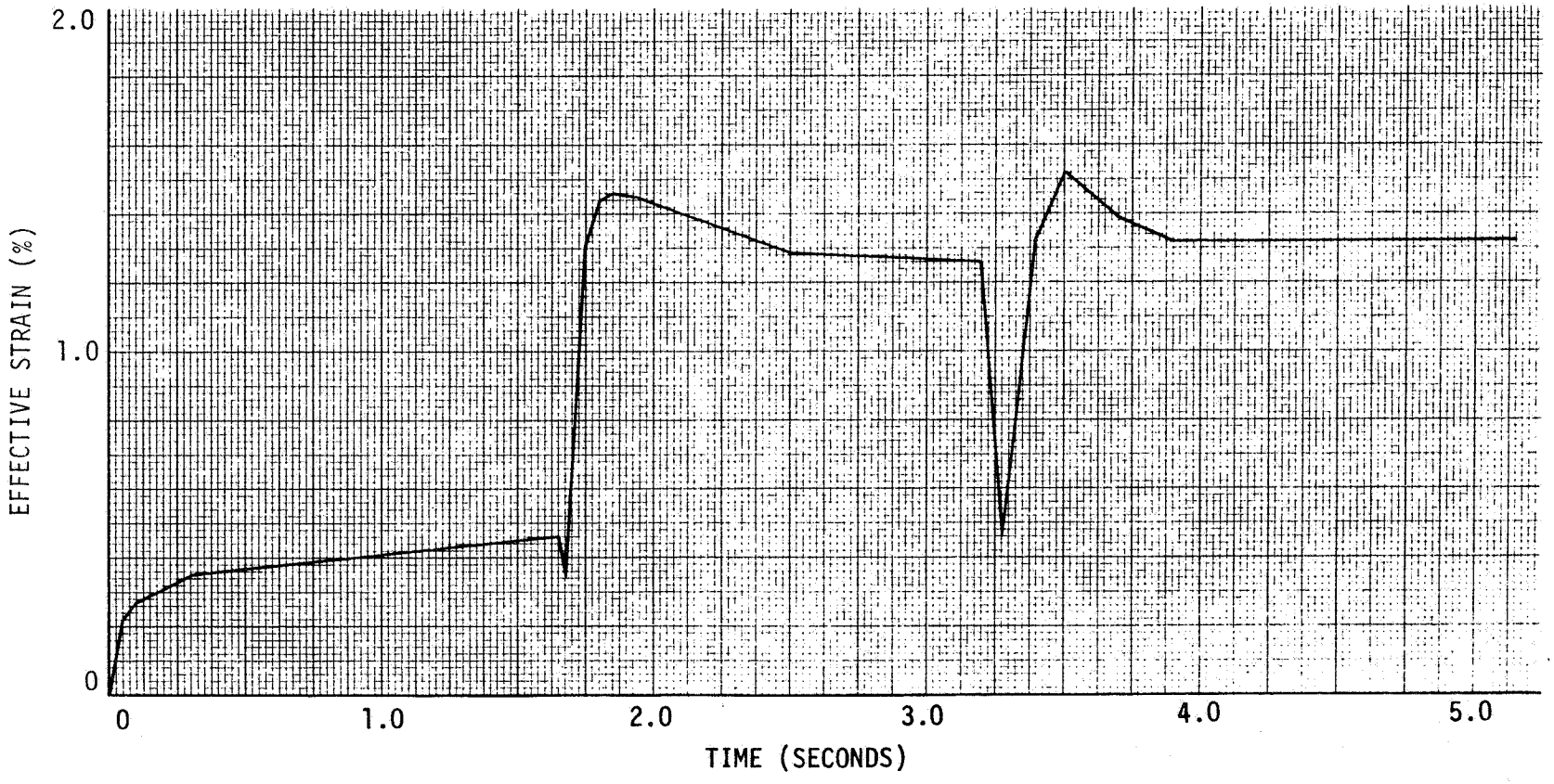

FIGURE 6.1-18 EFFECTIVE STRAIN VS. TIME, ELEMENT #133, CONFIGURATION P.3

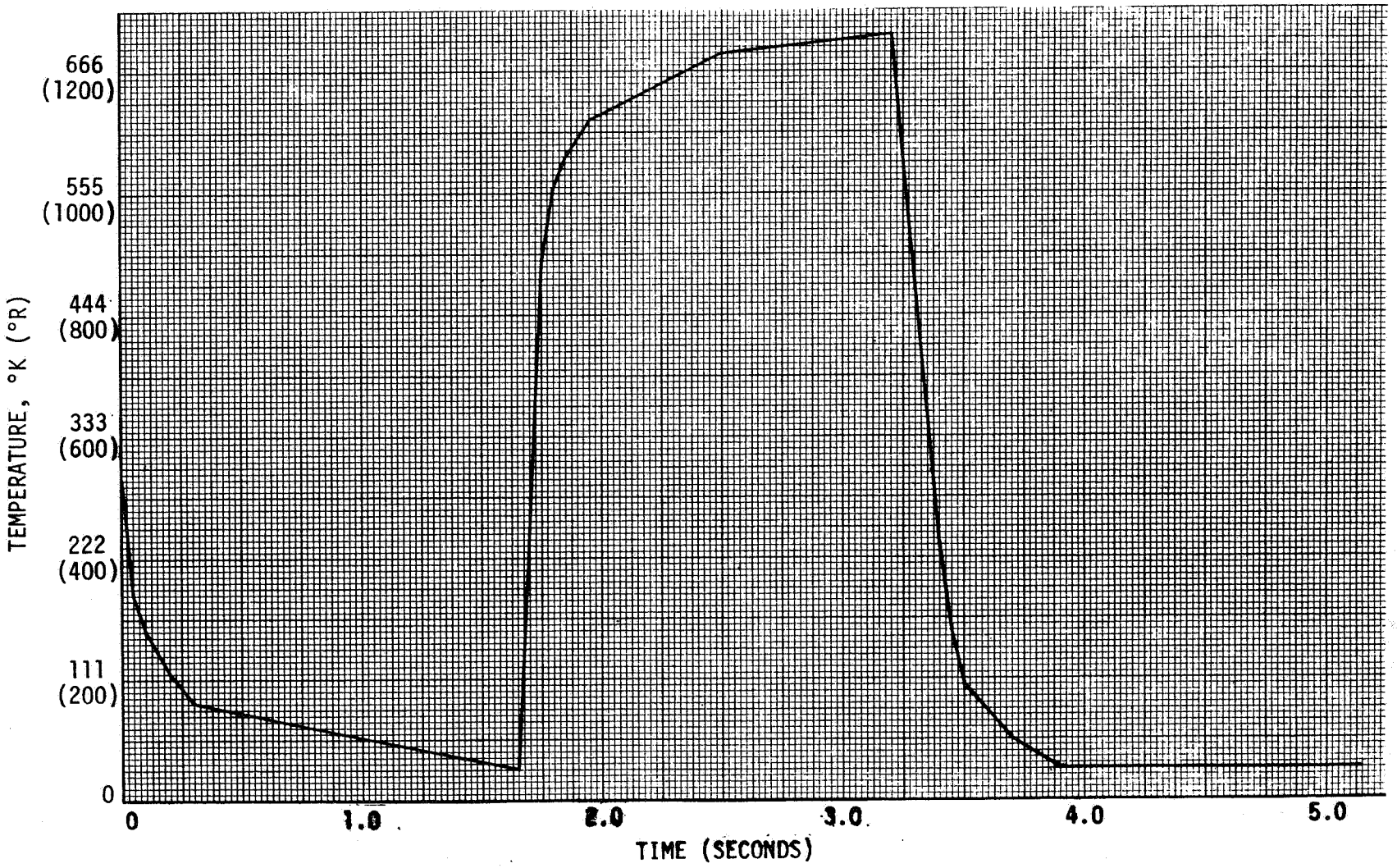

FIGURE 6.1-19 TEMPERATURE VS. TIME, ELEMENT #133, CONFIGURATION P.3

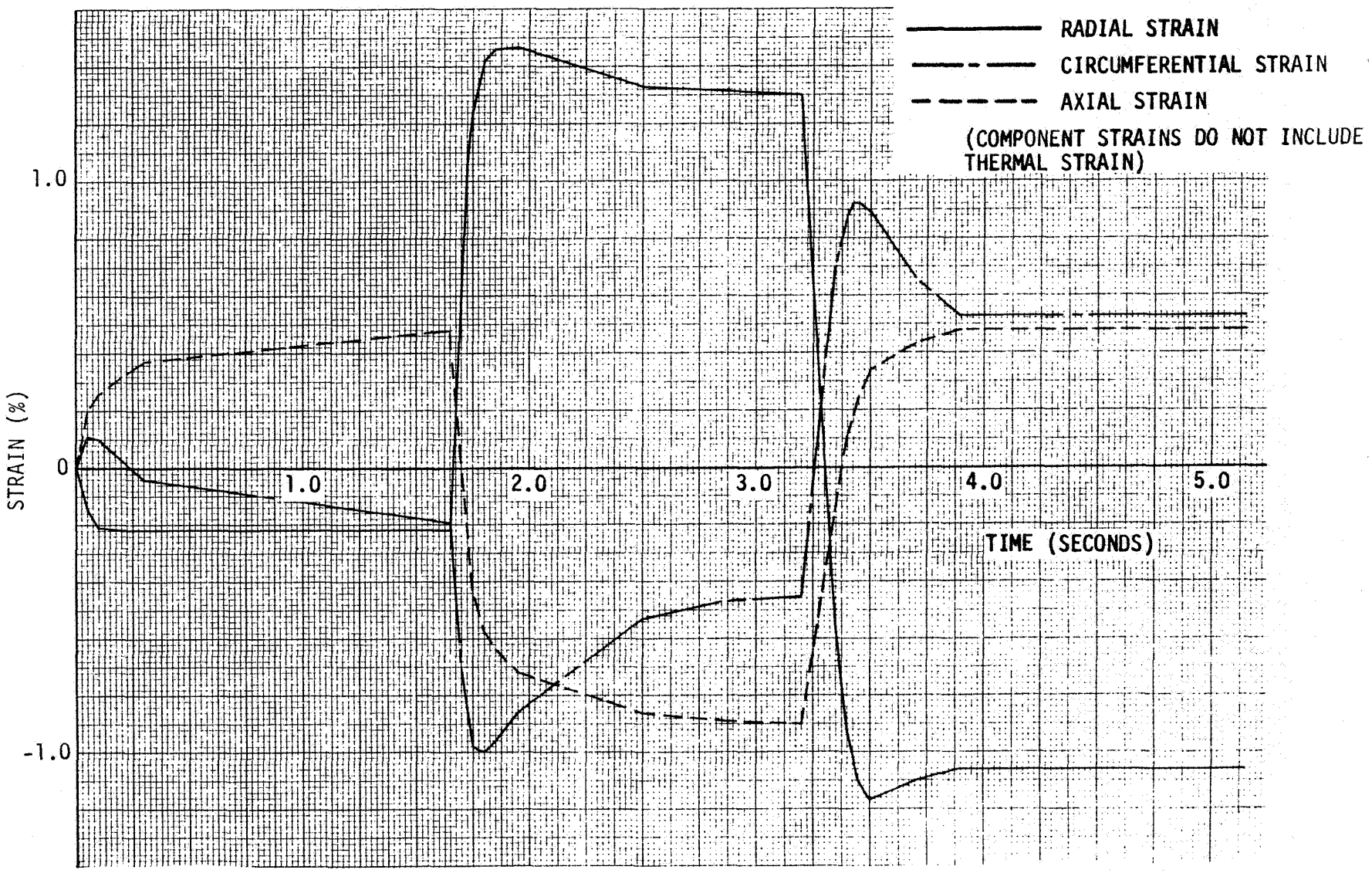

FIGURE 6.1-20 STRAIN VS. TIME, ELEMENT #131, CONFIGURATION P.3

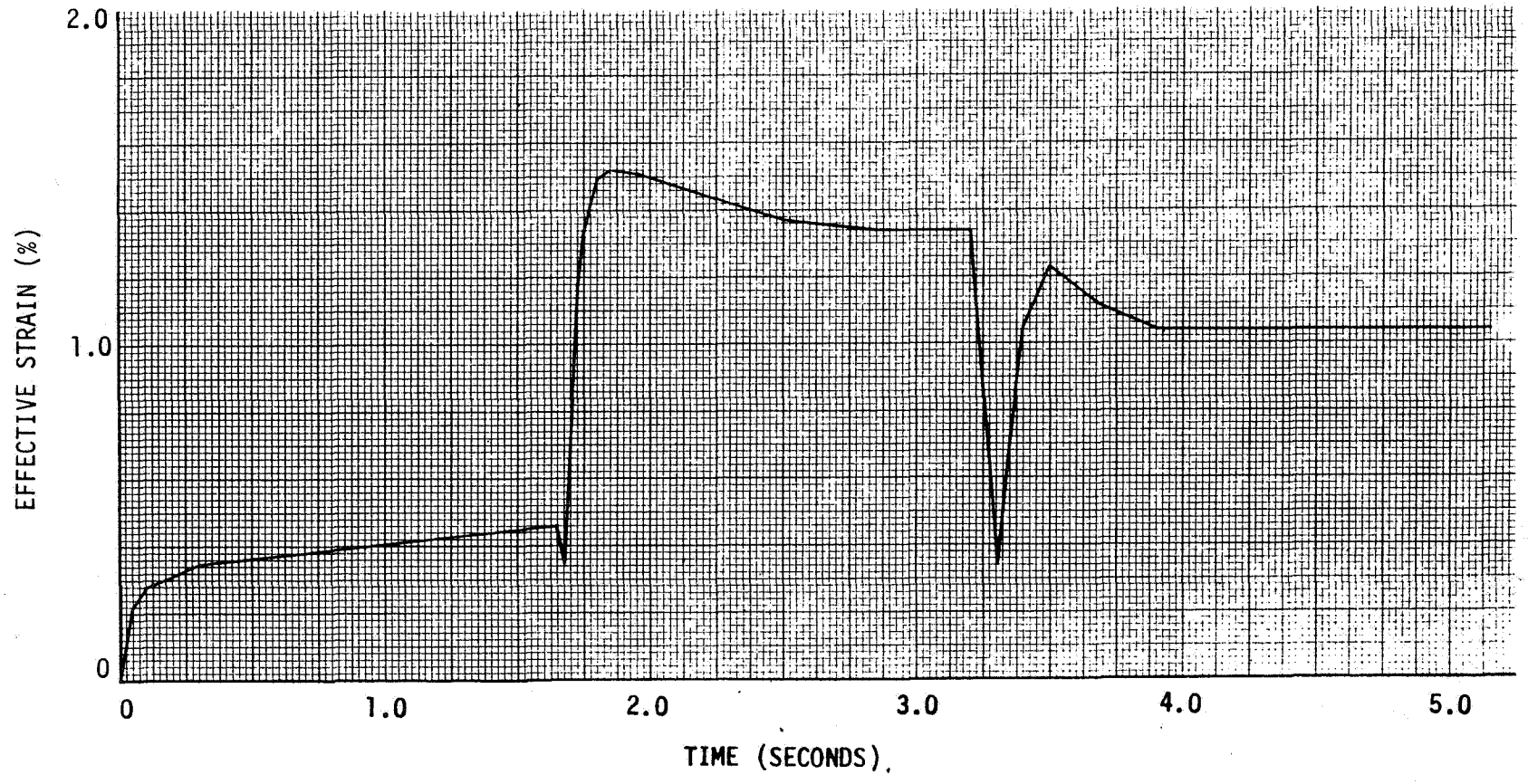

FIGURE 6.1-21 EFFECTIVE STRAIN VS. TIME, ELEMENT #131, CONFIGURATION P.3

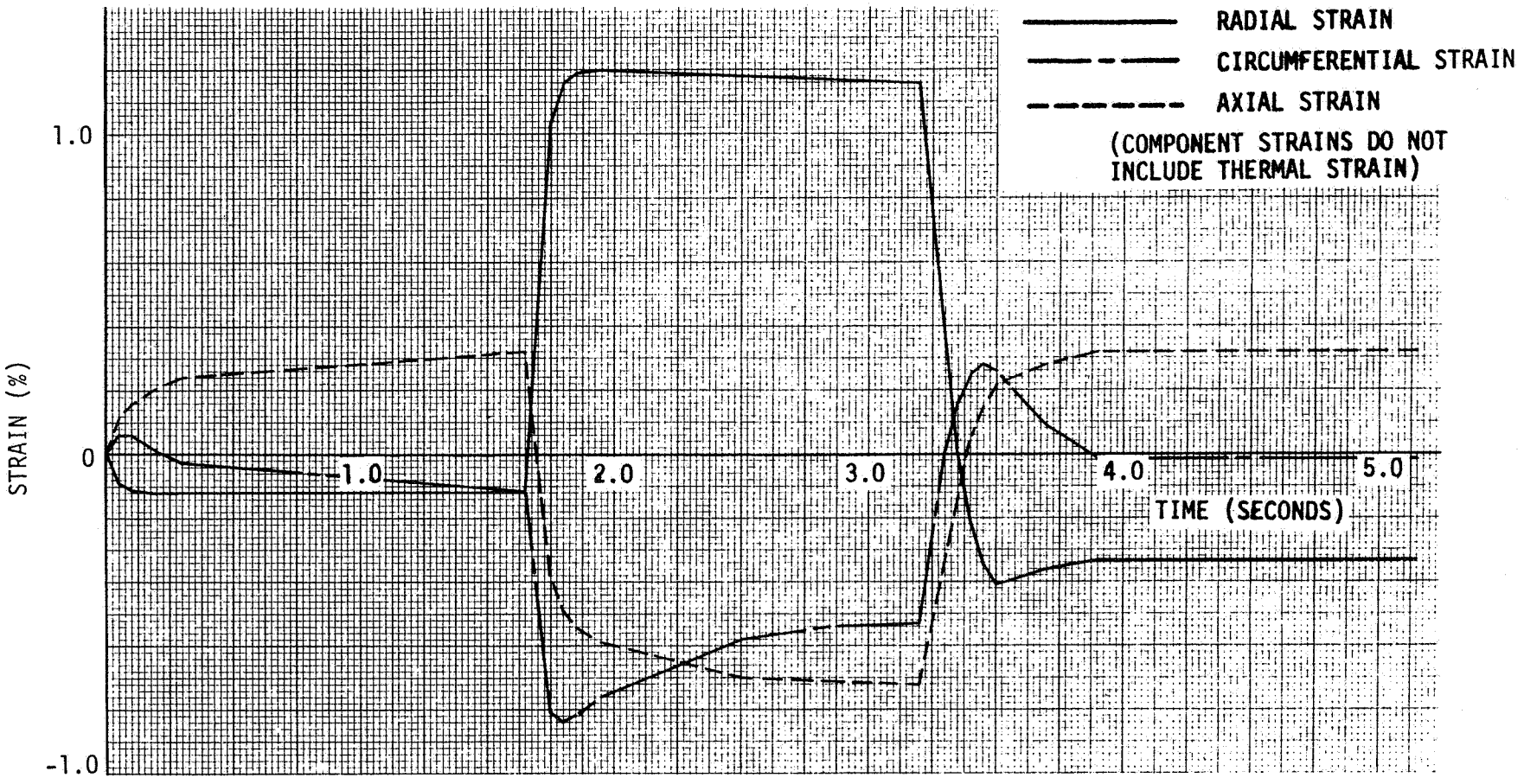

FIGURE 6.1-22 STRAIN VS. TIME, ELEMENT #10, CONFIGUPATION P.4

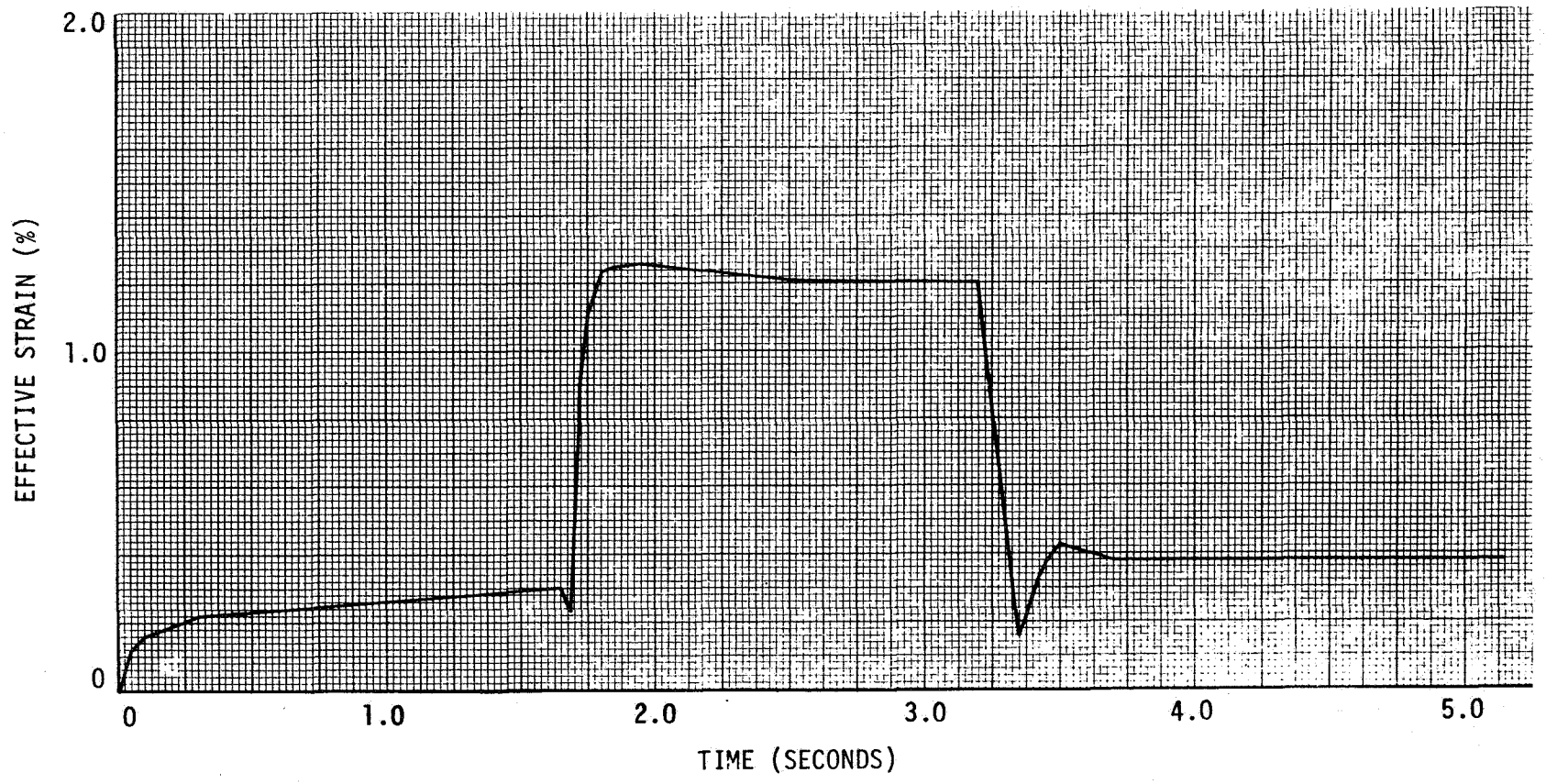

FIGURE 6.1-23 EFFECTIVE STRAIN VS. TIME, ELEMENT #10, CONFIGURATION P.4

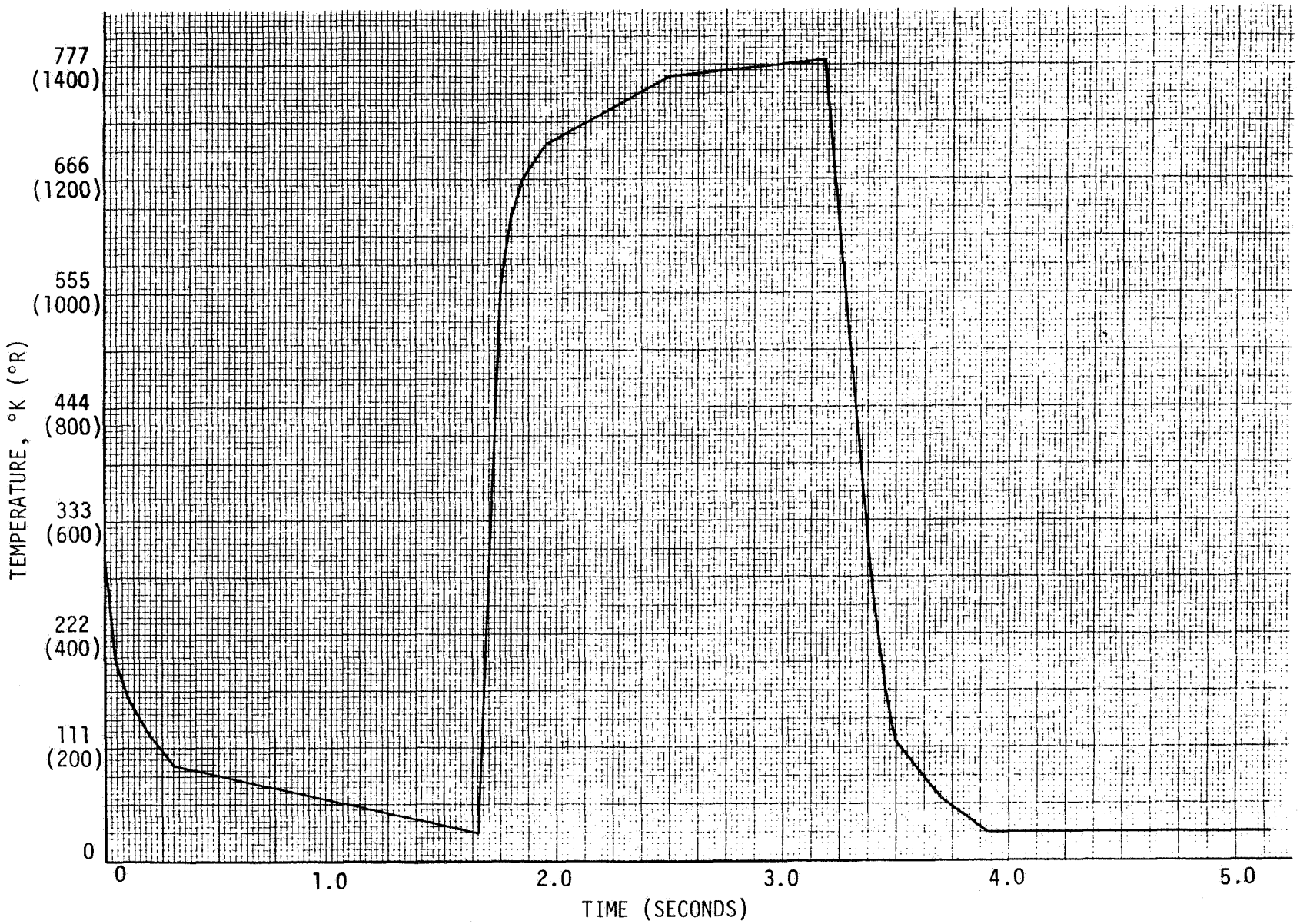

FIGURE 6.1-24 TEMPERATURE VS. TIME, ELEMENT #10, CONFIGURATION P.4

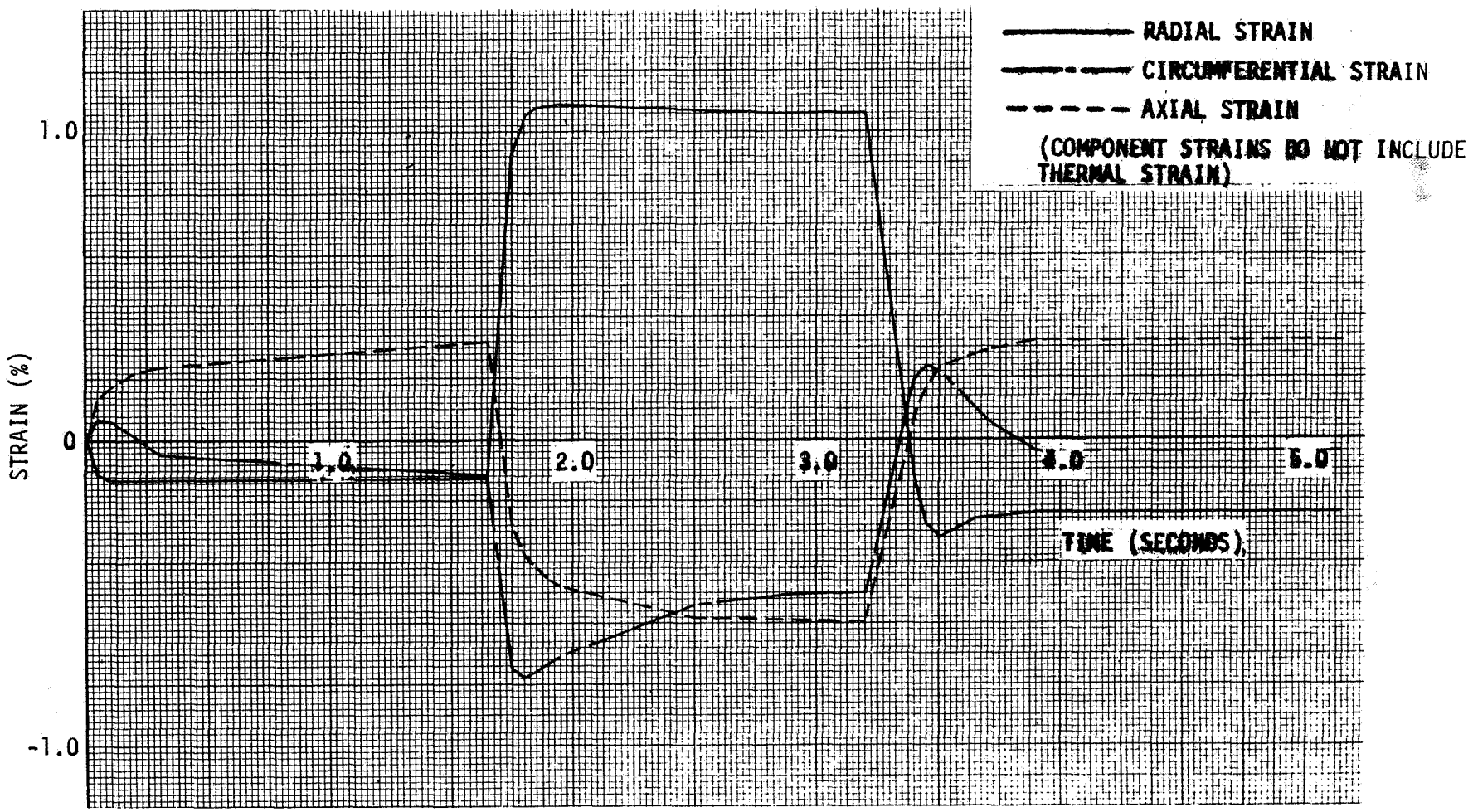

FIGURE 6.1-25 STRAIN VS. TIME, ELEMENT #131, CONFIGURATION P.4

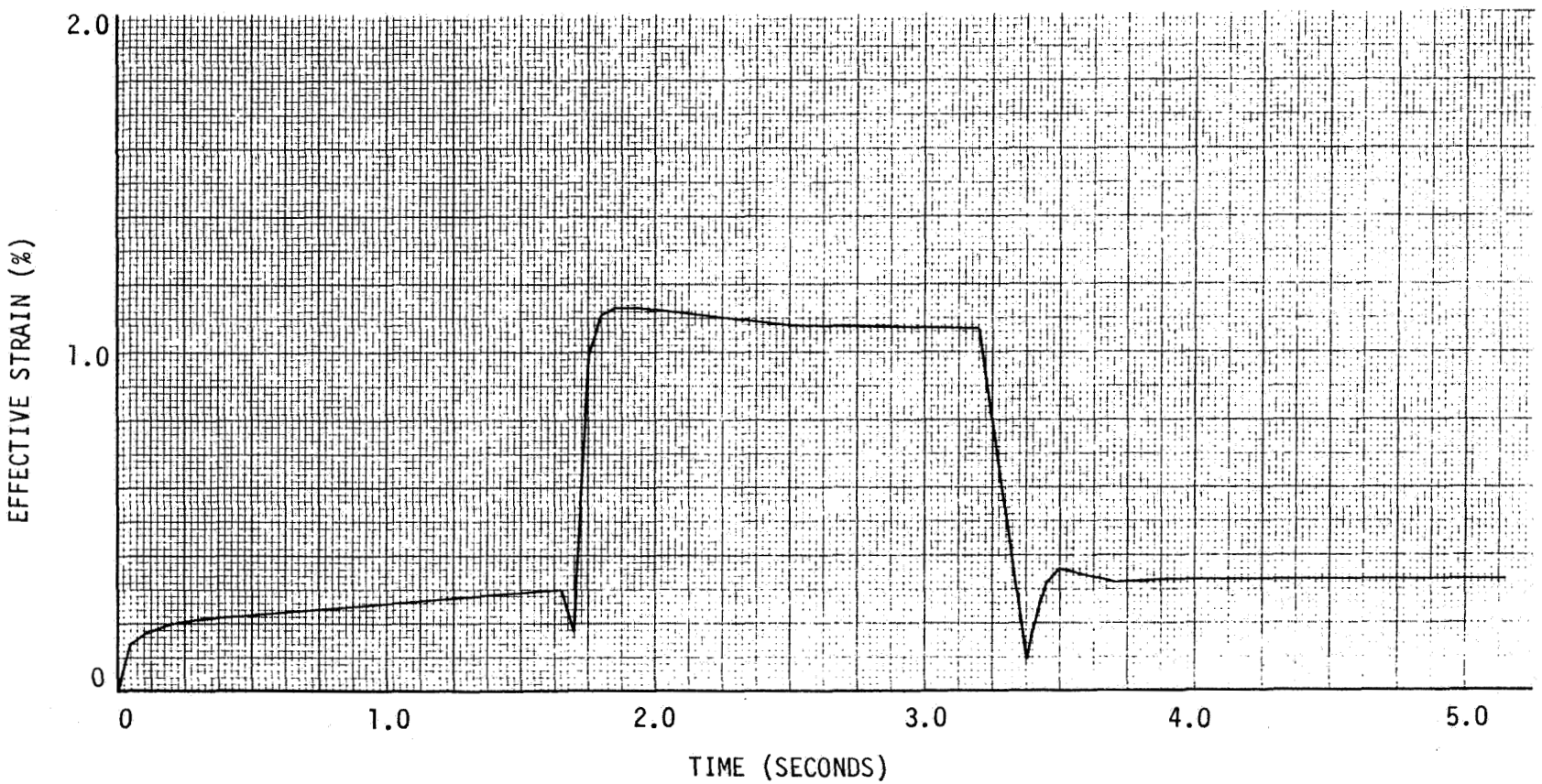

FIGURE 6.1-26 EFFECTIVE STRAIN VS. TIME, ELEMENT #131, CONFIGURATION P.4

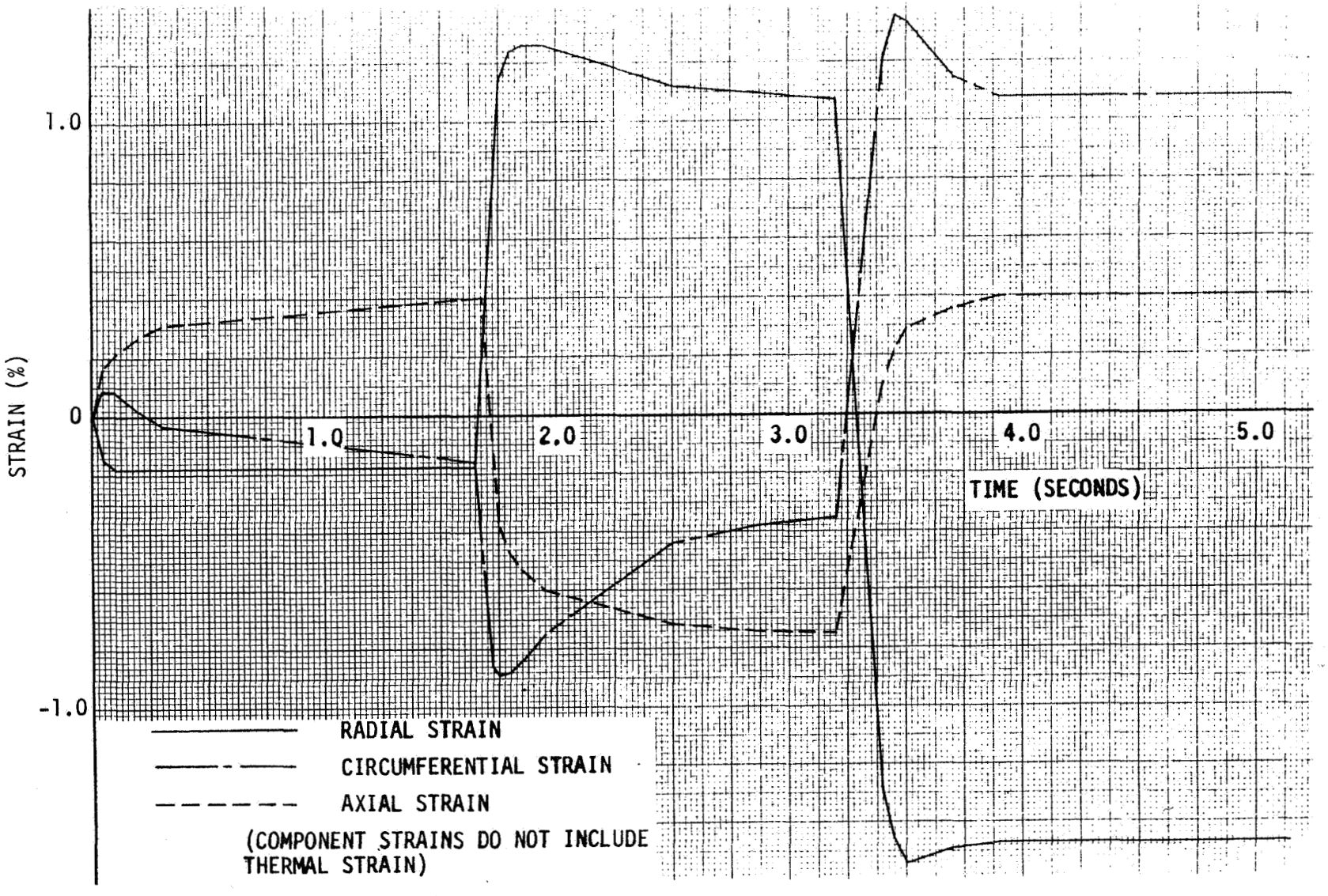

FIGURE 6.1-27 STRAIN VS. TIME, ELEMENT #131, CONFIGURATION P.5

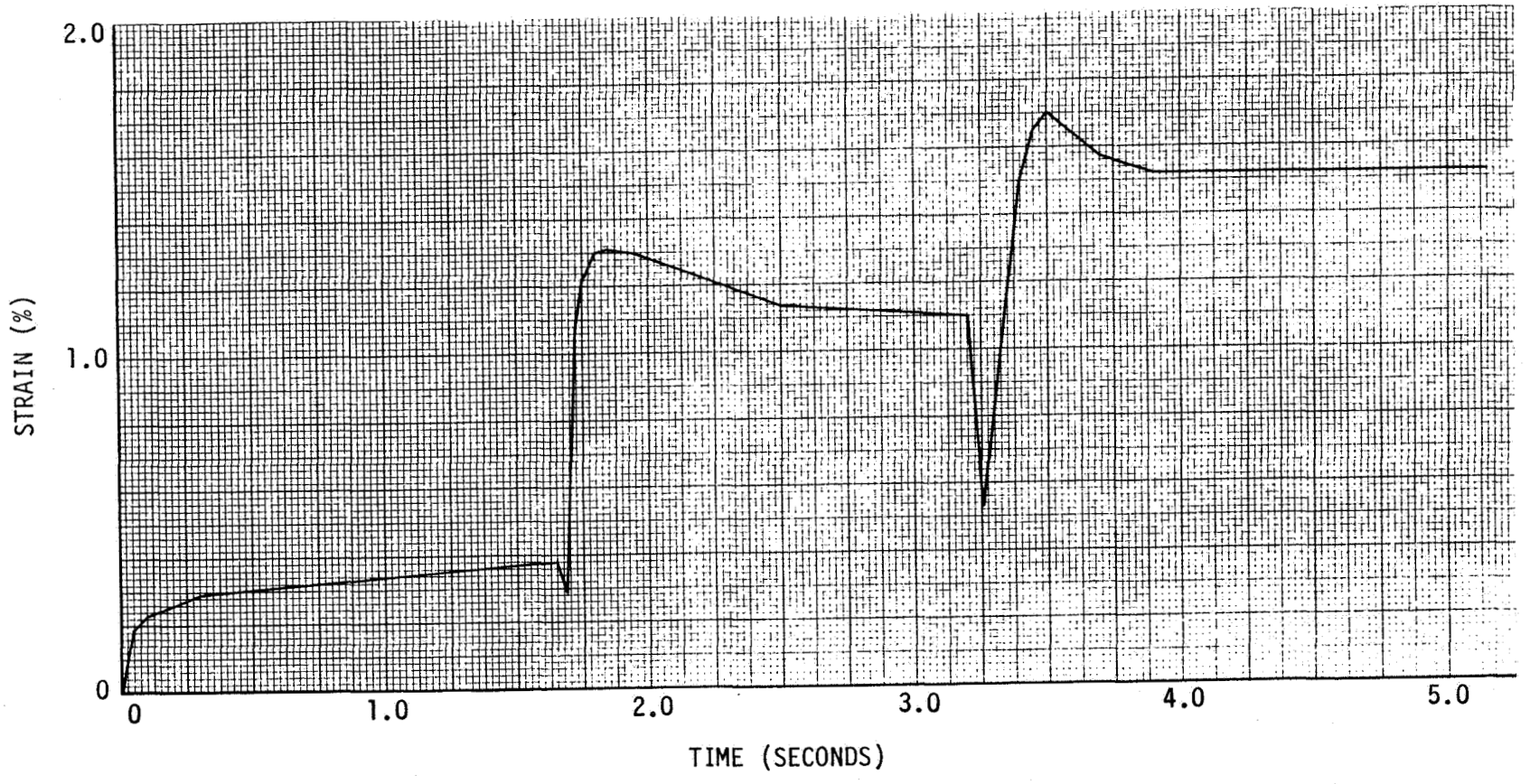

FIGURE 6.1-28 EFFECTIVE STRAIN VS. TIME, ELEMENT #131, CONFIGURATION P.5

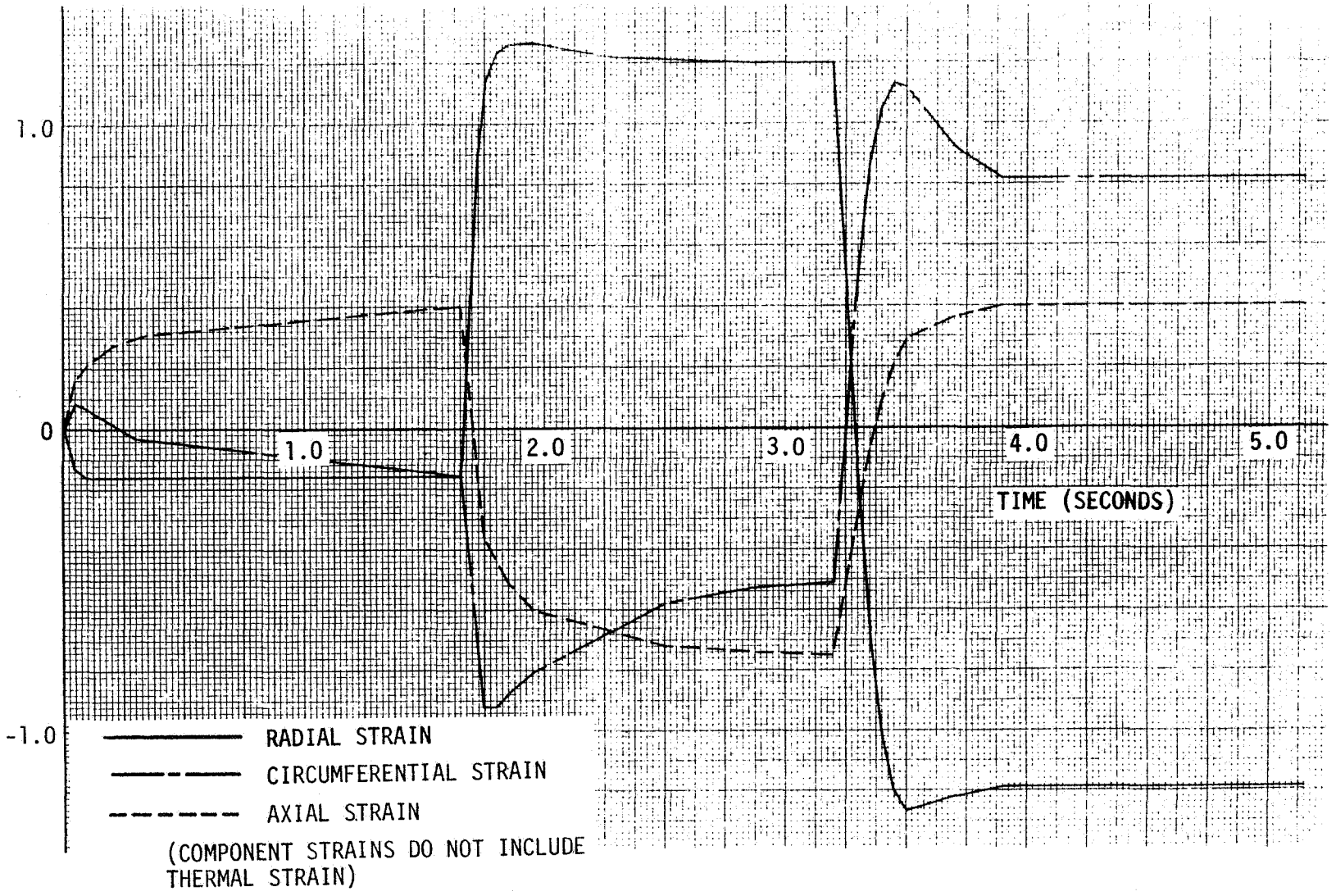

FIGURE 6.1-29 STRAIN VS. TIME, ELEMENT #131, CONFIGURATION P.6

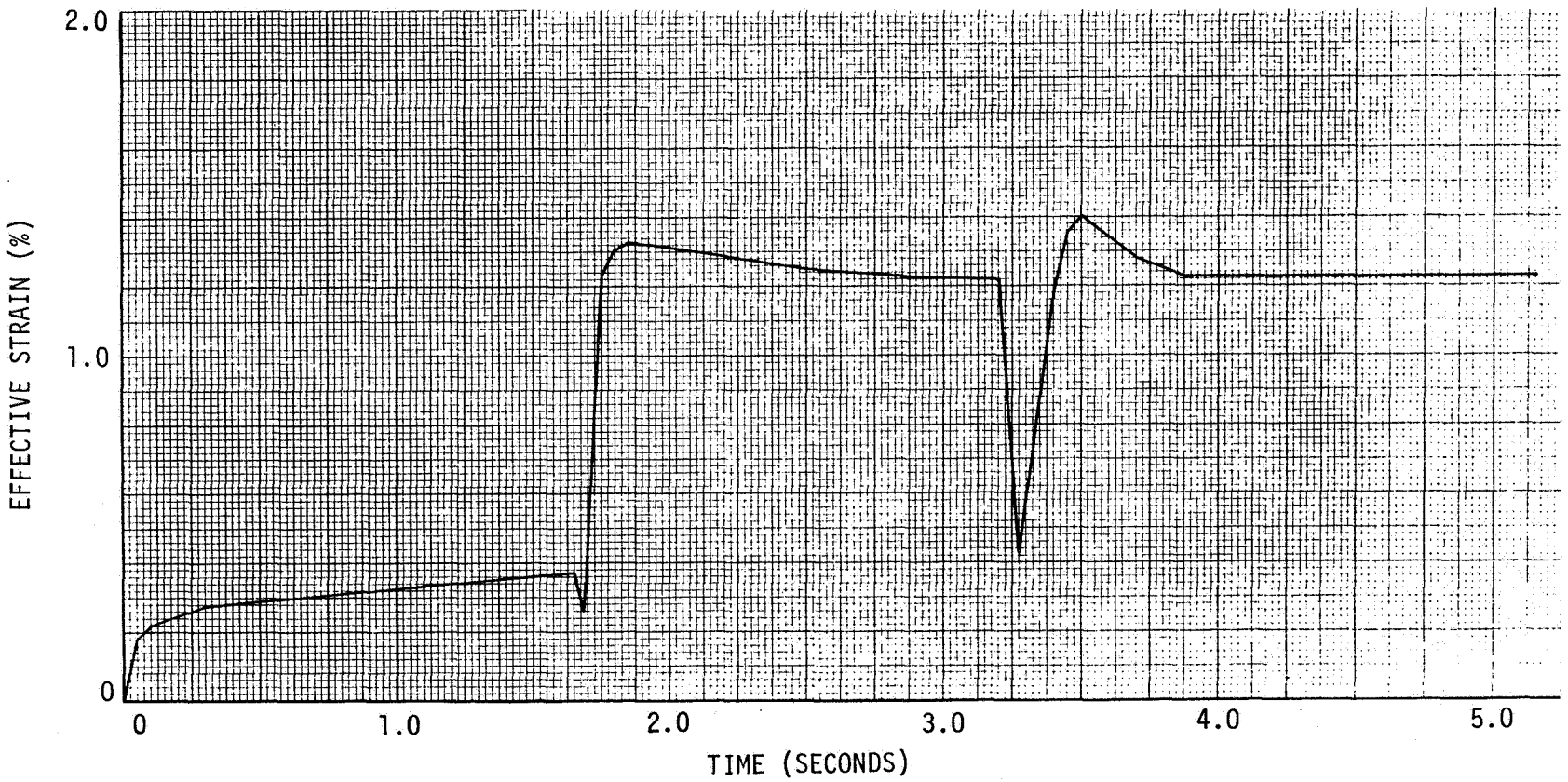

FIGURE 6.1-30 EFFECTIVE STRAIN VS. TIME, ELEMENT #131, CONFIGURATION P.6

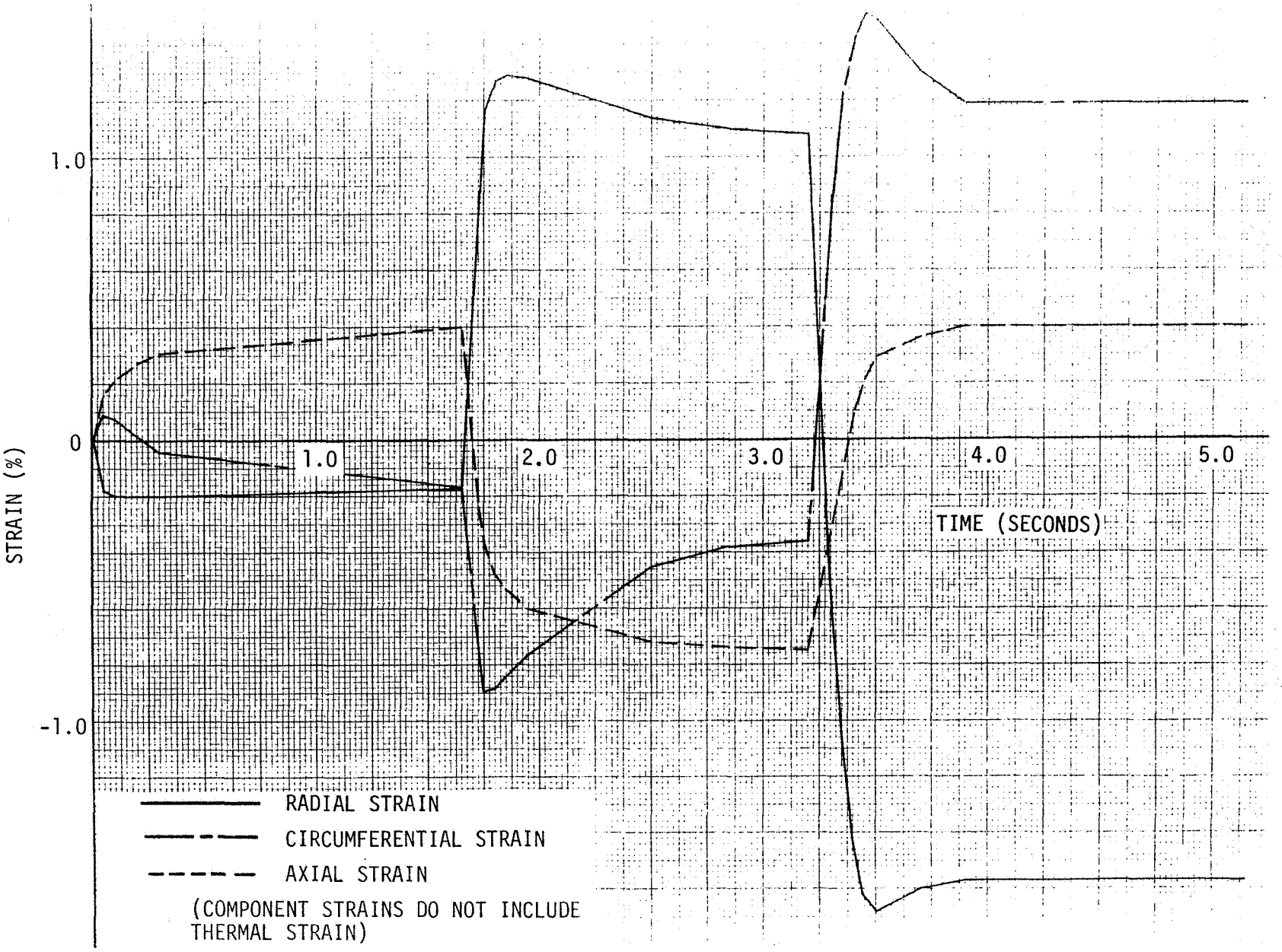

FIGURE 6.1.31 STRAIN VS. TIME, ELEMENT #131, CONFIGURATION P.7

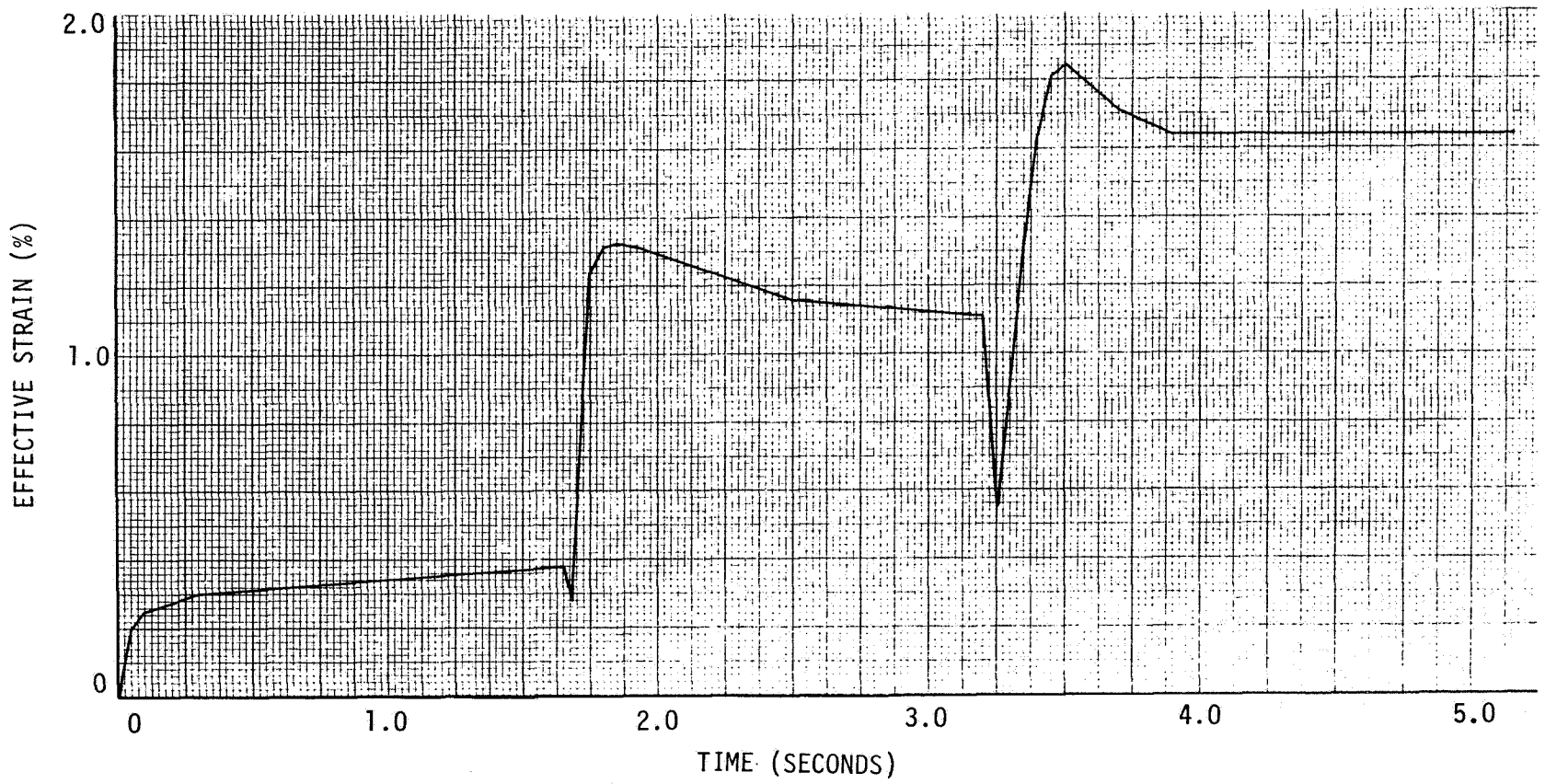

FIGURE 6.1-32 EFFECTIVE STRAIN VS. TIME, ELEMENT #131, CONFIGURATION P.7

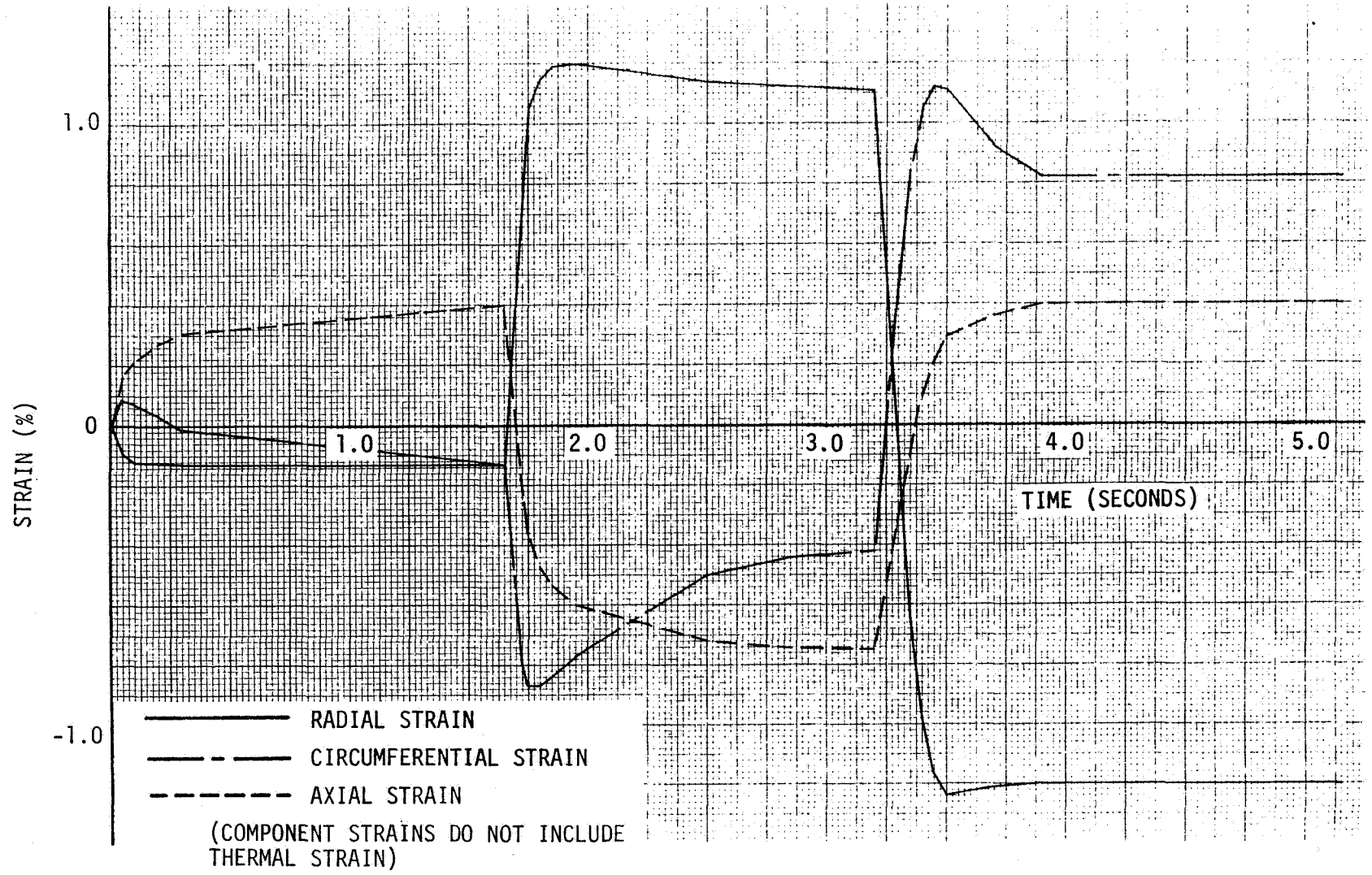

FIGURE 6.1-33 STRAIN VS. TIME, ELEMENT #131, CONFIGURATION P.8

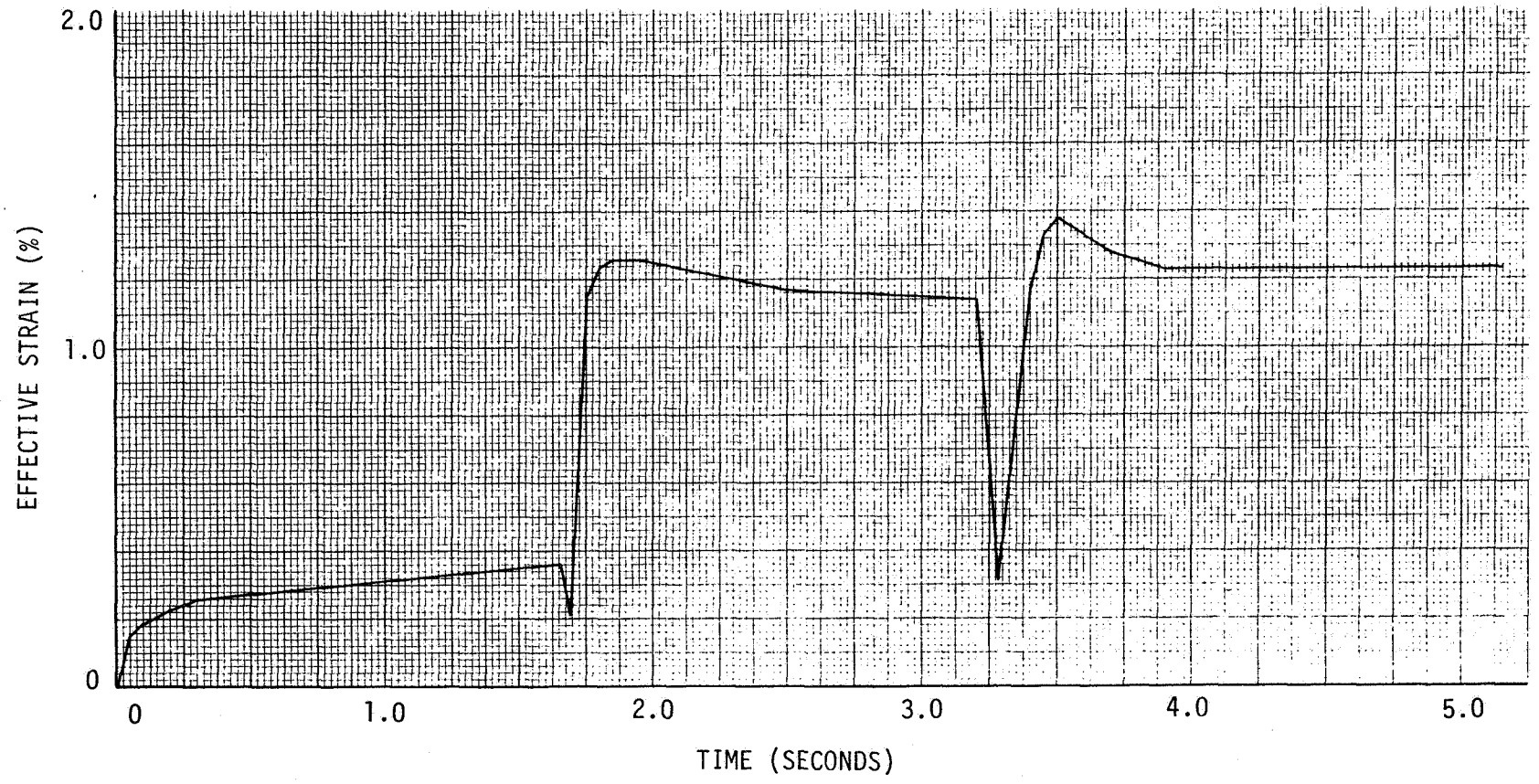

FIGURE 6.1-34 EFFECTIVE STRAIN VS. TIME, ELEMENT #131, CONFIGURATION P.8

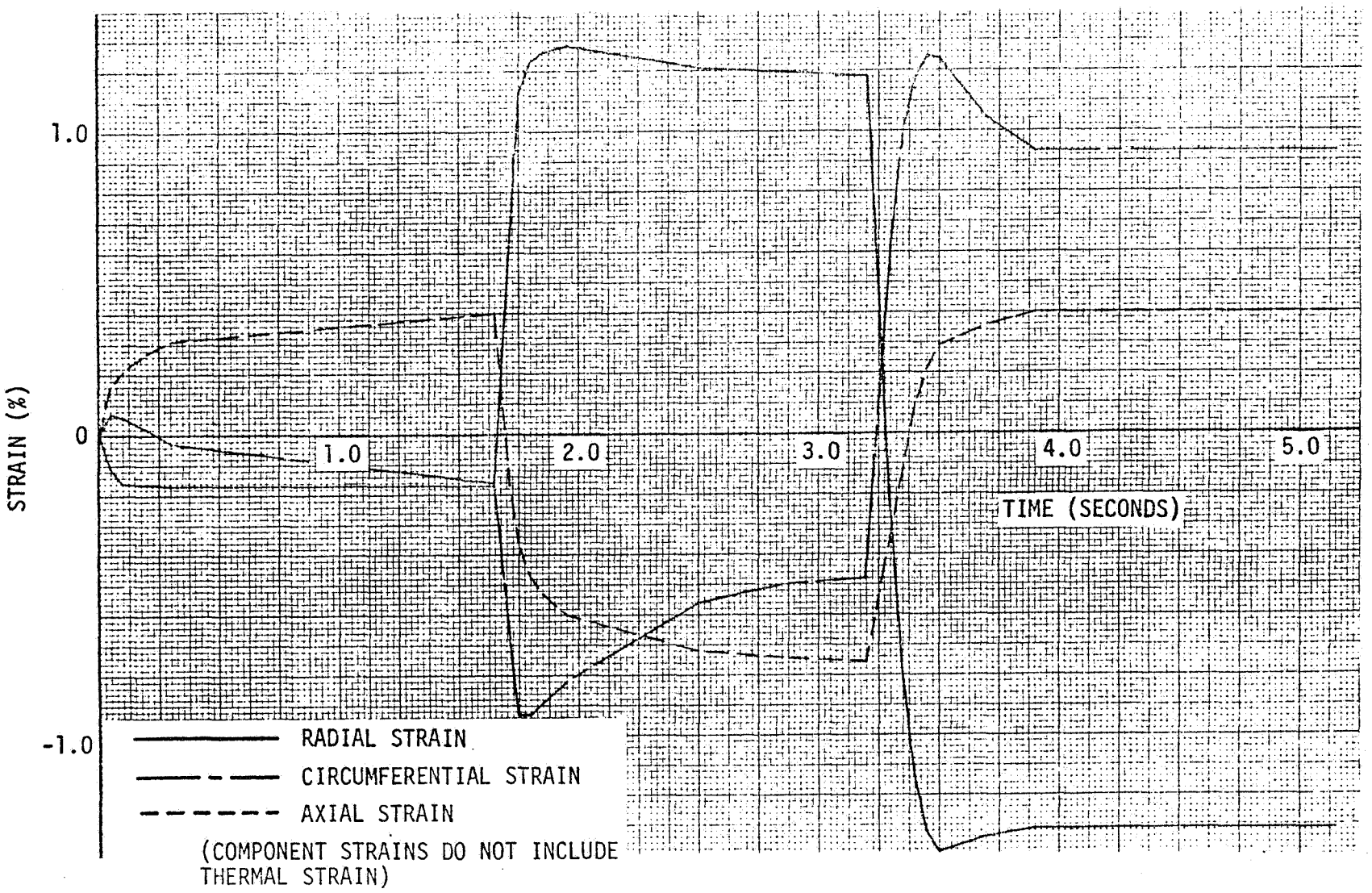

FIGURE 6.1-35 STRAIN VS. TIME, ELEMENT #131, CONFIGURATION P.9

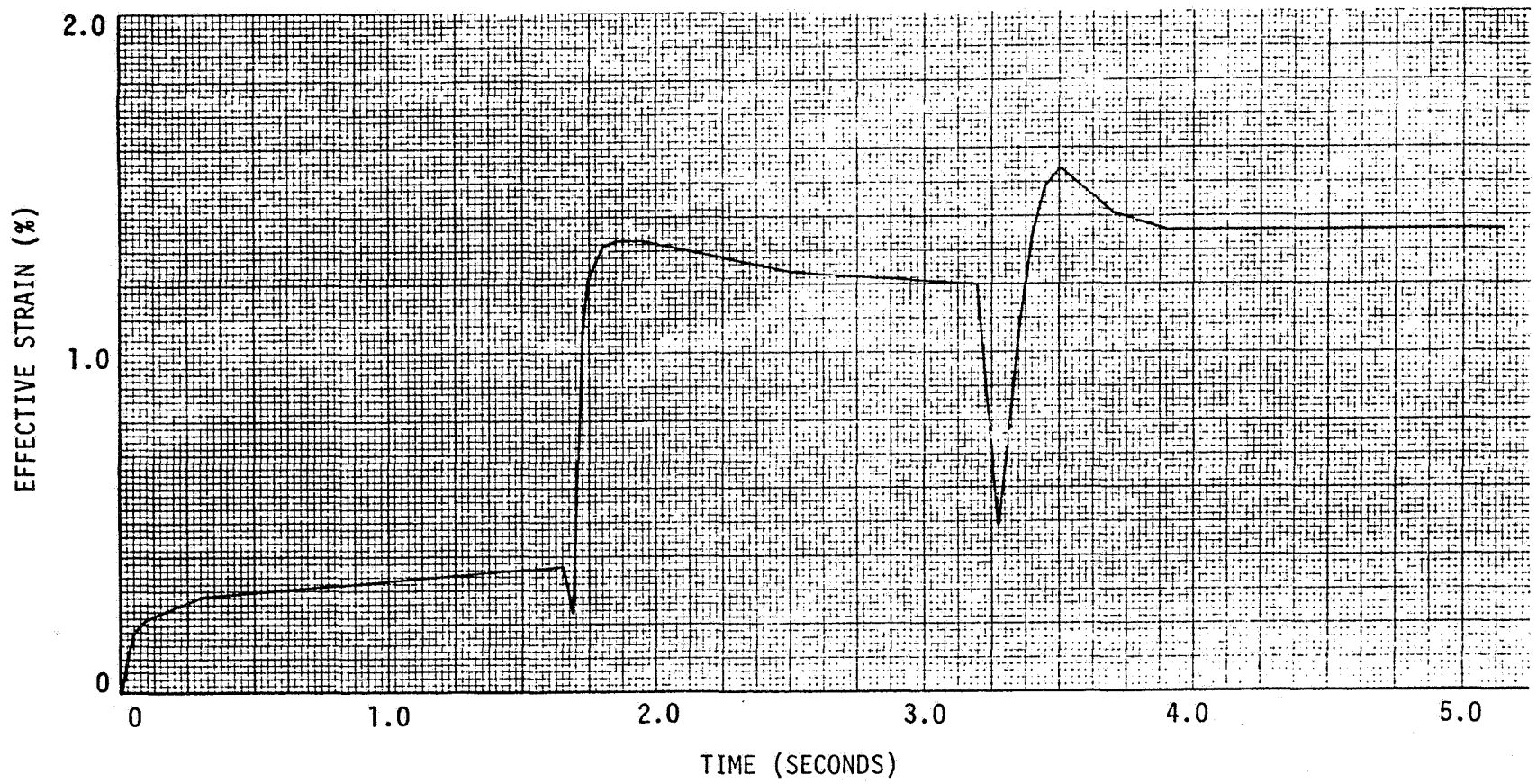

FIGURE 6.1-36 EFFECTIVE STRAIN VS. TIME, ELEMENT #131, CONFIGURATION P.9

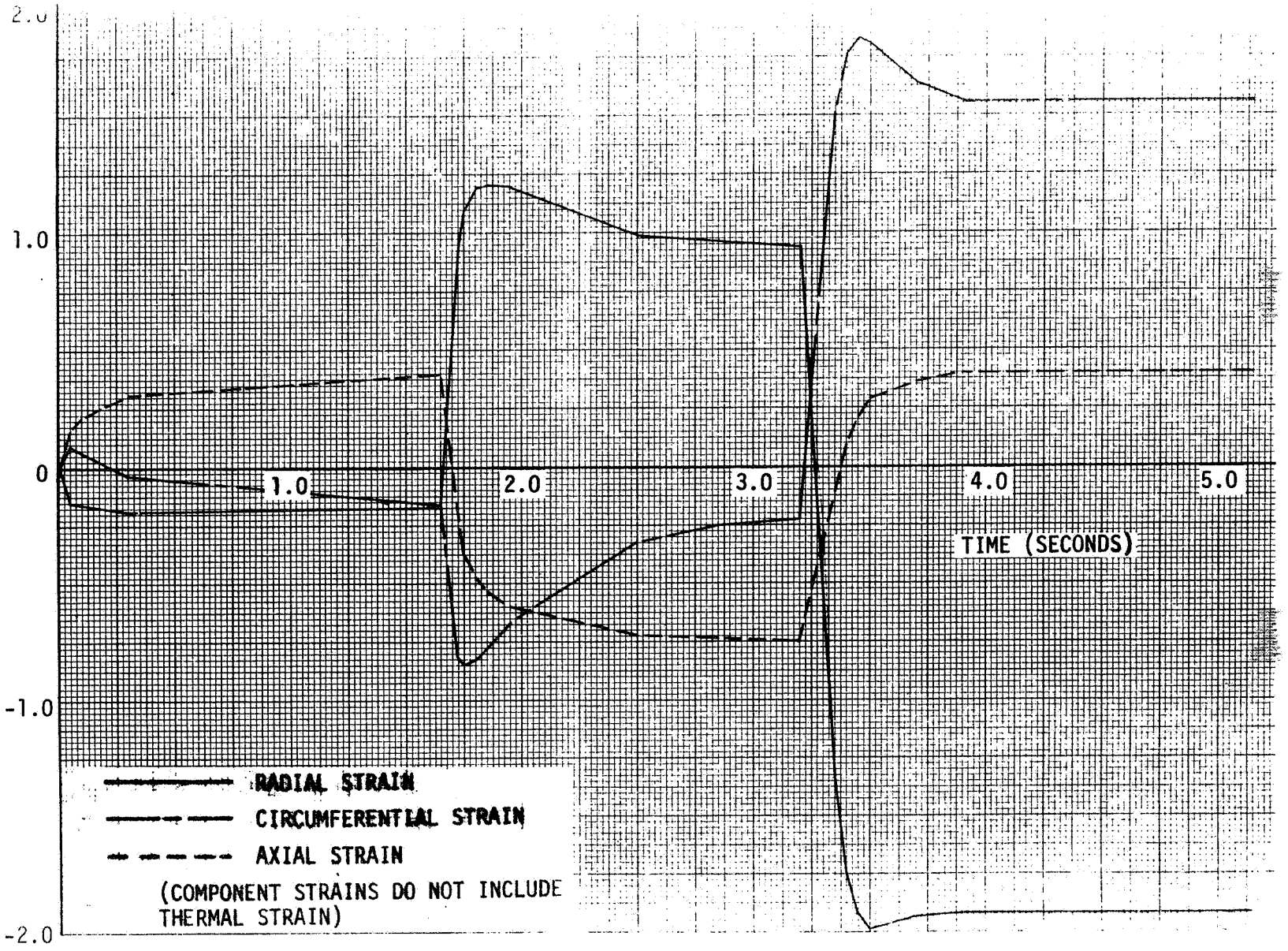

FIGURE 6.1-37 STRAIN VS. TIME, ELEMENT #131, CONFIGURATION P.10

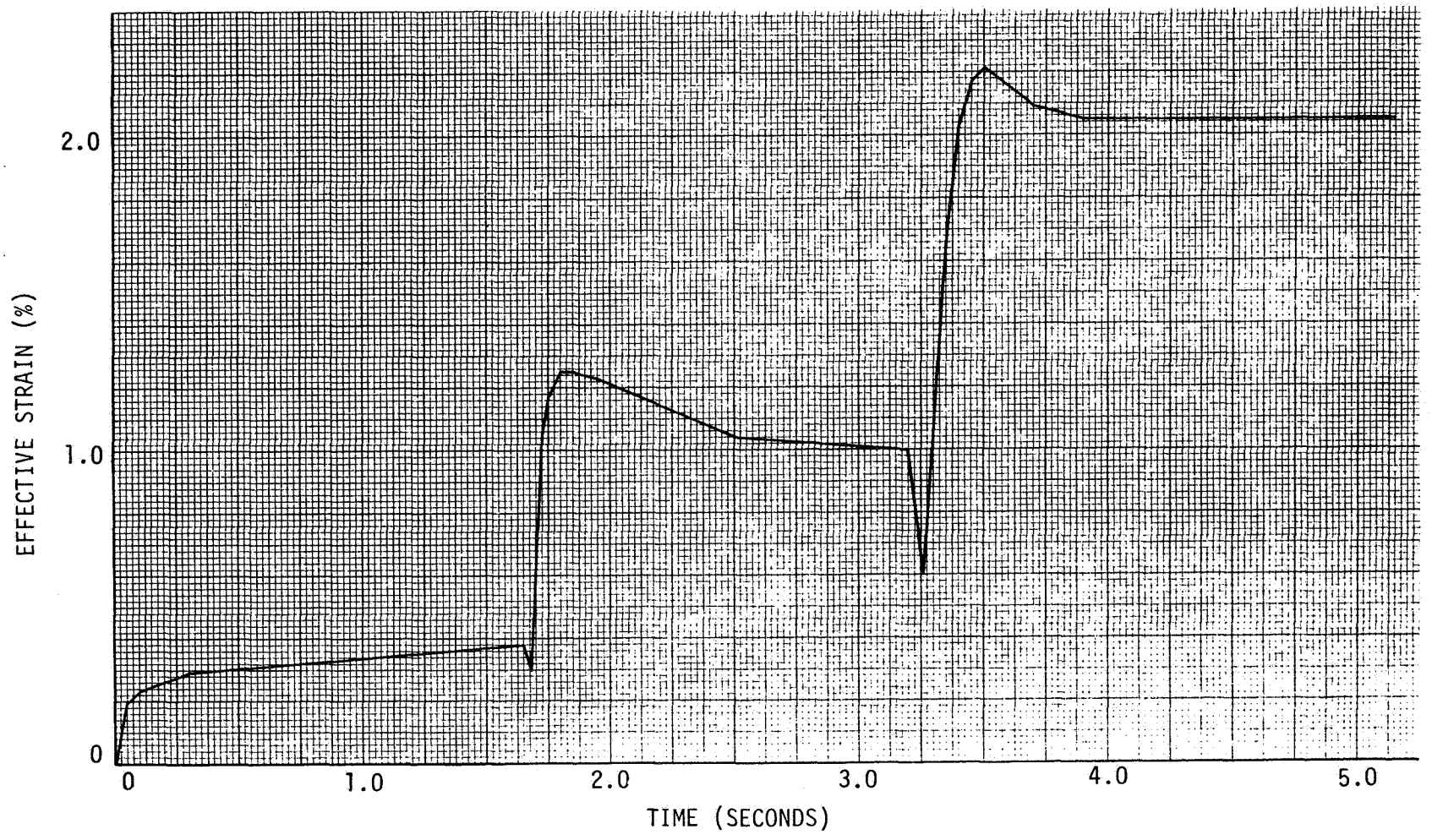

FIGURE 6.1-38 EFFECTIVE STRAIN VS. TIME, ELEMENT #131, CONFIGURATION P.10

TABLE 6.1-I SUMMARY OF PARAMETRIC EFFECTS ON MAXIMUM EFFECTIVE STRAIN RANGE

CONFIGURATION	PERCENT CHANGE IN PARAMETER	PERCENT CHANGE IN MAXIMUM EFFECTIVE STRAIN RANGE
P.1	+22	-26
P.2	-52	- 8
P.3	+20	-14
P.4	-20	-51
P.5	+20	-14
P.6	-20	-24
P.7	+19	-10
P.8	-26	-23
P.9	+25	-17
P.10	-25	- 2

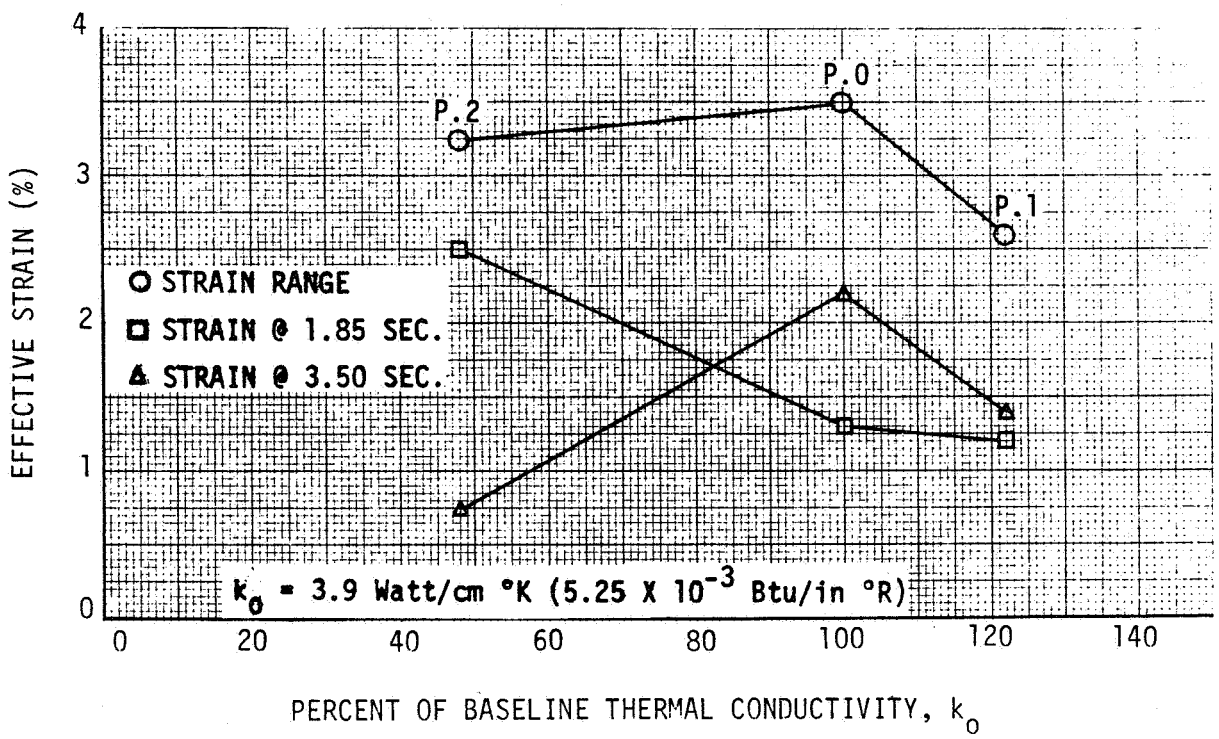

FIGURE 6.1-39 VARIATION OF MAXIMUM EFFECTIVE STRAIN WITH THERMAL CONDUCTIVITY

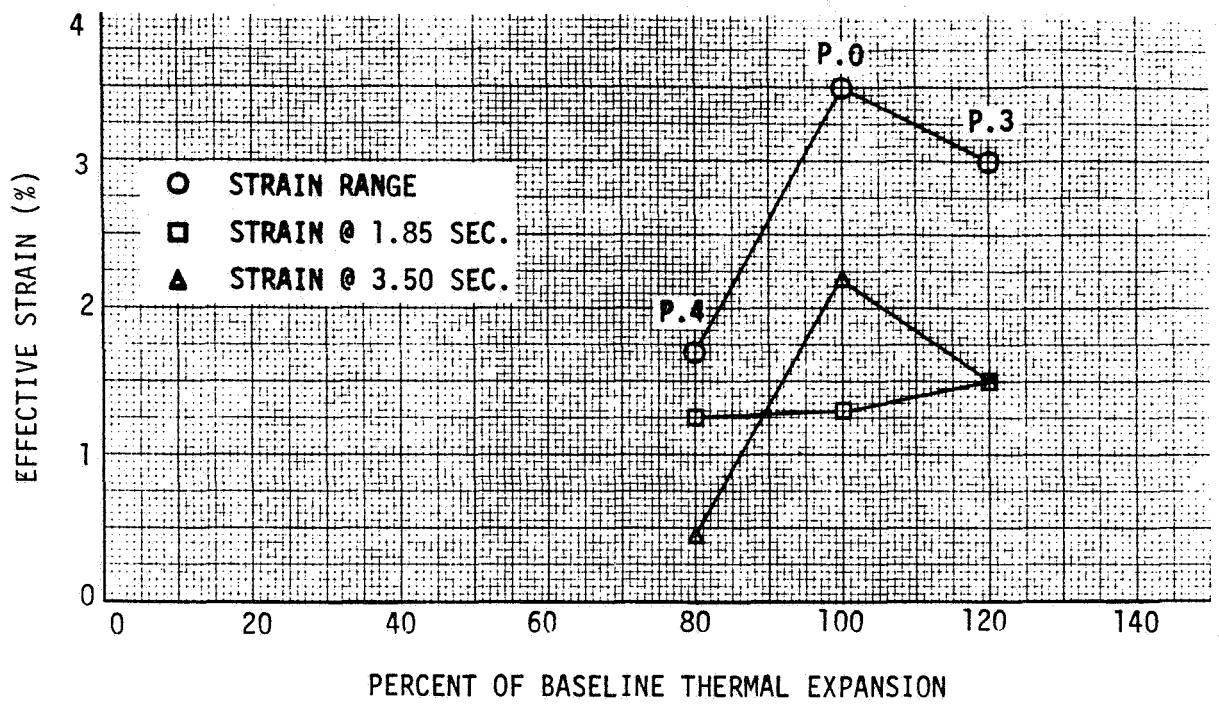

FIGURE 6.1-40 VARIATION OF MAXIMUM EFFECTIVE STRAIN WITH COEFFICIENT OF THERMAL EXPANSION

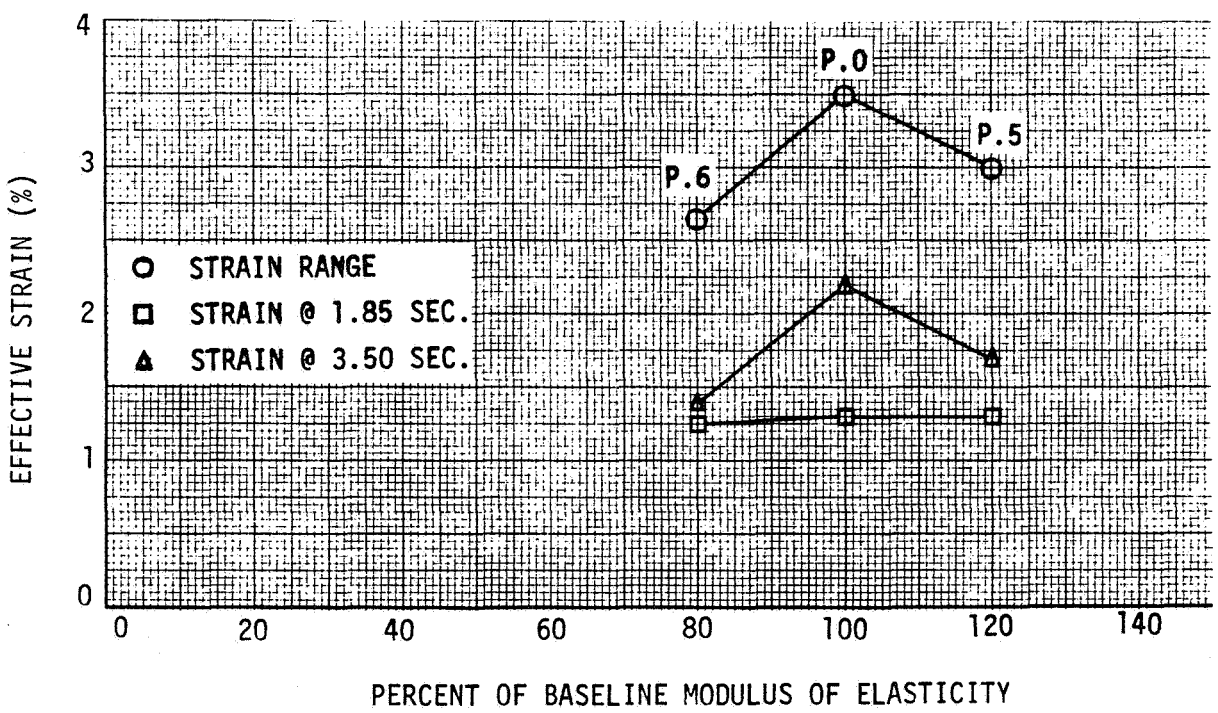

FIGURE 6.1-41 VARIATION OF MAXIMUM EFFECTIVE STRAIN WITH MODULUS OF ELASTICITY

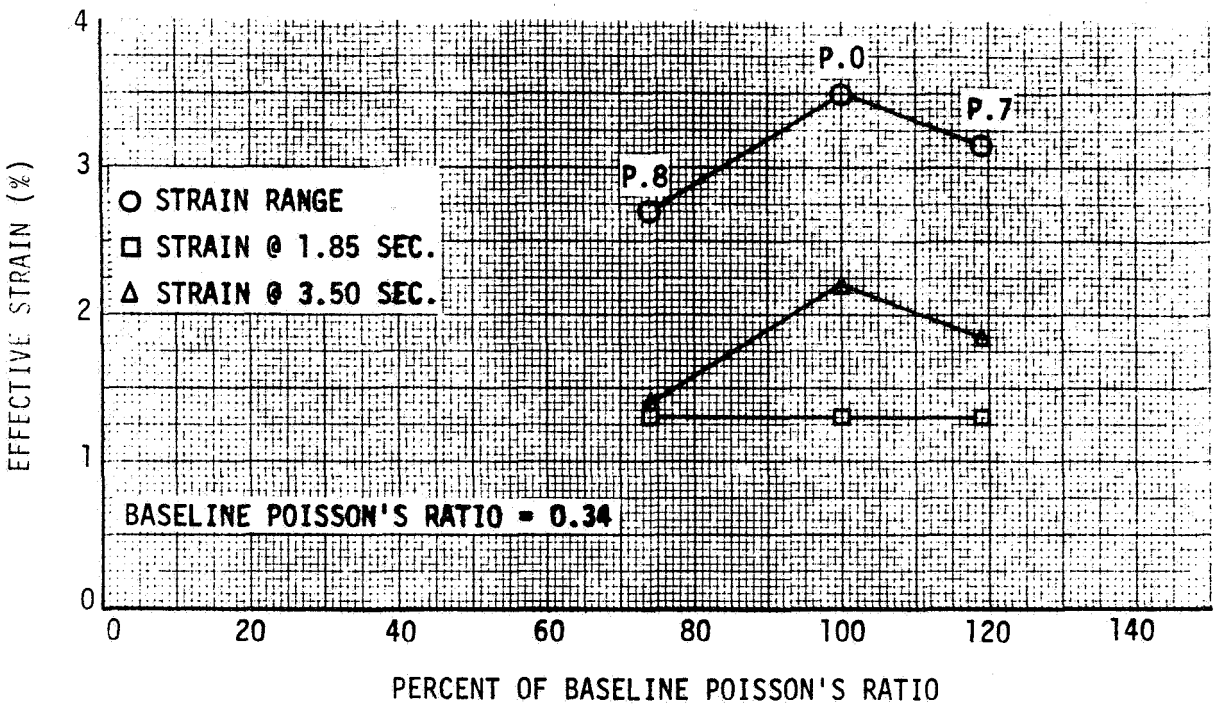

FIGURE 6.1-42 VARIATION OF MAXIMUM EFFECTIVE STRAIN WITH POISSON'S RATIO

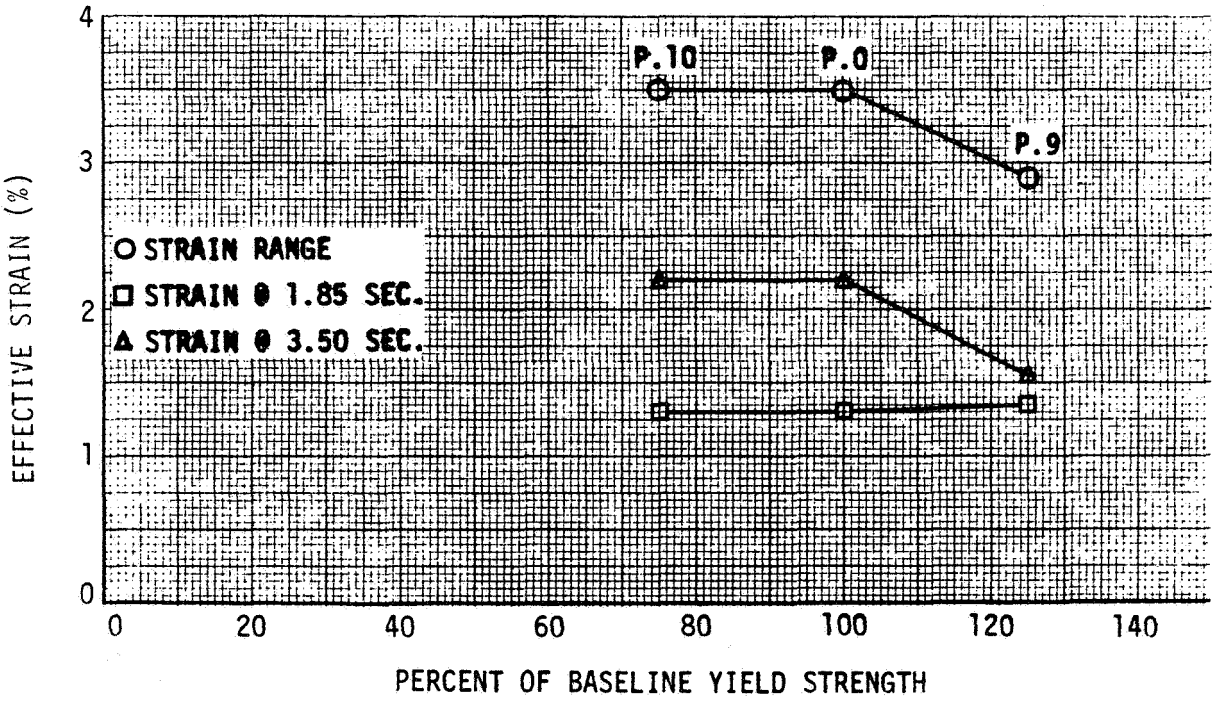

FIGURE 6.1-43 VARIATION OF MAXIMUM EFFECTIVE STRAIN WITH YIELD STRENGTH

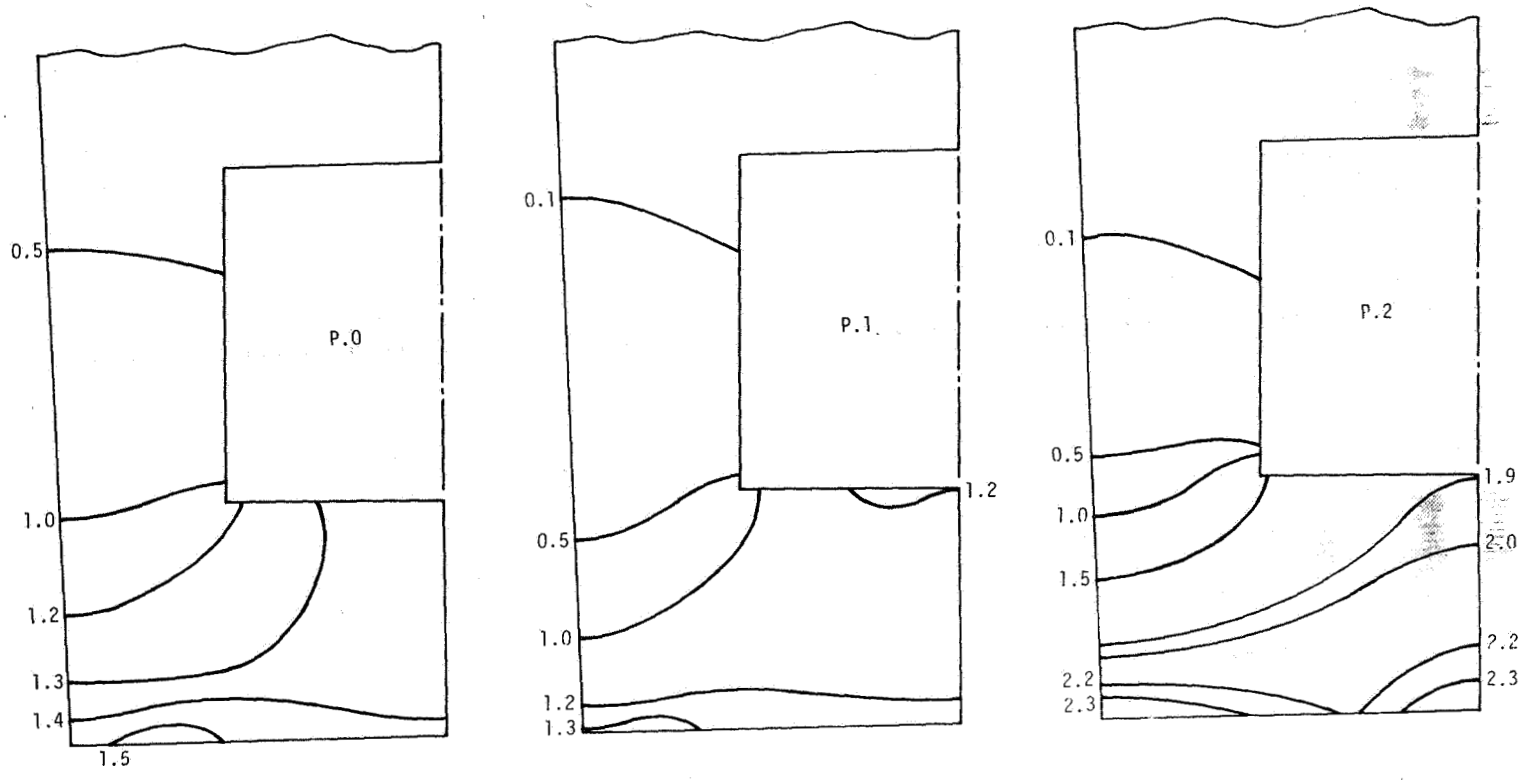

FIGURE 6.1-44 ISOGRAMS OF EFFECTIVE STRAIN AT TIME = 1.85 SECONDS, PARAMETRIC STUDY OF THERMAL PROPERTIES

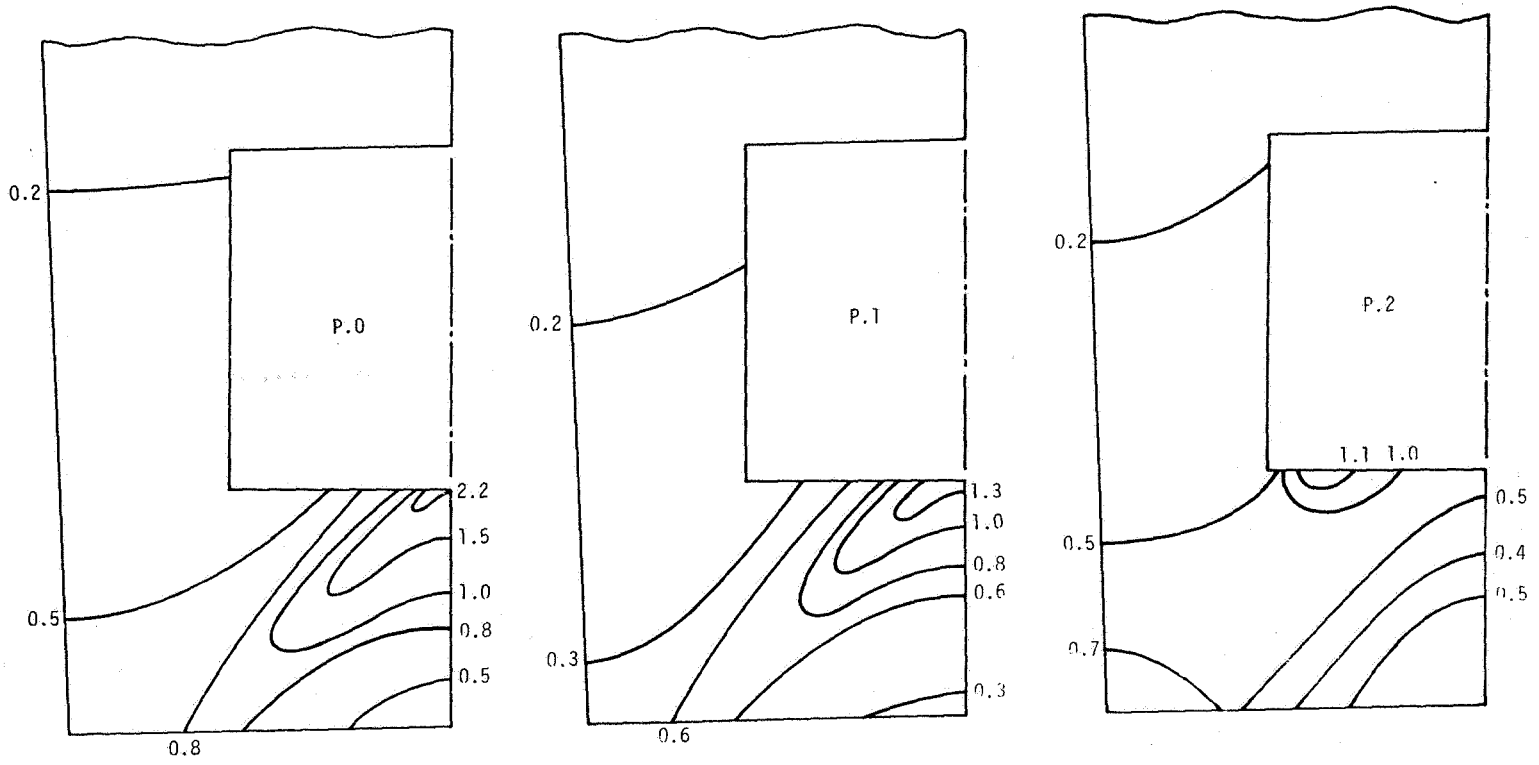

FIGURE 6.1-45 ISOGRAMS OF EFFECTIVE STRAIN AT TIME = 3.50 SECONDS, PARAMETRIC STUDY OF THERMAL PROPERTIES

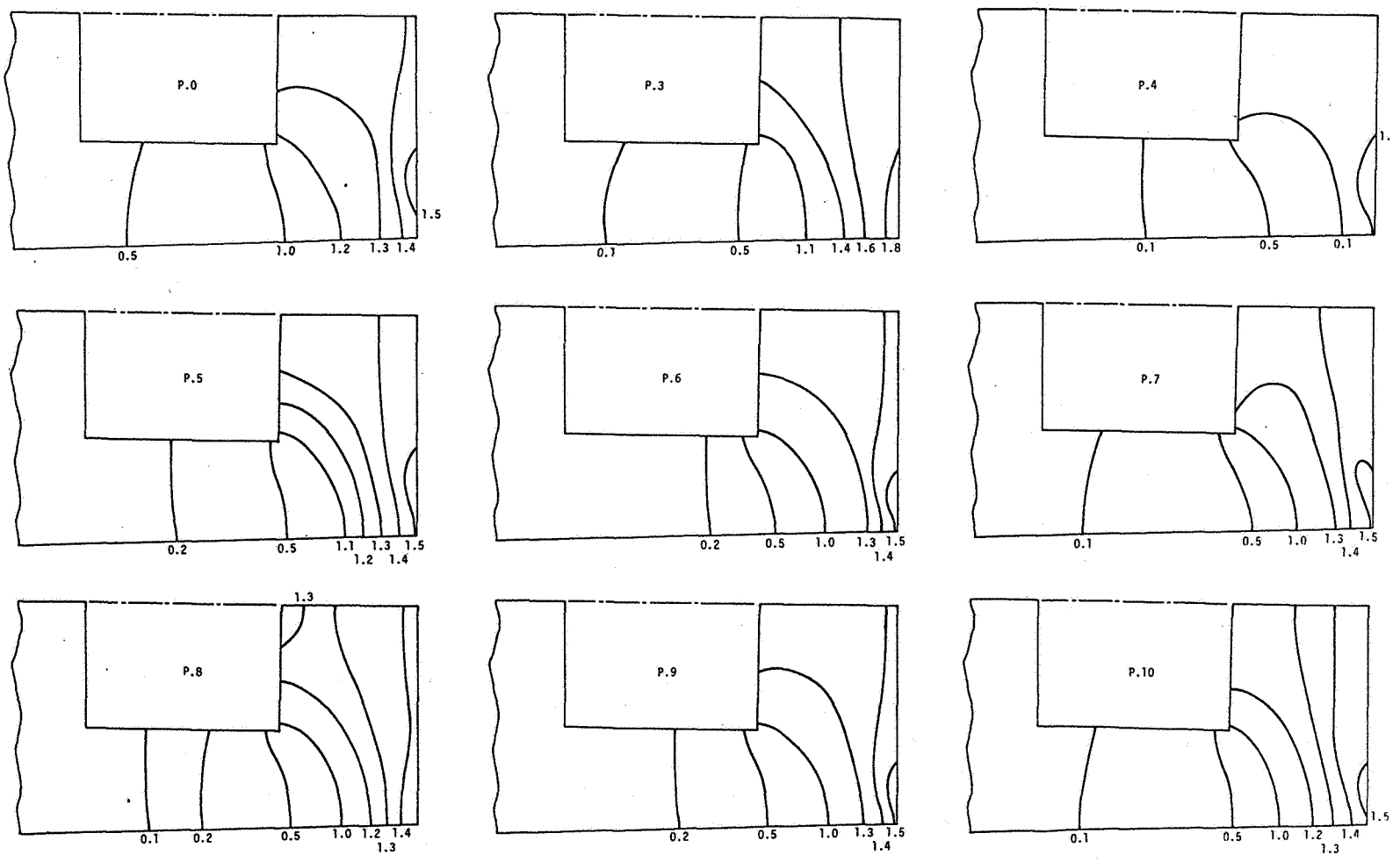

FIGURE 6.1-46 ISOGRAMS OF EFFECTIVE STRAIN AT TIME = 1.85 SECONDS, PARAMETRIC STUDY OF MECHANICAL PROPERTIES

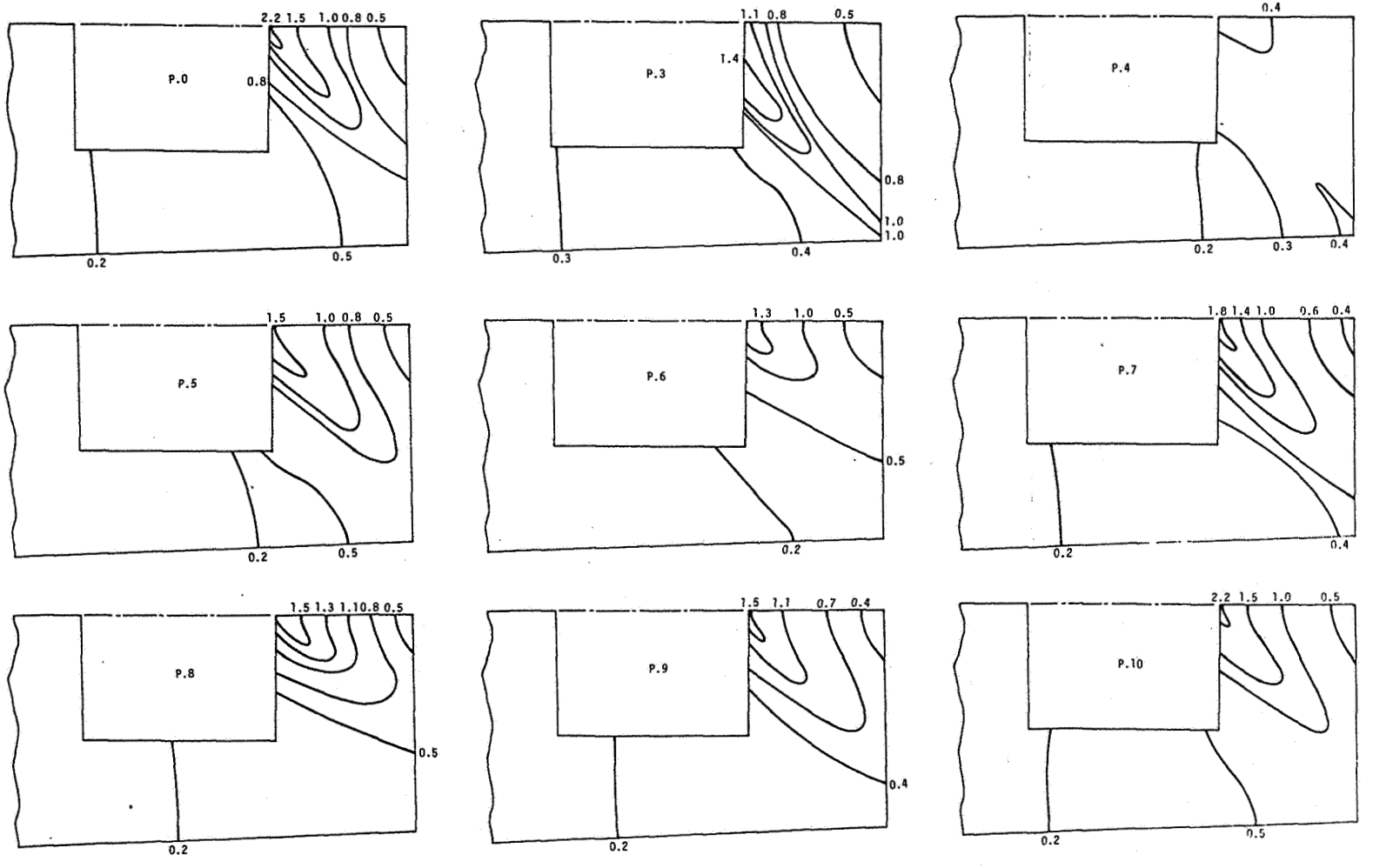

FIGURE 6.1-47 ISOGRAMS OF EFFECTIVE STRAIN AT TIME = 3.50 SECONDS, PARAMETRIC STUDY OF MECHANICAL PROPERTIES

7.0 CONCLUDING REMARKS

The parametric study revealed one consistent effect from all parameters: any change assigned to a material variable resulted in a reduction in the computed value of maximum effective strain range with respect to the baseline configuration. The reductions ranged from 2 to 51 percent, but this does not mean that any change in the properties of Amzirc is beneficial to fatigue life. For example, although the cyclic damage in the form of effective strain range was essentially the same in P.10 as in P.0, Figure 6.1-4 indicated that tolerance for damage in P.10 is less than in P.0. This figure shows that if the material condition is changed from half-hard to fully annealed the number of cycles to fracture decreases for strain ranges greater than 1.8 percent. It was concluded that configurations with yield strengths lower than the half-hard baseline case would consistently fail under fewer cycles than the baseline.

It remains for future analysis and tests to reveal the effect of all parameters on structural behavior and low-cycle fatigue life. Obviously the parameter easiest to investigate is yield strength. Variations in yield strength of Amzirc are obtained by changing the amount of cold work. Reference 1 states that the material is readily cold worked in the solution-annealed condition, and the strength of the material increases with the amount of cold working without sacrificing ductility or thermal conductivity. Material conditions between fully-annealed and full-hard should be assessed to provide material properties which characterize Amzirc for thrust chamber operating conditions. Then the optimum hardness could be selected for a thrust chamber design.

THIS PAGE LEFT INTENTIONALLY BLANK.

8.0 REFERENCES

1. J. J. Esposito and R. F. Zabora, Thrust Chamber Life Prediction - Mechanical and Physical Properties of High Performance Rocket Nozzle Materials, Boeing Report No. D180-18673-1, NASA Lewis Research Center Contract NAS3-17838, 1975.

2. J. B. Conway, R. H. Stentz and J. T. Berling, High Temperature, Low Cycle Fatigue of Copper Base Alloys in Argon; Part 1, Mar-Test Inc. Report MTI-4003-2-1, NASA Lewis Research Center Contract NAS3-16753, 1973.

THIS PAGE LEFT INTENTIONALLY BLANK.

APPENDIX A

TABLE A-I PLUG NOZZLE CYLINDER BETA NODE LOCATIONS

Node	R Inches	θ Degrees	Node	R Inches	θ Degrees	Node	R Inches	θ Degrees	Node	R Inches	θ Degrees	Node	R Inches	θ Degrees	Node	R Inches	θ Degrees
1	1.3000	2.5				59	1.3250	0	88	1.3550	1.7857	119	1.400	0	148	1.5050	.35714
2		2.1429	31	1.3150	2.5				90		1.3956				149		0
3		1.7857	32		2.1429	61	1.3300	2.5	91	1.3650	2.5	121	1.4250	2.5			
5		1.416	33		1.7857	62		2.1429	92		2.1429	122		2.1429	151	1.5450	2.5
6		1.0714	35		1.416	63		1.7857	93		1.7857	123		1.7857	152		2.1429
7		.71429	36		1.0714	65		1.416	95		1.3854	125		1.365	153		1.7857
8		.35714	37		.71429	66		1.0714	96	1.3750	2.5	126		1.0714	155		1.365
9		0	38		.35714	67		.71429	97		2.1429	127		.71429	156		1.0714
			39		0	68		.35714	98		1.7857	128		.35714	157		.71429
11	1.3050	2.5				69		0	100		1.3752	129		0	158		.35714
12		2.1429	41	1.3200	2.5				101	1.3850	2.5				159		0
13		1.7857	42		2.1429	71	1.33541	2.5	102		2.1429	131	1.4650	2.5			
15		1.416	43		1.7857	72		2.1429	103		1.7857	132		2.1429	161	1.585	2.5
16		1.0714	45		1.416	73		1.7857	105		1.365	133		1.7857	162		2.1429
17		.71429	46		1.0714	75		1.416	106		1.0714	135		1.365	163		1.7857
18		.35714	47		.71429	76	1.33531	1.0714	107		.71429	136		1.0714	165		1.365
19		0	48		.35714	77	1.3352	.71429	108		.35714	137		.71429	166		1.0714
			49		0	78	1.3351	.35714	109		0	138		.35714	167		.71429
21	1.3100	2.5				79	1.3350	0				139		0	168		.35714
22		2.1429	51	1.3250	2.5				111	1.400	2.5				169		0
23		1.7857	52		2.1429	81	1.3450	2.5	112		2.1429	141	1.5050	2.5			
25		1.416	53		1.7857	82		2.1429	113		1.7857	142		2.1429			
26		1.0714	55		1.416	83		1.7857	115		1.365	143		1.7857			
27		.71429	56		1.0714	85		1.4058	116		1.0714	145		1.365			
28		.35714	57		.71429	86	1.3550	2.5	117		.71429	146		1.0714			
29		0	58		.35714	87		2.1429	118		.35714	147		.71429			

APPENDIX B

TABLE B-I NODE IDENTIFICATION NUMBERS AND COORDINATES OF THE OUTER CYLINDER FINITE-ELEMENT MODEL

NODE I.D. NUMBER	COORDINATES RADIAL (inch)	CIRCUMFERENTIAL (degree)
1	1.300	0.00
2	1.300	0.25
3	1.300	0.50
4	1.300	0.75
5	1.300	1.00
6	1.300	1.25
7	1.300	1.50
8	1.300	1.75
9	1.300	2.00
10	1.300	2.25
11	1.300	2.50
12	1.305	0.00
13	1.305	0.25
14	1.305	0.50
15	1.305	0.75
16	1.305	1.00
17	1.305	1.25
18	1.305	1.50
19	1.305	1.75
20	1.305	2.00
21	1.305	2.25
22	1.305	2.50
23	1.310	0.00
24	1.310	0.25
25	1.310	0.50
26	1.310	0.75
27	1.310	1.00
28	1.310	1.25
29	1.310	1.50
30	1.310	1.75
31	1.310	2.00
32	1.310	2.25
33	1.310	2.50
34	1.315	0.00
35	1.315	0.25
36	1.315	0.50
37	1.315	0.75
38	1.315	1.00
39	1.315	1.25
40	1.315	1.50
41	1.315	1.75
42	1.315	2.00

TABLE B-I (CONTINUED)

NODE I.D. NUMBER	COORDINATES RADIAL (inch)	CIRCUMFERENTIAL (degrees)
43	1.315	2.25
44	1.315	2.50
45	1.320	0.00
46	1.320	0.25
47	1.320	0.50
48	1.320	0.75
49	1.320	1.00
50	1.320	1.25
51	1.320	1.50
52	1.320	1.75
53	1.320	2.00
54	1.320	2.25
55	1.320	2.50
56	1.325	0.00
57	1.325	0.25
58	1.325	0.50
59	1.325	0.75
60	1.325	1.00
61	1.325	1.25
62	1.325	1.50
63	1.325	1.75
64	1.325	2.00
65	1.325	2.25
66	1.325	2.50
67	1.330	0.00
68	1.330	0.25
69	1.330	0.50
70	1.330	0.75
71	1.330	1.00
72	1.330	1.25
73	1.330	1.50
74	1.330	1.75
75	1.330	2.00
76	1.330	2.25
77	1.330	2.50
78	1.335	0.00
79	1.335	0.25

TABLE B-I (CONTINUED)

NODE I.D. NUMBER	COORDINATES RADIAL (inch)	CIRCUMFERENTIAL (degree)
80	1.3351	0.500
81	1.3351	0.750
82	1.3352	1.000
83	1.3354	1.416
84	1.3354	1.750
85	1.3354	2.000
86	1.3354	2.250
87	1.3354	2.500
88	1.3387	1.582
89	1.3419	1.410
90	1.3419	1.750
91	1.3419	2.000
92	1.3419	2.250
93	1.3419	2.500
94	1.3485	1.405
95	1.3485	1.750
96	1.3485	2.000
97	1.3485	2.250
98	1.3485	2.500
99	1.3517	1.750
100	1.3517	2.250
101	1.3550	1.395
102	1.3550	2.000
103	1.3550	2.500
104	1.3600	1.750
105	1.3600	2.250
106	1.3650	1.385
107	1.3650	2.000
108	1.3650	2.500
109	1.3700	1.750
110	1.3700	2.250
111	1.3750	1.375
112	1.3750	2.000
113	1.3750	2.500
114	1.3800	1.750
115	1.3800	2.250
116	1.3850	0.000
117	1.3850	0.500

TABLE B-I (CONTINUED)

NODE I.D. NUMBER	COORDINATES RADIAL (inch)	CIRCUMFERENTIAL (degree
118	1.3850	1.000
119	1.3850	1.365
120	1.3850	2.000
121	1.3850	2.500
122	1.3900	0.250
123	1.3900	0.750
124	1.3900	1.250
125	1.3900	1.750
126	1.3900	2.250
127	1.3950	0.000
128	1.3950	0.500
129	1.3950	1.000
130	1.3950	1.500
131	1.3950	2.000
132	1.3950	2.500
133	1.4150	0.000
134	1.4150	0.500
135	1.4150	1.000
136	1.4150	1.500
137	1.4150	2.000
138	1.4150	2.500
139	1.4350	0.000
140	1.4350	1.000
141	1.4350	2.000
142	1.4550	0.000
143	1.4550	0.500
144	1.4550	1.000
145	1.4550	1.500
146	1.4550	2.000
147	1.4550	2.500
148	1.4750	0.000
149	1.4750	1.000
150	1.4750	2.000
151	1.4950	0.000
152	1.4950	0.500
153	1.4950	1.000

TABLE B-I (CONTINUED)

NODE I.D. NUMBER	COORDINATES RADIAL (inch)	CIRCUMFERENTIAL (degree)
154	1.4950	1.500
155	1.4950	2.000
156	1.4950	2.500
157	1.5150	0.000
158	1.5150	1.000
159	1.5150	2.000
160	1.5350	0.000
161	1.5350	0.500
162	1.5350	1.000
163	1.5350	1.500
164	1.5350	2.000
165	1.5350	2.500
166	1.5600	0.000
167	1.5600	1.000
168	1.5600	2.000
169	1.5800	0.000
170	1.5800	0.500
171	1.5800	1.000
172	1.5800	1.500
173	1.5800	2.000
174	1.5800	2.500

TABLE B-II FINITE ELEMENT AND CORRESPONDING NODE IDENTIFICATION NUMBERS OF THE OUTER CYLINDER FINITE-ELEMENT MODEL

ELEMENT I.D. NO.	NODE 1	NODE 2	NODE 3
1	1	12	2
2	2	13	3
3	3	14	4
4	4	15	5
5	5	16	6
6	6	17	7
7	7	18	8
8	8	19	9
9	9	20	10
10	10	21	11
11	13	2	12
12	14	3	13
13	15	4	14
14	16	5	15
15	17	6	16
16	18	7	17
17	19	8	18
18	20	9	19
19	21	10	20
20	22	11	21
21	12	23	13
22	13	24	14
23	14	25	15
24	15	26	16
25	16	27	17
26	17	28	18
27	18	29	19
28	19	30	20
29	20	31	21
30	21	32	22
31	24	13	23
32	25	14	24
33	26	15	25
34	27	16	26
35	28	17	27
36	29	18	28
37	30	19	29
38	31	20	30
39	32	21	31
40	33	22	32
41	23	34	24
42	24	35	25
43	25	36	26

TABLE B-II (CONTINUED)

ELEMENT I.D. NO.	NODE 1	NODE 2	NODE 3
44	26	37	27
45	27	38	28
46	28	39	29
47	29	40	30
48	30	41	31
49	31	42	32
50	32	43	33
51	35	24	34
52	36	25	35
53	37	26	36
54	38	27	37
55	39	28	38
56	40	29	39
57	41	30	40
58	42	31	41
59	43	32	42
60	44	33	43
61	34	45	35
62	35	46	36
63	36	47	37
64	37	48	38
65	38	49	39
66	39	50	40
67	40	51	41
68	41	52	42
69	42	53	43
70	43	54	44
71	46	35	45
72	47	36	46
73	48	37	47
74	49	38	48
75	50	39	49
76	51	40	50
77	52	41	51
78	53	42	52
79	54	43	53
80	55	44	54
81	45	56	46
82	46	57	47
83	47	58	48
84	48	59	49
85	49	60	50

TABLE B-II (CONTINUED)

ELEMENT I.D. NO.	NODE 1	NODE 2	NODE 3
86	50	61	51
87	51	62	52
88	52	63	53
89	53	64	54
90	54	65	55
91	57	46	56
92	58	47	57
93	59	48	58
94	60	49	59
95	61	50	60
96	62	51	61
97	63	52	62
98	64	53	63
99	65	54	64
100	66	55	65
101	56	67	57
102	57	68	58
103	58	69	59
104	59	70	60
105	60	71	61
106	61	72	62
107	62	73	63
108	63	74	64
109	64	75	65
110	65	76	66
111	68	57	67
112	69	58	68
113	70	59	69
114	71	60	70
115	72	61	71
116	73	62	72
117	74	63	73
118	75	64	74
119	76	65	75
120	77	66	76
121	67	78	68
122	68	79	69
123	69	80	70
124	70	81	71
125	71	82	72
126	73	72	83
127	84	74	73
128	74	84	75

TABLE B-II (CONTINUED)

ELEMENT I.D. NO.	NODE 1	NODE 2	NODE 3
129	75	85	76
130	76	86	77
131	79	68	78
132	80	69	79
133	81	70	80
134	82	71	81
135	82	83	72
136	83	84	73
137	85	75	84
138	86	76	85
139	87	77	86
140	84	83	88
141	84	90	85
142	92	86	85
143	86	92	87
144	83	89	88
145	89	90	88
146	90	84	88
147	91	85	90
148	85	91	92
149	93	87	92
150	89	94	90
151	96	91	90
152	91	96	92
153	98	93	92
154	95	90	94
155	90	95	96
156	97	92	96
157	92	97	98
158	99	95	94
159	95	99	96
160	100	97	96
161	97	100	98
162	94	101	99
163	101	102	99
164	102	96	99
165	96	102	100
166	102	103	100
167	103	98	100
168	102	101	104
169	103	102	105
170	101	106	104
171	106	107	104
172	107	102	104
173	102	107	105
174	107	108	105

TABLE B-II (CONTINUED)

ELEMENT I.D. NO.	NODE 1	NODE 2	NODE 3
175	108	103	105
176	107	106	109
177	108	107	110
178	106	111	109
179	111	112	109
180	112	107	109
181	107	112	110
182	112	113	110
183	113	108	110
184	112	111	114
185	113	112	115
186	111	119	114
187	119	120	114
188	120	112	114
189	112	120	115
190	120	121	115
191	121	113	115
192	117	116	122
193	118	117	123
194	119	118	124
195	120	119	125
196	121	120	126
197	116	127	122
198	127	128	122
199	128	117	122
200	117	128	123
201	128	129	123
202	129	118	123
203	118	129	124
204	129	130	124
205	130	119	124
206	119	130	125
207	130	131	125
208	131	120	125
209	120	131	126
210	131	132	126
211	132	121	126
212	134	128	127
213	128	134	129
214	136	130	129
215	130	136	131
216	138	132	131
217	127	133	134
218	135	129	134
219	129	135	136

TABLE B-II (CONTINUED)

ELEMENT I.D. NO.	NODE 1	NODE 2	NODE 3
220	137	131	136
221	131	137	138
222	133	139	134
223	140	135	134
224	135	140	136
225	141	137	136
226	137	141	138
227	143	134	139
228	134	143	140
229	145	136	140
230	136	145	141
231	147	138	141
232	139	142	143
233	144	140	143
234	140	144	145
235	146	141	145
236	141	146	147
237	142	148	143
238	149	144	143
239	144	149	145
240	150	146	145
241	146	150	147
242	152	143	148
243	143	152	149
244	154	145	149
245	145	154	150
246	156	147	150
247	148	151	152
248	153	149	152
249	149	153	154
250	155	150	154
251	150	155	156
252	151	157	152
253	158	153	152
254	153	158	154
255	159	155	154
256	155	159	156
257	161	152	157
258	152	161	158
259	163	154	158

TABLE B-II (CONTINUED)

ELEMENT I.D. NO.	NODE 1	NODE 2	NODE 3
260	154	163	159
261	165	156	159
262	157	160	161
263	162	158	161
264	158	162	163
265	164	159	163
266	159	164	165
267	160	166	161
268	167	162	161
269	162	167	163
270	168	164	163
271	164	168	165
272	170	161	166
273	161	170	167
274	172	163	167
275	163	172	168
276	174	165	168
277	166	169	170
278	171	167	170
279	167	171	172
280	173	168	172
281	168	173	174

THIS PAGE LEFT INTENTIONALLY BLANK.

APPENDIX C

TABLE C-I

CONFIGURATION P.O RESULTS

ELEMENT	TIME (sec)	CUMULATIVE STRAINS (%) ε_r	ε_θ	ε_z	ε_{eff}	TEMP. (°R)
1	.03	-.068	.040	.092	.095	419
4		-.067	.038	.092	.093	421
10		-.068	.047	.088	.094	424
131		-.079	.051	.098	.11	412
1	.05	-.11	.064	.15	.16	346
4		-.11	.062	.15	.16	348
10		-.12	.083	.15	.16	354
131		-.14	.088	.16	.18	333
1	.10	-.14	.057	.21	.20	282
4		-.14	.055	.20	.20	284
10		-.15	.076	.20	.20	290
131		-.17	.079	.21	.22	272
1	.20	-.15	.008	.26	.24	212
4		-.15	.005	.26	.24	214
10		-.16	.018	.26	.24	218
131		-.17	.021	.27	.25	206
1	.30	-.16	-.040	.30	.28	165
4		-.16	-.043	.30	.28	165
10		-.16	-.037	.30	.28	168
131		-.17	-.034	.31	.28	160
1	1.65	-.17	-.15	.40	.37	50
4		-.16	-.15	.40	.37	50
10		-.16	-.16	.40	.37	50
131		-.17	-.16	.40	.38	50
1	1.665	-.13	-.16	.35	.33	107
4		-.13	-.17	.35	.34	106
10		-.13	-.18	.35	.34	104
131		-.14	-.17	.36	.34	97
1	1.68	-.045	-.22	.24	.27	244
4		-.045	-.23	.24	.27	241
10		-.009	-.29	.25	.31	235
131		-.081	-.20	.28	.2	196
1	1.685	.030	-.27	.18	.26	315
4		.028	-.27	.18	.27	312
10		.053	-.32	.19	.30	303
131		-.029	-.24	.28	.29	249

CONFIGURATION P.0 RESULTS (Cont'd)

ELEMENT	TIME (sec)	CUMULATIVE STRAINS (%) ε_r	ε_θ	ε_z	ε_{eff}	TEMP. (°R)
1	1.69	.12	-.31	.12	.28	392
4		.12	-.31	.12	.29	388
10		.19	-.40	.13	.37	376
131		.065	-.31	.18	.30	307
1	1.695	.25	-.36	.032	.36	492
4		.25	-.37	.036	.36	487
10		.37	-.51	.050	.51	470
131		.23	-.43	.12	.41	383
1	1.70	.40	-.42	-.057	.48	590
4		.40	-.43	-.052	.48	584
10		.54	-.62	-.032	.67	563
131		.39	-.52	.057	.54	461
1	1.706	.58	-.49	-.16	.63	701
4		.58	-.51	-.16	.64	693
10		.76	-.75	-.13	.88	668
131		.59	-.64	-.030	.71	561
1	1.712	.72	-.55	-.25	.77	792
4		.73	-.57	-.24	.78	783
10		.94	-.85	-.21	1.05	753
131		.77	-.75	-.11	.88	645
1	1.725	.92	-.64	-.37	.96	917
4		.94	-.66	-.36	.98	906
10		1.11	-.95	-.33	1.22	876
131		.98	-.86	-.22	1.08	764
1	1.738	1.06	-.70	-.46	1.10	1009
4		1.07	-.72	-.45	1.11	998
10		1.22	-1.01	-.42	1.33	967
131		1.08	-.89	-.31	1.17	852
1	1.744	1.10	-.72	-.49	1.15	1039
4		1.11	-.74	-.48	1.16	1028
10		1.26	-1.02	-.45	1.37	996
131		1.10	-.89	-.34	1.19	880
1	1.75	1.14	-.74	-.52	1.18	1064
4		1.14	-.76	-.51	1.19	1054
10		1.30	-1.04	-.48	1.41	1022
131		1.13	-.89	-.36	1.21	905

CONFIGURATION P.0 RESULTS (Cont'd)

ELEMENT	TIME (sec)	CUMULATIVE STRAINS (%) ε_r	ε_θ	ε_z	ε_{eff}	TEMP. (°R)
1	1.775	1.21	-.75	-.59	1.26	1125
4		1.22	-.78	-.58	1.27	1114
10		1.37	-1.05	-.54	1.47	1083
131		1.17	-.89	-.41	1.25	963
1	1.80	1.28	-.77	-.66	1.33	1184
4		1.28	-.79	-.64	1.34	1174
10		1.44	-1.06	-.61	1.54	1143
131		1.22	-.88	-.47	1.29	1021
1	1.85	1.32	-.75	-.71	1.37	1239
4		1.32	-.77	-.70	1.38	1229
10		1.49	-1.04	-.67	1.58	1199
131		1.25	-.85	-.53	1.31	1074
1	1.95	1.34	-.69	-.78	1.38	1299
4		1.34	-.71	-.77	1.39	1290
10		1.51	-.96	-.74	1.58	1263
131		1.25	-.76	-.60	1.29	1133
1	2.50	1.30	-.50	-.91	1.36	1413
4		1.30	-.51	-.90	1.35	1406
10		1.44	-.70	-.87	1.49	1383
131		1.14	-.46	-.72	1.16	1244
1	3.20	1.29	-.45	-.94	1.35	1438
4		1.29	-.46	-.93	1.35	1430
10		1.43	-.65	-.90	1.48	1408
131		1.03	-.27	-.75	1.06	1267
1	3.21	1.26	-.43	-.89	1.31	1400
4		1.25	-.43	-.88	1.30	1392
10		1.39	-.62	-.86	1.42	1372
131		.89	-.16	-.71	.94	1235
1	3.22	1.22	-.41	-.85	1.26	1361
4		1.19	-.39	-.84	1.24	1355
10		1.36	-.62	-.82	1.39	1336
131		.71	.004	-.68	.80	1203
1	3.23	1.17	-.39	-.81	1.20	1323
4		1.12	-.36	-.80	1.16	1317
10		1.35	-.63	-.78	1.37	1300
131		.51	.19	-.64	.69	1171

CONFIGURATION P.0 RESULTS (Cont'd)

ELEMENT	TIME (sec)	CUMULATIVE STRAINS (%) ε_r	ε_θ	ε_z	ε_{eff}	TEMP. (°R)
1	3.24	1.09	-.35	-.76	1.13	1285
4		1.04	-.31	-.76	1.08	1279
10		1.31	-.63	-.74	1.33	1265
131		.34	.33	-.60	.63	1139
1	3.26	.92	-.28	-.66	.95	1186
4		.84	-.22	-.65	.81	1181
10		1.14	-.55	-.64	1.16	1170
131		-.034	.63	-.51	.66	1053
1	3.28	.71	-.20	-.53	.74	1068
4		.61	-.12	-.52	.66	1065
10		.94	-.46	-.51	.95	1058
131		-.40	.90	-.40	.87	950
1	3.30	.51	-.11	-.40	.54	951
4		.39	-.013	-.40	.46	950
10		.74	-.37	-.40	.75	946
131		-.66	1.08	-.30	1.06	846
1	3.325	.31	-.038	-.27	.34	814
4		.17	.079	-.27	.27	814
10		.56	-.30	-.27	.56	81[illegible]
131		-1.01	1.32	-.19	1.36	727
1	3.35	.12	.034	-.14	.15	679
4		-.046	.17	-.14	.19	680
10		.37	-.23	-.14	.38	682
131		-1.28	1.50	-.075	1.61	608
1	3.375	-.027	.079	-.037	.074	569
4		-.21	.23	-.039	.25	570
10		.23	-.19	-.043	.24	574
131		-1.51	1.64	.015	1.82	512
1	3.40	-.16	.12	.059	.16	460
4		-.35	.28	.057	.38	462
10		.10	-.15	.052	.16	468
131		-1.69	1.75	.094	1.99	417
1	3.425	-.24	.13	.13	.24	374
4		-.43	.30	.13	.44	377
10		.022	-.14	.12	.15	384
131		-1.81	1.82	.16	2.10	343

CONFIGURATION P.0 RESULTS (Cont'd)

ELEMENT	TIME (sec)	CUMULATIVE STRAINS (%) ε_r	ε_θ	ε_z	ε_{eff}	TEMP. (°R)
1	3.45	-.30	.13	.19	.31	298
4		-.50	.31	.19	.51	301
10		-.042	-.14	.18	.19	309
131		-1.91	1.85	.21	2.18	276
1	3.50	-.37	.11	.28	.39	196
4		-.58	.29	.28	.57	199
10		-.10	-.17	.27	.27	206
131		-1.97	1.84	.29	2.21	186
1	3.70	-.34	-.073	.36	.40	104
4		-.55	.12	.36	.54	104
10		-.058	-.39	.35	.43	106
131		-1.91	1.64	.36	2.08	101
1	3.90	-.31	-.17	.40	.43	50
4		-.52	.023	.40	.54	50
10		-.001	-.53	.40	.54	50
131		-1.89	1.55	.40	2.02	50

CONFIGURATION P.1 RESULTS

ELEMENT	TIME (sec)	CUMULATIVE STRAIN (%) ε_r	ε_θ	ε_z	ε_{eff}	TEMP. (°R)
1	.03	-.068	.040	.092	.095	419
10		-.068	.047	.088	.094	424
131		-.079	.051	.098	.11	412
1	.05	-.11	.064	.15	.16	346
10		-.12	.083	.15	.16	354
131		-.14	.088	.16	.18	333
1	.10	-.14	.057	.21	.20	282
10		-.15	.076	.20	.20	290
131		-.17	.079	.21	.22	272
1	.20	-.16	.008	.26	.24	212
10		-.16	.018	.26	.24	218
131		-.17	.021	.27	.25	206
1	.30	-.16	-.040	.30	.28	165
10		-.16	-.037	.30	.28	168
131		-.17	-.034	.31	.28	160
1	1.65	-.17	-.15	.40	.37	50
10		-.16	-.16	.40	.37	50
131		-.16	-.16	.40	.38	50
1	1.665	-.13	-.17	.35	.33	110
10		-.12	-.19	.35	.34	108
131		-.14	-.17	.36	.34	98
1	1.68	-.043	-.23	.25	.28	235
10		-.033	-.26	.25	.30	228
131		-.078	-.21	.28	.29	194
1	1.685	.022	-.27	.19	.27	301
10		.047	-.32	.20	.31	291
131		-.026	-.25	.24	.28	247
1	1.69	.11	-.30	.13	.29	368
10		.17	-.39	.15	.38	355
131		.067	-.32	.19	.30	300

CONFIGURATION P.1 RESULTS (Cont'd)

ELEMENT	TIME (sec)	CUMULATIVE STRAIN (%) ε_r	ε_θ	ε_z	ε_{eff}	TEMP. (°R)
1	1.695	.23	-.35	.059	.35	460
10		.32	-.49	.074	.48	441
131		.20	-.41	.13	.39	373
1	1.70	.37	-.40	-.020	.44	551
10		.48	-.59	.002	.62	527
131		.36	-.51	.070	.51	446
1	1.706	.52	-.46	-.11	.58	650
10		.68	-.70	-.087	.80	621
131		.54	-.61	-.007	.66	538
1	1.712	.66	-.52	-.20	.70	736
10		.84	-.80	-.16	.96	703
131		.71	-.71	-.085	.82	619
1	1.725	.83	-.58	-.31	.87	852
10		1.01	-.88	-.27	1.12	816
131		.92	-.82	-.19	1.02	732
1	1.738	.94	-.63	-.38	.97	928
10		1.09	-.91	-.34	1.19	891
131		1.01	-.85	-.26	1.10	805
1	1.744	.97	-.64	-.40	1.00	954
10		1.12	-.92	-.37	1.22	917
131		1.03	-.85	-.29	1.11	830
1	1.75	.99	-.65	-.43	1.03	977
10		1.14	-.92	-.39	1.24	940
131		1.05	-.86	-.31	1.13	853
1	1.775	1.06	-.66	-.50	1.10	1041
10		1.20	-.93	-.46	1.29	1004
131		1.10	-.85	-.37	1.17	916
1	1.80	1.10	-.65	-.54	1.13	1083
10		1.24	-.92	-.50	1.32	1047
131		1.12	-.83	-.41	1.18	956

CONFIGURATION P.1 RESULTS (Cont'd)

ELEMENT	TIME (sec)	CUMULATIVE STRAIN (%) ε_r	ε_θ	ε_z	ε_{eff}	TEMP. (°R)
1	1.85	1.13	-.62	-.60	1.16	1137
10		1.27	-.88	-.46	1.35	1103
131		1.14	-.78	-.46	1.19	1010
1	1.95	1.15	-.55	-.68	1.18	1205
10		1.28	-.79	-.64	1.33	1174
131		1.14	-.68	-.54	1.17	1077
1	2.225	1.14	-.42	-.78	1.18	1205
10		1.24	-.60	-.75	1.28	1274
131		1.09	-.49	-.64	1.11	1171
1	2.50	1.14	-.36	-.83	1.18	1340
10		1.21	-.52	-.80	1.26	1314
131		1.06	-.40	-.68	1.08	1209
1	2.85	1.14	-.34	-.85	1.19	1357
10		1.20	-.48	-.82	1.25	1333
131		1.04	-.36	-.70	1.07	1227
1	3.20	1.13	-.33	-.85	1.19	1363
10		1.20	-.47	-.82	1.24	1339
131		1.03	-.34	-.71	1.06	1232
1	3.205	1.13	-.33	-.84	1.18	1357
10		1.19	-.46	-.82	1.24	1333
131		1.03	-.34	-.70	1.05	1228
1	3.21	1.12	-.32	-.84	1.17	1349
10		1.18	-.45	-.81	1.22	1326
131		1.02	-.33	-.70	1.04	1222
1	3.215	1.11	-.31	-.82	1.16	1335
10		1.16	-.43	-.80	1.20	1312
131		1.00	-.32	-.68	1.03	1210
1	3.22	1.10	-.30	-.80	1.14	1320
10		1.14	-.41	-.78	1.18	1298
131		.98	-.30	-.67	1.00	1198

CONFIGURATION P.1 RESULTS (Cont'd)

ELEMENT	TIME (sec)	CUMULATIVE STRAIN (%) ε_r	ε_θ	ε_z	ε_{eff}	TEMP. (°R)	
1	3.225	1.08	-.30	-.78	1.12	1300	
10		1.10	-.38	-.76	1.13	1280	
131		.94	-.25	-.65	.95	1181	
1	3.23	1.06	-.29	-.76	1.09	1280	
10		1.05	-.35	-.74	1.09	1261	
131		.86	-.19	-.63	.89	1163	
1	3.24	1.01	-.28	-.71	1.04	1234	
10		.98	-.32	-.69	1.01	1218	
131		.64	.005	-.59	.71	1122	
1	3.25	.93	-.24	-.66	.95	1185	
10		.89	-.28	-.64	.92	1170	
131		.43	.18	-.54	.58	1078	
1	3.26	.84	-.21	-.60	.86	1133	
10		.79	-.22	-.58	.82	1121	
131		.24	.32	-.48	.51	1031	
1	3.28	.66	-.14	-.50	.67	1026	
10		.58	-.11	-.47	.62	1018	
131		-.055	.52	-.39	.53	935	
1	3.30	.50	-.087	-.37	.51	920	
10		.40	-.02	-.37	.44	916	
131		-.27	.66	-.30	.62	839	
1	3.325	.32	-.033	-.25	.34	791	
10		.20	.071	-.25	.27	792	
131		-.54	.82	-.18	.81	724	
1	3.35	.17	.008	-.14	.18	673	
10		.025	.14	-.14	.16	677	
131		-.77	.96	-.083	1.00	616	
1	3.375	.041	.040	-.034	.050	566	
10		-.13	.20	-.040	.20	572	
131		-.95	1.07	.008	1.17	520	rev

CONFIGURATION P.1 RESULTS (Cont'd)

ELEMENT	TIME (sec)	CUMULATIVE STRAIN (%) ε_r	ε_θ	ε_z	ε_{eff}	TEMP. (°R)
1	3.40	-.058	.058	.050	.074	470
10		-.24	.24	.043	.28	478
131		-1.08	1.12	.080	1.27	434
1	3.425	-.13	.059	.12	.15	387
10		-.31	.25	.11	.34	396
131		-1.17	1.15	.14	1.34	359
1	3.45	-.18	.048	.18	.21	316
10		-.36	.24	.17	.38	326
131		-1.22	1.15	.20	1.38	295
1	3.50	-.23	.010	.26	.29	212
10		-.42	.20	.26	.44	221
131		-1.28	1.12	.27	1.40	200
1	3.70	-.21	-.17	.36	.37	96
10		-.39	-.013	.36	.43	99
131		-1.26	.94	.36	1.32	92
1	3.90	-.18	-.27	.40	.42	50
10		-.34	-.14	.40	.44	50
131		-1.23	.85	.40	1.26	50

CONFIGURATION P.2 RESULTS

ELEMENT	TIME (sec)	CUMULATIVE STRAINS (%) ε_r	ε_θ	ε_z	ε_{eff}	TEMP. (°R)
1	.03	-.068	.040	.092	.095	419
10		-.068	.047	.088	.094	424
131		-.079	.051	.098	.11	412
1	.05	-.11	.064	.15	.16	346
10		-.12	.083	.15	.16	354
131		-.14	.088	.16	.18	333
1	.10	-.14	.057	.21	.20	282
10		-.15	.076	.20	.20	290
131		-.17	.079	.21	.22	272
1	.20	-.16	.007	.26	.24	212
10		-.16	.017	.26	.24	218
131		-.17	.021	.27	.25	206
1	.30	-.16	-.040	.30	.28	165
10		-.16	-.037	.30	.28	168
131		-.17	-.034	.31	.28	160
1	1.65	-.17	-.15	.40	.37	50
10		-.16	-.16	.40	.37	50
131		-.16	-.16	.40	.38	50
1	1.665	-.10	-.20	.33	.32	136
10		-.099	-.21	.33	.33	134
131		-.13	-.18	.35	.34	104
1	1.672	-.063	-.23	.28	.30	192
10		-.057	-.25	.28	.31	189
131		-.11	-.19	.33	.32	138
1	1.68	.061	-.30	.18	.29	311
10		.080	-.34	.19	.32	304
131		-.049	-.24	.27	.30	209
1	1.685	.20	-.37	.11	.36	402
10		.23	-.43	.12	.40	391
131		.28	-.30	.22	.30	265

CONFIGURATION P.2 RESULTS (Cont'd)

ELEMENT	TIME (sec)	CUMULATIVE STRAINS (%) ε_r	ε_θ	ε_z	ε_{eff}	TEMP. (°R)
1	1.69	.36	-.44	.025	.46	500
10		.40	-.53	.038	.54	485
131		.16	-.39	.17	.37	327
1	1.695	.58	-.55	-.094	.66	629
10		.64	-.68	-.074	.76	607
131		.34	-.51	.099	.51	411
1	1.70	.81	-.66	-.21	.87	754
10		.89	-.82	-.19	1.00	726
131		.52	-.62	.027	.66	498
1	1.706	1.03	-.78	-.34	1.09	890
10		1.10	-.96	-.31	1.22	854
131		.77	-.76	-.082	.89	615
1	1.712	1.20	-.87	-.46	1.27	1004
10		1.27	-1.08	-.41	1.40	962
131		.96	-.87	-.18	1.07	716
1	1.718	1.32	-.94	-.54	1.39	1079
10		1.40	-1.17	-.49	1.54	1034
131		1.04	-.90	-.24	1.15	786
1	1.725	1.49	-1.02	-.64	1.57	1175
10		1.61	-1.28	-.59	1.74	1127
131		1.17	-.96	-.33	1.26	875
1	1.738	1.72	-1.14	-.80	1.80	1294
10		1.89	-1.43	-.71	2.02	1243
131		1.31	-1.02	-.44	1.40	986
1	1.744	1.81	-1.18	-.81	1.88	1334
10		1.97	-1.47	-.76	2.09	1283
131		1.36	-1.04	-.48	1.45	1024
1	1.75	1.88	-1.21	-.85	1.95	1370
10		2.04	-1.50	-.80	2.16	1319
131		1.42	-1.07	-.51	1.51	1058

CONFIGURATION P.2 RESULTS (Cont'd)

ELEMENT	TIME (sec)	CUMULATIVE STRAIN (%) ε_r	ε_θ	ε_z	ε_{eff}	TEMP. (°R)
1	1.775	2.06	-1.29	-.96	2.14	1473
10		2.22	-1.58	-.91	2.34	1420
131		1.61	-1.17	-.62	1.70	1154
1	1.80	2.15	-1.32	-1.03	2.22	1530
10		2.31	-1.60	-.97	2.43	1479
131		1.72	-1.23	-.68	1.81	1209
1	1.85	2.23	-1.33	-1.09	2.29	1588
10		2.38	-1.61	-1.04	2.49	1539
131		1.80	-1.25	-.74	1.89	1263
1	1.95	2.25	-1.29	-1.13	2.31	1629
10		2.40	-1.56	-1.08	2.50	1582
131		1.80	-1.19	-.78	1.87	1302
1	2.225	2.22	-1.17	-1.18	2.27	1667
10		2.37	-1.42	-1.13	2.43	1625
131		1.77	-1.06	-.82	1.81	1339
1	2.50	2.20	-1.10	-1.20	2.23	1686
10		2.32	-1.31	-1.15	2.37	1645
131		1.73	-.96	-.84	1.75	1357
1	2.85	2.17	-1.05	-1.21	2.20	1697
10		2.26	-1.23	-1.17	2.31	1658
131		1.69	-.90	-.85	1.71	1368
1	3.20	2.15	-1.03	-1.21	2.19	1703
10		2.24	-1.18	-1.17	2.28	1664
131		1.67	-.87	-.86	1.69	1373
1	3.205	2.15	-1.02	-1.21	2.18	1695
10		2.22	-1.17	-1.16	2.26	1657
131		1.67	-.87	-.85	1.68	1369
1	3.21	2.14	-1.02	-1.20	2.16	1685
10		2.20	-1.15	-1.15	2.24	1647
131		1.66	-.87	-.84	1.68	1363

CONFIGURATION P.2 RESULTS (Cont'd)

ELEMENT	TIME (sec)	CUMULATIVE STRAIN (%) ε_r	ε_θ	ε_z	ε_{eff}	TEMP. (°R)
1	3.215	2.12	-1.00	-1.18	2.14	1667
10		2.17	-1.12	-1.14	2.20	1631
131		1.65	-.86	-.83	1.66	1350
1	3.22	2.09	-.99	-1.15	2.11	1647
10		2.12	-1.08	-1.12	2.15	1613
131		1.63	-.85	-.82	1.64	1336
1	3.225	2.06	-.97	-1.13	2.07	1623
10		2.05	-1.03	-1.09	2.08	1590
131		1.61	-.84	-.80	1.62	1317
1	3.23	2.01	-.95	-1.10	2.03	1598
10		1.98	-.97	-1.07	2.00	1566
131		1.58	-.83	-.77	1.59	1298
1	3.25	1.78	-.84	-.96	1.79	1474
10		1.68	-.78	-.94	1.70	1450
131		1.37	-.72	-.66	1.38	1197
1	3.26	1.64	-.78	-.89	1.65	1404
10		1.52	-.67	-.87	1.53	1383
131		1.26	-.66	-.60	1.27	1140
1	3.28	1.36	-.64	-.73	1.36	1258
10		1.18	-.47	-.72	1.19	1243
131		1.02	-.54	-.47	1.02	1020
1	3.30	1.07	-.51	-.57	1.08	1110
10		.85	-.28	-.56	.86	1101
131		.77	-.43	-.35	.79	899
1	3.325	.74	-.35	-.38	.74	930
10		.50	-.094	-.38	.52	927
131		.50	-.28	-.21	.50	752

CONFIGURATION P.2 RESULTS (Cont'd)

ELEMENT	TIME (sec)	CUMULATIVE STRAIN (%) ε_r	ε_θ	ε_z	ε_{eff}	TEMP. (°R)
1	3.335	.63	-.30	-.32	.63	869
10		.40	-.034	-.32	.42	868
131		.40	-.22	-.16	.39	703
1	3.35	.45	-.22	-.22	.45	763
10		.18	.094	-.22	.24	764
131		.23	-.13	-.084	.23	618
1	3.375	-.11	-.030	-.079	.045	613
10		-.31	.24	-.084	.32	618
131		-.24	.075	.027	.20	498
1	3.40	-.20	.039	.042	.16	480
10		-.40	.32	.035	.42	488
131		-.30	.11	.11	.28	393
1	3.425	-.27	.084	.14	.26	367
10		-.47	.37	.13	.50	376
131		-.36	.14	.19	.35	304
1	3.45	-.33	.12	.22	.33	271
10		-.52	.40	.21	.56	282
131		-.40	.16	.25	.41	229
1	3.50	-.44	.15	.33	.47	138
10		-.70	.49	.32	.74	148
131		-.56	.26	.34	.58	123
1	3.60	-.44	.098	.37	.47	90
10		-.69	.42	.36	.72	98
131		-.54	.19	.37	.56	84
1	4.00	-.35	-.090	.39	.44	58
10		-.59	.20	.39	.60	59
131		-.44	-.023	.39	.48	56
1	5.15	-.33	-.14	.40	.44	50
10		-.56	.14	.40	.58	50
131		-.41	-.090	.40	.47	50

CONFIGURATION P.3 RESULTS

ELEMENT	TIME (sec)	CUMULATIVE STRAIN (%) ε_r	ε_θ	ε_z	ε_{eff}	TEMP. (°R)
1	.03	-.081	.048	.11	.11	419
10		-.083	.057	.10	.11	424
131		-.094	.061	.12	.13	412
1	.05	-.14	.076	.18	.19	346
10		-.15	.10	.18	.20	354
131		-.18	.11	.20	.22	333
1	.10	-.18	.068	.25	.25	282
10		-.19	.095	.24	.25	290
131		-.21	.10	.26	.28	272
1	.20	-.20	.007	.32	.30	212
10		-.20	.022	.31	.30	218
131		-.22	.027	.32	.31	206
1	.30	-.20	-.051	.36	.34	165
10		-.21	-.044	.36	.34	168
131		-.22	-.039	.37	.35	160
1	1.65	-.21	-.18	.48	.45	50
10		-.20	-.20	.48	.45	50
131		-.21	-.19	.48	.46	50
1	1.665	-.17	-.20	.42	.41	107
10		-.16	-.22	.42	.41	104
131		-.18	-.20	.43	.42	97
1	1.68	-.039	-.29	.29	.33	244
10		-.026	-.32	.30	.36	235
131		-.088	-.26	.33	.36	196
1	1.685	.07	-.33	.21	.33	315
10		.13	-.42	.23	.40	303
131		.025	-.35	.28	.36	249
1	1.69	.20	-.39	.14	.37	392
10		.28	-.51	.15	.49	376
131		.18	-.46	.22	.44	307

CONFIGURATION P.3 RESULTS (Cont'd)

ELEMENT	TIME (sec)	CUMULATIVE STRAIN (%) ε_r	ε_θ	ε_z	ε_{eff}	TEMP. (°R)
1	1.695	.38	-.46	.038	.49	492
10		.48	-.63	.060	.65	470
131		.36	-.58	.15	.57	383
1	1.70	.57	-.55	-.069	.65	590
10		.68	-.75	-.038	.82	563
131		.55	-.68	.069	.72	461
1	1.706	.80	-.66	-.20	.86	701
10		.88	-.86	-.16	1.01	668
131		.77	-.80	-.036	.90	561
1	1.712	.96	-.74	-.30	1.02	792
10		1.04	-.96	-.26	1.17	755
131		.90	-.87	-.13	1.03	645
1	1.725	1.16	-.84	-.44	1.23	917
10		1.26	-1.07	-.40	1.38	876
131		1.06	-.92	-.27	1.17	764
1	1.738	1.31	-.92	-.56	1.38	1009
10		1.44	-1.15	-.50	1.56	967
131		1.18	-.96	-.37	1.28	852
1	1.744	1.38	-.94	-.59	1.44	1039
10		1.50	-1.18	-.54	1.61	996
131		1.22	-.97	-.40	1.31	880
1	1.75	1.42	-.95	-.63	1.49	1064
10		1.54	-1.20	-.57	1.66	1022
131		1.25	-.98	-.43	1.34	905
1	1.775	1.52	-.97	-.71	1.58	1125
10		1.65	-1.21	-.65	1.75	1083
131		1.33	-.99	-.50	1.42	963
1	1.80	1.62	-.99	-.78	1.68	1184
10		1.75	-1.23	-.73	1.84	1143
131		1.42	-1.00	-.57	1.49	1021

CONFIGURATION P.3 RESULTS (Cont'd)

ELEMENT	TIME (sec)	CUMULATIVE STRAIN (%) ε_r	ε_θ	ε_z	ε_{eff}	TEMP. (°R)
1	1.85	1.67	-.96	-.86	1.72	1239
10		1.79	-1.19	-.80	1.87	1199
131		1.46	-.96	-.64	1.52	1074
1	1.95	1.69	-.87	-.94	1.73	1299
10		1.80	-1.08	-.89	1.86	1263
131		1.47	-.86	-.72	1.51	1133
1	2.50	1.63	-.63	-1.09	1.68	1413
10		1.66	-.73	-1.05	1.71	1383
131		1.33	-.53	-.86	1.37	1244
1	2.85	1.62	-.58	-1.11	1.67	1432
10		1.64	-.66	-1.07	1.68	1402
131		1.31	-.47	-.89	1.34	1262
1	3.20	1.61	-.57	-1.12	1.67	1438
10		1.62	-.64	-1.08	1.68	1408
131		1.30	-.45	-.90	1.34	1267
1	3.205	1.59	-.56	-1.10	1.64	1419
10		1.60	-.61	-1.06	1.64	1391
131		1.28	-.43	-.87	1.31	1252
1	3.21	1.57	-.54	-1.07	1.61	1400
10		1.56	-.58	-1.03	1.60	1372
131		1.25	-.41	-.85	1.28	1235
1	3.215	1.55	-.53	-1.04	1.59	1382
10		1.50	-.53	-1.01	1.54	1356
131		1.21	-.38	-.83	1.24	1220
1	3.22	1.53	-.53	-1.02	1.56	1361
10		1.41	-.46	-.98	1.46	1336
131		1.15	-.34	-.81	1.18	1203
1	3.225	1.50	-.52	-1.00	1.53	1344
10		1.34	-.41	-.96	1.39	1320
131		1.11	-.31	-.79	1.14	1189

CONFIGURATION P.3 RESULTS (Cont'd)

ELEMENT	TIME (sec)	CUMULATIVE STRAIN (%) ε_r	ε_θ	ε_z	ε_{eff}	TEMP. (°R)	
1	3.23	1.46	-.50	-.97	1.49	1323	
10		1.26	-.35	-.94	1.31	1300	
131		1.06	-.28	-.77	1.09	1171	
1	3.24	1.38	-.46	-.92	1.40	1285	
10		1.15	-.27	-.89	1.21	1265	
131		.94	-.20	-.73	.99	1139	
1	3.25	1.30	-.43	-.87	1.33	1250	
10		1.05	-.20	-.85	1.11	1232	
131		.84	-.13	-.69	.90	1110	
1	3.26	1.17	-.38	-.79	1.19	1186	
10		.86	-.093	-.77	.95	1170	
131		.66	-.020	-.61	.73	1053	
1	3.28	.92	-.28	-.63	.94	1068	
10		.55	.090	-.62	.68	1058	
131		.35	.17	-.48	.50	950	
1	3.30	.68	-.18	-.48	.70	951	
10		.25	.25	-.48	.49	946	
131		.063	.34	-.36	.41	846	
1	3.325	.44	-.098	-.33	.46	814	
10		-.025	.40	-.33	.42	813	
131		-.24	.51	-.23	.50	727	
1	3.35	.20	-.010	-.17	.22	679	
10		-.30	.54	-.18	.52	682	
131		-.55	.70	-.090	.73	608	
1	3.375	.023	.051	-.045	.057	569	
10		-.49	.62	-.051	.65	574	
131		-.74	.80	.018	.89	512	
1	3.40	-.14	.10	.070	.15	460	
10		-.68	.71	.62	.80	468	
131		-.92	.88	.11	1.04	417	rev

CONFIGURATION P.3 RESULTS (Cont'd)

ELEMENT	TIME (sec)	CUMULATIVE STRAIN (%) ε_r	ε_θ	ε_z	ε_{eff}	TEMP. (°R)
1	3.425	-.24	.12	.16	.25	374
10		-.80	.74	.15	.90	384
131		-1.02	.92	.19	1.13	343
1	3.45	-.32	.12	.23	.34	298
10		-.88	.75	.22	.96	309
131		-1.10	.92	.25	1.19	276
1	3.50	-.40	.091	.33	.43	196
10		-.97	.72	.32	1.02	206
131		-1.17	.89	.34	1.23	186
1	3.70	-.36	-.11	.43	.47	104
10		-.92	.48	.42	.92	106
131		-1.10	.66	.43	1.11	101
1	3.90	-.32	-.23	.48	.51	50
10		-.87	.33	.48	.86	50
131		-1.06	.53	.48	1.04	50

CONFIGURATION P.4 RESULTS

ELEMENT	TIME (sec)	CUMULATIVE STRAIN (%) ε_r	ε_θ	ε_z	ε_{eff}	TEMP. (°R)
1	.03	-.055	.034	.074	.076	419
10		-.054	.036	.070	.074	424
131		-.064	.040	.079	.085	412
1	.05	-.090	.052	.12	.12	346
10		-.092	.064	.12	.12	354
131		-.11	.068	.13	.14	333
1	.10	-.11	.045	.16	.16	282
10		-.11	.058	.16	.16	290
131		-.13	.061	.17	.17	272
1	.20	-.12	.007	.21	.19	212
10		-.12	.013	.21	.19	218
131		-.13	.015	.22	.20	206
1	.30	-.12	-.029	.24	.22	165
10		-.12	-.029	.24	.22	168
131		-.10	-.045	.24	.21	160
1	1.65	-.13	-.11	.32	.29	50
10		-.12	-.12	.32	.30	50
131		-.13	-.12	.32	.30	50
1	1.665	-.094	-.12	.28	.26	107
10		-.088	-.14	.28	.26	104
131		-.10	-.12	.29	.27	97
1	1.68	-.026	-.18	.19	.22	244
10		-.023	-.20	.20	.23	235
131		-.057	-.15	.22	.22	196
1	1.685	.019	-.21	.14	.20	315
10		.026	-.23	.15	.23	303
131		-.028	-.17	.19	.21	249
1	1.69	.076	-.24	.092	.22	392
10		.094	-.28	.10	.25	376
131		.011	-.20	.15	.20	307

CONFIGURATION P.4 RESULTS (Cont'd)

ELEMENT	TIME (sec)	CUMULATIVE STRAIN (%) ε_r	ε_θ	ε_z	ε_{eff}	TEMP. (°R)
1	1.695	.18	-.29	.026	.27	492
10		.20	-.35	.040	.33	470
131		.091	-.26	.098	.24	383
1	1.70	.30	-.34	-.046	.37	590
10		.34	-.43	-.025	.44	563
131		.20	-.33	.046	.31	461
1	1.706	.44	-.40	-.13	.50	701
10		.52	-.54	-.10	.61	668
131		.36	-.44	-.024	.46	561
1	1.712	.56	-.45	-.20	.60	792
10		.66	-.62	-.17	.75	755
131		.52	-.53	-.087	.61	645
1	1.725	.71	-.51	-.29	.75	917
10		.83	-.72	-.26	.92	876
131		.71	-.64	-.18	.79	764
1	1.738	.82	-.55	-.37	.86	1009
10		.96	-.78	-.33	1.04	967
131		.85	-.72	-.24	.93	852
1	1.744	.86	-.56	-.39	.90	1039
10		1.00	-.79	-.36	1.08	996
131		.89	-.74	-.27	.97	880
1	1.75	.89	-.57	-.42	.93	1064
10		1.04	-.81	-.38	1.12	1022
131		.93	-.75	-.28	1.00	905
1	1.775	.96	-.58	-.47	.99	1125
10		1.10	-.82	-.43	1.18	1083
131		.98	-.76	-.33	1.05	963
1	1.80	1.02	-.59	-.52	1.06	1184
10		1.16	-.84	-.49	1.23	1143
131		1.05	-.78	-.38	1.11	1021

CONFIGURATION P.4 RESULTS (Cont'd)

ELEMENT	TIME (sec)	CUMULATIVE STRAIN (%) ε_r	ε_θ	ε_z	ε_{eff}	TEMP. (°R)
1	1.85	1.07	-.58	-.57	1.10	1239
10		1.19	-.82	-.54	1.25	1199
131		1.08	-.76	-.42	1.13	1074
1	1.95	1.09	-.54	-.63	1.12	1299
10		1.20	-.76	-.59	1.26	1263
131		1.09	-.71	-.48	1.13	1133
1	2.50	1.08	-.39	-.73	1.11	1413
10		1.18	-.58	-.70	1.21	1383
131		1.07	-.54	-.58	1.08	1244
1	2.85	1.07	-.36	-.74	1.10	1432
10		1.16	-.54	-.72	1.20	1402
131		1.06	-.51	-.59	1.07	1262
1	3.20	1.07	-.36	-.75	1.10	1438
10		1.16	-.53	-.72	1.20	1408
131		1.06	-.50	-.60	1.07	1267
1	3.205	1.06	-.34	-.73	1.09	1419
10		1.15	-.52	-.71	1.18	1391
131		1.04	-.49	-.58	1.06	1252
1	3.21	1.04	-.33	-.72	1.07	1400
10		1.13	-.50	-.69	1.16	1372
131		1.03	-.48	-.57	1.04	1235
1	3.215	1.02	-.32	-.70	1.05	1382
10		1.11	-.48	-.68	1.13	1356
131		1.02	-.47	-.56	1.02	1220
1	3.22	1.01	-.31	-.68	1.03	1361
10		1.09	-.46	-.66	1.11	1336
131		1.00	-.45	-.54	1.00	1203
1	3.225	.99	-.30	-.67	1.01	1344
10		1.07	-.45	-.64	1.08	1320
131		.98	-.44	-.53	.98	1189

CONFIGURATION P.4 RESULTS (Cont'd)

ELEMENT	TIME (sec)	CUMULATIVE STRAIN (%) ε_r	ε_θ	ε_z	ε_{eff}	TEMP. (°R)
1	3.23	.97	-.29	-.65	.98	1323
10		1.04	-.42	-.63	1.05	1300
131		.96	-.42	-.51	.95	1171
1	3.24	.93	-.26	-.61	.94	1285
10		.99	-.38	-.60	.99	1265
131		.92	-.39	-.48	.91	1139
1	3.25	.89	-.24	-.58	.89	1250
10		.92	-.33	-.57	.92	1232
131		.88	-.37	-.46	.87	1110
1	3.26	.81	-.20	-.52	.80	1186
10		.79	-.25	-.51	.79	1170
131		.81	-.32	-.41	.79	1053
1	3.28	.66	-.14	-.42	.65	1068
10		.55	-.11	-.41	.57	1058
131		.68	-.26	-.32	.65	950
1	3.30	.50	-.076	-.32	.49	951
10		.34	.010	-.32	.38	946
131		.53	-.18	-.24	.50	846
1	3.325	.34	-.018	-.22	.32	814
10		.18	.083	-.22	.24	813
131		.33	-.066	-.15	.30	727
1	3.35	.18	.039	-.11	.17	679
10		.009	.16	-.12	.16	682
131		.13	.058	-.059	.11	608
1	3.375	.066	.075	-.030	.067	569
10		-.12	.21	.034	.20	574
131		-.022	.14	.012	.098	512
1	3.40	-.039	.11	.047	.085	460
10		-.22	.25	.042	.27	468
131		-.12	.19	.075	.18	417

CONFIGURATION P.4 RESULTS (Cont'd)

ELEMENT	TIME (sec)	CUMULATIVE STRAIN (%) ε_r	ε_θ	ε_z	ε_{eff}	TEMP. (°R)
1	3.425	-.11	.12	.10	.14	374
10		-.29	.27	.097	.33	384
131		-.21	.22	.12	.26	343
1	3.45	-.16	.12	.15	.20	298
10		-.35	.28	.15	.38	309
131		-.28	.24	.17	.32	276
1	3.50	-.22	.11	.22	.27	196
10		-.41	.26	.22	.43	206
131		-.32	.22	.23	.36	186
1	3.70	-.20	-.034	.28	.28	104
10		-.36	.085	.28	.38	106
131		-.26	.058	.29	.32	101
1	3.90	-.18	-.11	.32	.31	50
10		-.33	-.016	.32	.38	50
131		-.24	-.040	.32	.33	50

CONFIGURATION P.5 RESULTS

ELEMENT	TIME (sec)	CUMULATIVE STRAIN (%) ε_r	ε_θ	ε_z	ε_{eff}	TEMP. (°R)
1	.03	-.068	.040	.092	.094	419
10		-.069	.048	.088	.094	424
131		-.079	.051	.098	.11	412
1	.05	-.12	.064	.15	.16	346
10		-.13	.086	.15	.17	354
131		-.15	.093	.16	.19	333
1	.10	-.16	.058	.21	.21	282
10		-.16	.080	.20	.21	290
131		-.18	.085	.21	.23	272
1	.20	-.17	.006	.26	.25	212
10		-.17	.018	.26	.25	218
131		-.18	.022	.27	.26	206
1	.30	-.17	-.043	.30	.28	165
10		-.18	-.038	.30	.28	168
131		-.19	-.034	.31	.29	160
1	1.65	-.18	-.15	.40	.38	50
10		-.17	-.17	.40	.38	50
131		-.18	-.16	.40	.38	50
1	1.665	-.14	-.17	.35	.34	107
10		-.14	-.19	.35	.35	104
131		-.15	-.17	.36	.35	97
1	1.68	-.035	-.24	.24	.28	244
10		-.025	-.27	.25	.30	235
131		-.078	-.22	.28	.30	196
1	1.685	.050	-.28	.18	.27	315
10		.081	-.33	.19	.32	303
131		.004	-.28	.23	.29	249
1	1.69	.16	-.32	.12	.31	392
10		.22	-.42	.13	.40	376
131		.14	-.37	.18	.36	307

CONFIGURATION P.5 RESULTS (Cont'd)

ELEMENT	TIME (sec)	CUMULATIVE STRAIN (%) ε_r	ε_θ	ε_z	ε_{eff}	TEMP. (°R)
1	1.695	.31	-.38	.032	.40	492
10		.38	-.52	.050	.52	470
131		.30	-.47	.12	.47	383
1	1.70	.47	-.46	-.057	.53	590
10		.56	-.62	-.032	.68	563
131		.45	-.57	.057	.59	461
1	1.706	.66	-.54	-.16	.70	701
10		.77	-.74	-.13	.88	668
131		.66	-.69	-.030	.78	561
1	1.712	.81	-.60	-.25	.85	792
10		.92	-.82	-.21	1.02	755
131		.83	-.79	-.11	.94	645
1	1.725	.97	-.69	-.37	1.03	917
10		1.10	-.93	-.33	1.20	876
131		.99	-.86	-.22	1.08	764
1	1.738	1.11	-.75	-.46	1.16	1009
10		1.22	-.99	-.42	1.33	967
131		1.09	-.89	-.31	1.17	852
1	1.744	1.16	-.77	-.49	1.20	1039
10		1.26	-1.01	-.45	1.36	996
131		1.11	-.89	-.34	1.19	880
1	1.75	1.19	-.78	-.52	1.24	1064
10		1.30	-1.02	-.48	1.40	1022
131		1.14	-.89	-.36	1.22	905
1	1.775	1.26	-.80	-.59	1.31	1125
10		1.39	-1.04	-.54	1.48	1083
131		1.18	-.89	-.41	1.26	963
1	1.80	1.34	-.81	-.66	1.38	1184
10		1.48	-1.06	-.61	1.57	1143
131		1.24	-.88	-.47	1.30	1021

CONFIGURATION P.5 RESULTS (Cont'd)

ELEMENT	TIME (sec)	CUMULATIVE STRAIN (%) ε_r	ε_θ	ε_z	ε_{eff}	TEMP. (°R)
1	1.85	1.38	-.79	-.71	1.42	1239
10		1.52	-1.03	-.67	1.59	1199
131		1.26	-.84	-.53	1.31	1074
1	1.95	1.40	-.72	-.78	1.43	1299
10		1.53	-.94	-.74	1.59	1263
131		1.26	-.75	-.60	1.30	1133
1	2.50	1.35	-.52	-.91	1.40	1413
10		1.45	-.68	-.87	1.49	1383
131		1.12	-.44	-.72	1.14	1244
1	2.85	1.34	-.48	-.93	1.39	1432
10		1.44	-.64	-.90	1.48	1402
131		1.09	-.38	-.74	1.12	1262
1	3.20	1.34	-.48	-.94	1.39	1438
10		1.43	-.63	-.90	1.47	1408
131		1.07	-.35	-.75	1.10	1267
1	3.205	1.32	-.46	-.91	1.37	1419
10		1.41	-.61	-.88	1.45	1391
131		1.05	-.33	-.73	1.08	1252
1	3.21	1.30	-.45	-.89	1.34	1400
10		1.39	-.59	-.86	1.42	1372
131		1.01	-.30	-.71	1.04	1235
1	3.215	1.28	-.44	-.87	1.32	1382
10		1.38	-.59	-.84	1.40	1356
131		.94	-.24	-.69	.97	1220
1	3.22	1.26	-.42	-.85	1.28	1361
10		1.37	-.60	-.82	1.40	1336
131		.85	-.15	-.68	.89	1203
1	3.225	1.23	-.41	-.83	1.26	1344
10		1.36	-.61	-.80	1.39	1320
131		.78	-.091	-.66	.83	1189

CONFIGURATION P.5 RESULTS (Cont'd)

ELEMENT	TIME (sec)	CUMULATIVE STRAIN (%) ε_r	ε_θ	ε_z	ε_{eff}	TEMP. (°R)
1	3.23	1.19	-.39	-.81	1.21	1323
10		1.35	-.61	-.78	1.37	1300
131		.69	-.018	-.64	.77	1171
1	3.24	1.11	-.35	-.76	1.14	1285
10		1.30	-.60	-.74	1.32	1265
131		.54	.10	-.60	.67	1139
1	3.25	1.05	-.33	-.73	1.08	1250
10		1.25	-.58	-.71	1.26	1232
131		.42	.20	-.57	.60	1110
1	3.26	.93	-.28	-.66	.96	1186
10		1.16	-.54	-.63	1.17	1170
131		.20	.35	-.51	.53	1053
1	3.28	.72	-.19	-.52	.74	1068
10		1.00	-.49	-.51	1.00	1058
131		-.14	.58	-.40	.59	950
1	3.30	.52	-.11	-.40	.54	951
10		.85	-.45	-.40	.85	946
131		-.38	.74	-.30	.72	846
1	3.325	.32	-.032	-.27	.34	814
10		.70	-.41	-.27	.70	813
131		-.66	.90	-.19	.92	727
1	3.35	.12	.044	-.14	.15	679
10		.53	-.36	-.14	.54	682
131		-.92	1.07	-.075	1.16	608
1	3.375	-.036	.092	-.037	.086	569
10		.39	-.33	-.043	.42	574
131		-1.11	1.17	.015	1.32	512
1	3.40	-.16	.13	.058	.18	460
10		.28	-.31	.052	.34	468
131		-1.30	1.21	.094	1.50	417

CONFIGURATION P.5 RESULTS (Cont'd)

ELEMENT	TIME (sec)	CUMULATIVE STRAIN (%) ε_r	ε_θ	ε_z	ε_{eff}	TEMP. (°R)
1	3.425	-.25	.14	.13	.26	374
10		.20	-.30	.12	.32	384
131		-1.39	1.33	.16	1.58	343
1	3.45	-.31	.14	.19	.32	298
10		.15	-.31	.18	.32	309
131		-1.48	1.36	.21	1.65	276
1	3.50	-.37	.11	.28	.39	196
10		.093	-.35	.27	.37	206
131		-1.54	1.34	.29	1.70	186
1	3.70	-.34	-.066	.36	.40	104
10		.15	-.59	.35	.58	106
131		-1.49	1.15	.36	1.57	101
1	3.90	-.30	-.16	.40	.43	50
10		.24	-.76	.40	.72	50
131		-1.47	1.08	.40	1.52	50

CONFIGURATION P.6 RESULTS

ELEMENT	TIME (sec)	CUMULATIVE STRAIN (%) ε_r	ε_θ	ε_z	ε_{eff}	TEMP. (°R)
1	.03	-.069	.042	.092	.095	419
10		-.068	.046	.088	.093	424
131		-.079	.050	.098	.11	412
1	.05	-.11	.065	.15	.15	346
10		-.12	.080	.15	.16	354
131		-.13	.085	.16	.18	333
1	.10	-.14	.056	.21	.20	282
10		-.14	.072	.20	.20	290
131		-.16	.076	.21	.22	272
1	.20	-.14	.008	.26	.24	212
10		-.14	.015	.26	.24	218
131		-.16	.018	.27	.25	206
1	.30	-.14	-.036	.30	.27	165
10		-.14	-.036	.30	.27	168
131		-.16	-.033	.31	.28	160
1	1.65	-.16	-.14	.40	.37	50
10		-.15	-.16	.40	.37	50
131		-.16	-.16	.40	.37	50
1	1.665	-.11	-.15	.35	.32	107
10		-.11	-.17	.35	.33	104
131		-.12	-.16	-.36	.33	97
1	1.68	-.030	-.22	.24	.27	244
10		-.026	-.24	.25	.28	235
131		-.071	-.19	.28	.28	196
1	1.685	.026	-.26	.18	.26	315
10		.035	-.29	.19	.28	303
131		-.036	-.22	.23	.26	249
1	1.69	.10	-.30	.12	.27	392
10		.12	-.36	.13	.32	376
131		.017	-.26	.18	.26	307

CONFIGURATION P.6 RESULTS (Cont'd)

ELEMENT	TIME (sec)	CUMULATIVE STRAIN (%) ε_r	ε_θ	ε_z	ε_{eff}	TEMP. (°R)
1	1.695	.23	-.36	.032	.35	492
10		.27	-.44	.050	.42	470
131		.12	-.34	.12	.30	383
1	1.70	.39	-.43	-.057	.47	590
10		.44	-.54	-.032	.57	563
131		.27	-.44	.057	.42	461
1	1.706	.57	-.50	-.16	.64	701
10		.66	-.68	-.13	.78	668
131		.49	-.57	-.030	.61	561
1	1.712	.72	-.57	-.25	.77	792
10		.84	-.78	-.21	.95	755
131		.68	-.69	-.11	.79	645
1	1.725	.91	-.64	-.37	.96	917
10		1.06	-.90	-.33	1.16	876
131		.92	-.82	-.22	1.02	764
1	1.738	1.06	-.70	-.46	1.10	1009
10		1.18	-.96	-.42	1.28	967
131		1.08	-.90	-.31	1.17	852
1	1.744	1.10	-.72	-.49	1.15	1030
10		1.21	-.97	-.44	1.32	996
131		1.11	-.91	-.34	1.20	880
1	1.75	1.13	-.73	-.52	1.18	1064
10		1.25	-.99	-.48	1.35	1022
131		1.14	-.92	-.36	1.23	905
1	1.775	1.20	-.75	-.59	1.25	1125
10		1.32	-1.01	-.54	1.42	1083
131		1.18	-.92	-.41	1.27	963
1	1.80	1.27	-.76	-.66	1.32	1184
10		1.39	-1.03	-.61	1.49	1143
131		1.23	-.92	-.41	1.31	1021

CONFIGURATION P.6 RESULTS (Cont'd)

ELEMENT	TIME (sec)	CUMULATIVE STRAIN (%) ε_r	ε_θ	ε_z	ε_{eff}	TEMP. (°R)
1	1.85	1.31	-.74	-.71	1.36	1239
10		1.42	-1.00	-.67	1.52	1199
131		1.26	-.88	-.53	1.33	1074
1	1.95	1.33	-.69	-.78	1.38	1299
10		1.44	-.93	-.74	1.52	1263
131		1.27	-.81	-.60	1.32	1133
1	2.50	1.31	-.51	-.91	1.37	1413
10		1.40	-.70	-.87	1.46	1383
131		1.22	-.58	-.72	1.25	1244
1	2.85	1.31	-.47	-.93	1.36	1432
10		1.39	-.65	-.90	1.45	1402
131		1.20	-.53	-.74	1.23	1262
1	3.20	1.30	-.46	-.94	1.36	1438
10		1.38	-.64	-.90	1.44	1408
131		1.20	-.51	-.75	1.22	1267
1	3.205	1.29	-.45	-.91	1.34	1419
10		1.36	-.62	-.88	1.42	1391
131		1.18	-.50	-.73	1.20	1252
1	3.21	1.27	-.44	-.89	1.32	1400
10		1.34	-.60	-.86	1.39	1372
131		1.16	-.48	-.71	1.18	1235
1	3.215	1.25	-.42	-.87	1.30	1382
10		1.32	-.58	-.84	1.36	1356
131		1.14	-.46	-.69	1.15	1220
1	3.22	1.24	-.41	-.85	1.27	1361
10		1.28	-.55	-.82	1.32	1336
131		1.11	-.43	-.68	1.12	1203
1	3.225	1.22	-.41	-.83	1.25	1344
10		1.25	-.52	-.80	1.28	1320
131		1.06	-.39	-.66	1.07	1189

CONFIGURATION P.6 RESULTS (Cont'd)

ELEMENT	TIME (sec)	CUMULATIVE STRAIN (%) ε_r	ε_θ	ε_z	ε_{eff}	TEMP. (°R)
1	3.23	1.19	-.39	-.81	1.22	1323
10		1.21	-.50	-.78	1.25	1300
131		1.01	-.34	-.64	1.02	1171
1	3.24	1.14	-.37	-.76	1.16	1285
10		1.15	-.47	-.74	1.18	1265
131		.88	-.23	-.60	.89	1139
1	3.25	1.08	-.34	-.73	1.10	1250
10		1.10	-.45	-.71	1.13	1232
131		.75	-.13	-.57	.78	1110
1	3.26	.96	-.29	-.66	.98	1186
10		.99	-.40	-.64	1.02	1170
131		.53	.052	-.51	.60	1053
1	3.28	.75	-.21	-.53	.77	1068
10		.78	-.29	-.51	.80	1058
131		.17	.30	-.40	.43	950
1	3.30	.55	-.12	-.40	.56	951
10		.58	-.20	-.40	.60	946
131		-.11	.49	-.30	.48	846
1	3.325	.35	-.052	-.27	.36	814
10		.38	-.11	-.27	.39	813
131		-.38	.67	-.19	.65	727
1	3.35	.16	.015	-.14	.18	679
10		.19	-.030	-.14	.20	682
131		-.67	.86	-.075	.89	608
1	3.375	.019	.058	-.037	.055	569
10		.045	.019	-.043	.052	574
131		-.85	.96	.015	1.05	512
1	3.40	-.10	.092	.058	.12	460
10		-.082	.060	.052	.092	468
131		-1.01	1.05	.094	1.19	417

CONFIGURATION P.6 RESULTS (Cont'd)

ELEMENT	TIME (sec)	CUMULATIVE STRAIN (%) ε_r	ε_θ	ε_z	ε_{eff}	TEMP. (°R)
1	3.425	-.18	.10	.13	.20	374
10		-.16	.076	.12	.18	384
131		-1.12	1.10	.16	1.29	343
1	3.45	-.25	.11	.19	.27	298
10		-.23	.085	.18	.25	309
131		-1.20	1.13	.21	1.36	276
1	3.50	-.33	.094	.28	.36	196
10		-.30	.069	.27	.34	206
131		-1.27	1.12	.29	1.40	186
1	3.70	-.29	-.086	.36	.38	104
10		-.26	-.15	.35	.38	106
131		-1.22	.92	.36	1.28	101
1	3.90	-.27	-.18	.40	.42	50
10		-.23	-.27	.40	.43	50
131		-1.19	.82	.40	1.23	50

CONFIGURATION P.7 RESULTS

ELEMENT	TIME (sec)	CUMULATIVE STRAIN (%) ε_r	ε_θ	ε_z	ε_{eff}	TEMP. (°R)
1	.03	-.087	.038	.092	.11	419
10		-.088	.046	.088	.11	424
131		-.10	.050	.098	.12	412
1	.05	-.14	.060	.15	.18	346
10		-.15	.081	.15	.18	354
131		-.18	.088	.16	.20	333
1	.10	-.18	.050	.21	.22	282
10		-.19	.072	.20	.23	290
131		-.20	.076	.21	.25	272
1	.20	-.19	-.003	.26	.26	212
10		-.19	.008	.26	.26	218
131		-.20	.013	.27	.27	206
1	.30	-.18	-.053	.30	.29	165
10		-.18	-.049	.30	.29	168
131		-.20	-.044	.31	.30	160
1	1.65	-.18	-.16	.40	.38	50
10		-.17	-.18	.40	.38	50
131		-.18	-.17	.40	.38	50
1	1.665	-.14	-.18	.35	.34	107
10		-.13	-.20	.35	.35	104
131		-.15	-.18	.36	.35	97
1	1.68	-.021	-.24	.24	.28	244
10		-.0005	-.28	.25	.30	235
131		-.073	-.21	.28	.29	196
1	1.685	.072	-.29	.18	.28	315
10		.099	-.34	.19	.33	303
131		-.003	-.26	.23	.28	249
1	1.69	.18	-.33	.12	.32	392
10		.23	-.42	.13	.40	376
131		.12	-.34	.18	.33	307

CONFIGURATION P.7 RESULTS (Cont'd)

ELEMENT	TIME (sec)	CUMULATIVE STRAIN (%) ε_r	ε_θ	ε_z	ε_{eff}	TEMP. (°R)
1	1.695	.32	-.39	.032	.42	492
10		.40	-.52	.050	.54	470
131		.28	-.45	.12	.44	383
1	1.70	.48	-.46	-.057	.55	590
10		.58	-.62	-.32	.69	563
131		.45	-.56	.057	.59	461
1	1.706	.67	-.54	-.16	.72	701
10		.79	-.75	-.13	.89	668
131		.65	-.68	-.030	.77	561
1	1.712	.82	-.61	-.25	.86	792
10		.95	-.83	-.21	1.04	755
131		.84	-.78	-.11	.94	645
1	1.725	1.02	-.70	-.37	1.05	917
10		1.13	-.92	-.33	1.22	876
131		1.02	-.87	-.22	1.11	764
1	1.738	1.15	-.76	-.46	1.18	1009
10		1.26	-.98	-.42	1.35	967
131		1.12	-.90	-.31	1.20	852
1	1.744	1.19	-.77	-.49	1.23	1039
10		1.30	-1.00	-.45	1.39	996
131		1.15	-.90	-.34	1.22	880
1	1.75	1.23	-.79	-.52	1.27	1064
10		1.34	-1.01	-.48	1.42	1022
131		1.17	-.90	-.36	1.24	905
1	1.775	1.30	-.80	-.59	1.34	1125
10		1.41	-1.02	-.54	1.49	1083
131		1.22	-.89	-.41	1.28	963
1	1.80	1.38	-.82	-.66	1.41	1184
10		1.49	-1.04	-.61	1.56	1143
131		1.27	-.88	-.47	1.32	1021

CONFIGURATION P.7 RESULTS (Cont'd)

ELEMENT	TIME (sec)	CUMULATIVE STRAIN (%) ε_r	ε_θ	ε_z	ε_{eff}
1	1.85	1.42	-.80	-.71	1.45
10		1.53	-1.01	-.67	1.59
131		1.29	-.84	-.53	1.33
1	1.95	1.43	-.73	-.78	1.46
10		1.54	-.92	-.74	1.58
131		1.28	-.76	-.60	1.31
1	2.50	1.38	-.54	-.91	1.42
10		1.45	-.67	-.87	1.49
131		1.14	-.45	-.72	1.16
1	2.85	1.38	-.50	-.93	1.42
10		1.44	-.63	-.90	1.48
131		1.10	-.38	-.74	1.13
1	3.20	1.37	-.49	-.94	1.41
10		1.43	-.62	-.90	1.47
131		1.08	-.36	-.75	1.11
1	3.205	1.35	-.48	-.91	1.39
10		1.41	-.60	-.88	1.44
131		1.05	-.33	-.73	1.08
1	3.21	1.33	-.47	-.89	1.36
10		1.38	-.58	-.86	1.41
131		1.00	-.29	-.71	1.03
1	3.215	1.30	-.45	-.87	1.33
10		1.36	-.58	-.84	1.39
131		.94	-.23	-.69	.97
1	3.22	1.27	-.44	-.85	1.30
10		1.36	-.59	-.82	1.38
131		.84	-.14	-.68	.88
1	3.225	1.24	-.43	-.83	1.27
10		1.35	-.60	-.80	1.37
131		.75	-.066	-.66	.82

CONFIGURATION P.7 RESULTS (Cont'd)

ELEMENT	TIME (sec)	CUMULATIVE STRAIN (%) ε_r	ε_θ	ε_z	ε_{eff}	TEMP. (°R)	
1	3.23	1.20	-.41	-.81	1.23	1323	
10		1.34	-.61	-.78	1.36	1300	
131		.65	.024	-.64	.74	1171	
1	3.24	1.13	-.37	-.76	1.16	1285	
10		1.30	-.61	-.74	1.32	1265	
131		.48	.16	-.60	.64	1139	
1	3.25	1.06	-.34	-.73	1.09	1250	
10		1.26	-.59	-.71	1.27	1232	
131		.35	.27	-.57	.59	1110	
1	3.26	.95	-.30	-.66	.98	1186	
10		1.16	-.56	-.64	1.18	1170	
131		.13	.43	-.51	.55	1053	
1	3.28	.74	-.22	-.53	.76	1068	
10		1.00	-.51	-.51	1.01	1058	
131		-.21	.67	-.40	.66	950	
1	3.30	.55	-.14	-.40	.57	951	
10		.86	-.47	-.40	.86	946	
131		-.49	.86	-.30	.85	846	
1	3.325	.35	-.077	-.27	.37	814	
10		.71	-.44	-.27	.72	813	
131		-.78	1.04	-.19	1.07	727	
1	3.35	.16	-.012	-.14	.18	679	
10		.57	-.42	-.14	.59	682	
131		-1.07	1.23	-.075	1.33	608	
1	3.375	.019	.030	-.037	.042	569	
10		.45	-.41	-.043	.50	574	
131		-1.26	1.33	.015	1.50	512	rev
1	3.40	-.11	.064	.058	.11	460	rev
10		.35	-.40	.052	.43	468	
131		-1.42	1.42	.094	1.64	417	

CONFIGURATION P.7 RESULTS (Cont'd)

ELEMENT	TIME (sec)	CUMULATIVE STRAIN (%) ε_r	ε_θ	ε_z	ε_{eff}	TEMP. (°R)
1	3.425	-.19	.075	.13	.20	374
10		.28	-.39	.12	.40	384
131		-1.54	1.48	.16	1.75	343
1	3.45	-.26	.080	.19	.27	238
10		.22	-.40	.18	.40	309
131		-1.62	1.51	.21	1.81	276
1	3.50	-.32	.056	.28	.35	196
10		.16	-.43	.27	.44	206
131		-1.68	1.49	.29	1.84	186
1	3.70	-.26	-.13	.36	.38	104
10		.25	-.68	.35	.66	106
131		-1.60	1.30	.36	1.71	101
1	3.90	-.22	-.22	.40	.42	50
10		.32	-.82	.40	.79	50
131		-1.57	1.19	.40	1.64	50

CONFIGURATION P.8 RESULTS

ELEMENT	TIME (sec)	CUMULATIVE STRAIN (%) ε_r	ε_θ	ε_z	ε_{eff}	TEMP. (°R)
1	.03	-.046	.045	.092	.081	419
10		-.045	.049	.088	.079	424
131		-.053	.053	.098	.090	412
1	.05	-.075	-.070	.15	.13	346
10		-.077	.086	.15	.13	354
131		-.093	.091	.16	.15	333
1	.10	-.10	.067	.21	.18	282
10		-.10	.083	.20	.18	290
131		-.12	.086	.21	.19	272
1	.20	-.11	.024	.26	.22	212
10		-.11	.032	.26	.22	218
131		-.12	.035	.27	.23	206
1	.30	-.12	-.020	.30	.26	165
10		-.12	-.019	.30	.25	168
131		-.13	-.016	.31	.26	160
1	1.65	-.14	-.12	.40	.35	50
10		-.13	-.14	.40	.36	50
131		-.14	-.14	.40	.36	50
1	1.665	-.11	-.14	.35	.32	107
10		-.11	-.16	.35	.33	104
131		-.12	-.14	.36	.33	97
1	1.68	-.059	-.21	.24	.26	244
10		-.052	-.24	.25	.28	235
131		-.086	-.18	.28	.28	196
1	1.685	-.011	-.25	.18	.25	315
10		.080	-.39	.19	.36	303
131		-.061	-.21	.23	.26	249
1	1.69	.078	-.30	.12	.26	392
10		.16	-.43	.13	.38	376
131		-.008	-.26	.18	.26	307

CONFIGURATION P.8 RESULTS (Cont'd)

ELEMENT	TIME (sec)	CUMULATIVE STRAIN (%) ε_r	ε_θ	ε_z	ε_{eff}	TEMP. (°R)
1	1.695	.23	-.37	.032	.35	492
10		.29	-.50	.050	.47	470
131		.12	-.35	.12	.31	383
1	1.70	.39	-.44	-.057	.48	590
10		.46	-.58	-.032	.60	563
131		.27	-.44	.057	.42	461
1	1.706	.58	-.52	-.16	.65	701
10		.66	-.70	-.13	.79	668
131		.47	-.56	-.030	.60	561
1	1.712	.73	-.59	-.25	.79	792
10		.82	-.79	-.21	.94	755
131		.64	-.66	-.11	.75	645
1	1.725	.94	-.68	-.37	.99	917
10		1.00	-.88	-.33	1.12	876
131		.88	-.79	-.22	.98	764
1	1.738	1.04	-.73	-.46	1.11	1009
10		1.11	-.94	-.42	1.23	967
131		1.00	-.86	-.31	1.10	852
1	1.744	1.08	-.75	-.49	1.15	1039
10		1.14	-.97	-.45	1.27	996
131		1.03	-.86	-.33	1.13	880
1	1.75	1.11	-.76	-.52	1.18	1064
10		1.17	-.98	-.48	1.30	1022
131		1.06	-.87	-.36	1.15	905
1	1.775	1.18	-.78	-.59	1.25	1125
10		1.24	-1.00	-.54	1.37	1083
131		1.10	-.87	-.41	1.20	963
1	1.80	1.24	-.80	-.66	1.32	1184
10		1.30	-1.02	-.61	1.43	1143
131		1.15	-.87	-.47	1.24	1021

CONFIGURATION P.8 RESULTS (Cont'd)

ELEMENT	TIME (sec)	CUMULATIVE STRAIN (%) ε_r	ε_θ	ε_z	ε_{eff}	TEMP. (°R)
1	1.85	1.29	-.79	-.71	1.36	1239
10		1.34	-.99	-.67	1.46	1199
131		1.19	-.84	-.53	1.26	1074
1	1.95	1.31	-.73	-.78	1.38	1299
10		1.37	-.91	-.74	1.47	1263
131		1.20	-.77	-.60	1.26	1133
1	2.50	1.30	-.53	-.91	1.36	1413
10		1.33	-.66	-.87	1.40	1383
131		1.14	-.50	-.72	1.17	1244
1	2.85	1.29	-.50	-.93	1.36	1432
10		1.32	-.61	-.90	1.39	1402
131		1.12	-.44	-.74	1.16	1262
1	3.20	1.29	-.48	-.94	1.36	1438
10		1.31	-.60	-.90	1.39	1408
131		1.11	-.42	-.75	1.14	1267
1	3.205	1.28	-.47	-.91	1.34	1419
10		1.29	-.58	-.88	1.36	1391
131		1.10	-.40	-.73	1.12	1252
1	3.21	1.27	-.46	-.89	1.32	1340
10		1.28	-.56	-.86	1.34	1372
131		1.08	-.38	-.71	1.10	1235
1	3.215	1.26	-.44	-.87	1.30	1382
10		1.26	-.54	-.84	1.32	1356
131		1.06	-.35	-.69	1.07	1220
1	3.22	1.24	-.42	-.85	1.27	1361
10		1.24	-.52	-.82	1.28	1336
131		1.01	-.30	-.68	1.02	1203
1	3.225	1.21	-.41	-.83	1.25	1344
10		1.22	-.51	-.80	1.26	1320
131		.96	-.26	-.66	.98	1189

CONFIGURATION P.8 RESULTS (Cont'd)

ELEMENT	TIME (sec)	CUMULATIVE STRAIN (%) ε_r	ε_θ	ε_z	ε_{eff}	TEMP. (°R)
1	3.23	1.18	-.39	-.81	1.21	1323
10		1.20	-.51	-.78	1.24	1300
131		.90	-.21	-.64	.92	1171
1	3.24	1.10	-.35	-.76	1.13	1285
10		1.15	-.49	-.74	1.19	1265
131		.77	-.11	-.60	.81	1139
1	3.25	1.04	-.32	-.73	1.06	1250
10		1.10	-.47	-.71	1.13	1232
131		.68	-.031	-.57	.72	1110
1	3.26	.92	-.27	-.66	.95	1186
10		.98	-.40	-.64	1.01	1170
131		.48	.12	-.51	.58	1053
1	3.28	.70	-.17	-.53	.73	1068
10		.75	-.28	-.51	.78	1058
131		.18	.31	-.40	.44	950
1	3.30	.50	-.082	-.40	.52	951
10		.54	-.17	-.40	.56	946
131		-.087	.48	-.30	.47	846
1	3.325	.30	-.004	-.27	.33	814
10		.32	-.071	-.27	.35	813
131		-.37	.66	-.19	.64	727
1	3.35	.10	.071	-.14	.15	679
10		.11	.028	-.14	.15	682
131		-.65	.84	-.075	.87	608
1	3.375	-.049	.12	-.087	.11	569
10		-.049	.093	-.043	.092	574
131		-.83	.95	.015	1.03	512
1	3.40	-.18	.16	.058	.20	460
10		-.18	.14	.052	.20	468
131		-.98	1.05	.094	1.17	417

CONFIGURATION P.8 RESULTS (Cont'd)

ELEMENT	TIME (sec)	CUMULATIVE STRAIN (%) ε_r	ε_θ	ε_z	ε_{eff}	TEMP. (°R)
1	3.425	-.26	.18	.13	.28	374
10		-.27	.16	.12	.28	384
131		-1.08	1.09	.16	1.26	343
1	3.45	-.33	.19	.19	.35	298
10		-.34	.18	.18	.35	309
131		-1.17	1.12	.21	1.33	276
1	3.50	-.40	.17	.28	.42	196
10		-.41	.15	.27	.42	206
131		-1.24	1.11	.29	1.38	186
1	3.70	-.40	-.009	.36	.44	104
10		-.41	-.072	.35	.44	106
131		-1.21	.92	.36	1.28	101
1	3.90	-.39	-.11	.40	.46	50
10		-.38	-.20	.40	.47	50
131		-1.20	.82	.40	1.23	50

CONFIGURATION P.9 RESULTS

ELEMENT	TIME (sec)	CUMULATIVE STRAIN (%) ε_r	ε_θ	ε_z	ε_{eff}	TEMP. (°R)
1	.03	-.068	.040	.092	.095	419
10		-.068	.047	.088	.094	424
131		-.079	.051	.098	.11	412
1	.05	-.11	.064	.15	.16	346
10		-.12	.082	.15	.16	354
131		-.13	.086	.16	.18	333
1	.10	-.14	.055	.21	.20	282
10		-.14	.075	.20	.20	290
131		-.16	.080	.21	.22	272
1	.20	-.15	.008	.26	.24	212
10		-.15	.018	.26	.24	218
131		-.16	.021	.27	.25	206
1	.30	-.16	-.038	.30	.28	165
10		-.15	-.034	.30	.27	168
131		-.17	-.031	.31	.28	160
1	1.65	-.17	-.14	.40	.37	50
10		-.16	-.16	.40	.37	50
131		-.17	-.16	.40	.37	50
1	1.665	-.12	-.16	.35	.33	107
10		-.12	-.18	.35	.34	104
131		-.14	-.16	.36	.34	97
1	1.68	-.043	-.23	.24	.27	244
10		-.039	-.25	.25	.29	235
131		-.083	-.20	.28	.29	196
1	1.685	.014	-.27	.18	.26	315
10		.023	-.30	.19	.29	303
131		-.047	-.22	.23	.26	249
1	1.69	.089	-.31	.12	.28	392
10		.11	-.36	.13	.32	376
131		.006	-.26	.18	.26	307

CONFIGURATION P.9 RESULTS (Cont'd)

ELEMENT	TIME (sec)	CUMULATIVE STRAIN (%) ε_r	ε_θ	ε_z	ε_{eff}	TEMP. (°R)
1	1.695	.22	-.37	.032	.35	492
10		.26	-.45	.050	.42	470
131		.12	-.35	.12	.31	383
1	1.70	.38	-.44	-.057	.47	590
10		.44	-.56	-.032	.58	563
131		.28	-.45	.057	.43	461
1	1.706	.56	-.51	-.16	.63	701
10		.66	-.70	-.13	.79	668
131		.50	-.59	-.030	.63	561
1	1.712	.71	-.57	-.25	.77	792
10		.84	-.81	-.21	.96	755
131		.69	-.71	-.11	.81	645
1	1.725	.90	-.65	-.37	.95	917
10		1.05	-.92	-.33	1.17	876
131		.93	-.85	-.22	1.04	764
1	1.738	1.04	-.71	-.46	1.10	1009
10		1.18	-.98	-.42	1.29	967
131		1.07	-.91	-.31	1.18	852
1	1.744	1.09	-.73	-.49	1.14	1039
10		1.22	-1.00	-.45	1.33	996
131		1.10	-.92	-.34	1.20	880
1	1.75	1.12	-.74	-.52	1.18	1064
10		1.25	-1.01	-.48	1.37	1022
131		1.13	-.93	-.36	1.23	905
1	1.775	1.19	-.76	-.59	1.25	1125
10		1.33	-1.03	-.54	1.44	1083
131		1.18	-.93	-.41	1.27	963
1	1.80	1.26	-.77	-.66	1.32	1184
10		1.40	-1.05	-.61	1.50	1143
131		1.23	-.93	-.47	1.31	1021

CONFIGURATION P.9 RESULTS (Cont'd)

ELEMENT	TIME (sec)	CUMULATIVE STRAIN (%) ε_r	ε_θ	ε_z	ε_{eff}	TEMP. (°R)
1	1.85	1.30	-.76	-.71	1.36	1239
10		1.44	-1.02	-.67	1.53	1199
131		1.26	-.89	-.53	1.33	1074
1	1.95	1.33	-.70	-.78	1.38	1299
10		1.46	-.95	-.74	1.54	1263
131		1.28	-.82	-.60	1.33	1133
1	2.50	1.31	-.51	-.91	1.37	1413
10		1.42	-.70	-.87	1.48	1383
131		1.21	-.56	-.72	1.24	1244
1	2.85	1.30	-.48	-.93	1.36	1432
10		1.40	-.66	-.90	1.46	1402
131		1.19	-.50	-.74	1.21	1262
1	3.20	1.30	-.46	-.94	1.36	1438
10		1.40	-.64	-.90	1.46	1408
131		1.18	-.48	-.75	1.20	1267
1	3.205	1.29	-.45	-.91	1.34	1419
10		1.38	-.62	-.88	1.43	1391
131		1.16	-.46	-.73	1.18	1252
1	3.21	1.27	-.43	-.81	1.32	1400
10		1.36	-.60	-.86	1.40	1372
131		1.13	-.44	-.71	1.15	1235
1	3.215	1.25	-.42	-.87	1.29	1382
10		1.34	-.58	-.84	1.37	1356
131		1.10	-.41	-.69	1.12	1220
1	3.22	1.23	-.41	-.85	1.27	1361
10		1.30	-.56	-.82	1.34	1336
131		1.06	-.37	-.68	1.07	1203
1	3.225	1.21	-.40	-.83	1.25	1344
10		1.28	-.55	-.80	1.31	1320
131		1.00	-.32	-.66	1.01	1189

CONFIGURATION P.9 RESULTS (Cont'd)

ELEMENT	TIME (sec)	CUMULATIVE STRAIN (%) ε_r	ε_θ	ε_z	ε_{eff}	TEMP. (°R)	
1	3.23	1.19	-.39	-.81	1.22	1323	
10		1.25	-.54	-.78	1.28	1300	
131		.92	-.25	-.64	.94	1171	
1	3.24	1.13	-.36	-.76	1.16	1285	
10		1.21	-.53	-.74	1.24	1265	
131		.75	-.098	-.60	.79	1139	
1	3.25	1.07	-.34	-.73	1.09	1250	
10		1.16	-.51	-.71	1.19	1232	
131		.61	.018	-.57	.68	1110	
1	3.26	.96	-.29	-.65	.98	1186	
10		1.06	-.46	-.64	1.08	1170	
131		.36	.21	-.51	.54	1053	
1	3.28	.75	-.21	-.53	.77	1068	
10		.84	-.35	-.51	.85	1058	
131		.031	.44	-.40	.49	950	
1	3.30	.55	-.13	-.40	.57	951	
10		.63	-.24	-.40	.64	946	
131		-.23	.62	-.30	.60	846	
1	3.325	.36	-.062	-.27	.37	814	
10		.42	-.16	-.27	.43	813	
131		-.52	.80	-.19	.79	727	
1	3.35	.17	.003	-.14	.18	679	
10		.22	-.070	-.14	.23	682	
131		-.80	.99	-.075	1.04	608	
1	3.375	.030	.044	-.037	.050	569	
10		.077	-.018	-.043	.073	574	
131		-.99	1.09	.015	1.20	512	rev
1	3.40	-.096	.079	.058	.11	460	rev
10		-.054	.024	.052	.063	468	rev
131		-1.14	1.18	.094	1.34	417	

CONFIGURATION P.9 RESULTS (Cont'd)

ELEMENT	TIME (sec)	CUMULATIVE STRAIN (%) ε_r	ε_θ	ε_z	ε_{eff}	TEMP. (°R)
1	3.425	-.18	.091	.13	.19	374
10		-.14	.042	.12	.15	384
131		-1.24	1.22	.16	1.43	343
1	3.45	-.24	.098	.19	.26	298
10		-.21	.053	.18	.23	309
131		-1.32	1.25	.21	1.49	276
1	3.50	-.32	.085	.28	.35	196
10		-.28	.039	.27	.32	206
131		-1.39	1.24	.29	1.54	186
1	3.70	-.29	-.095	.36	.38	104
10		-.22	-.17	.35	.37	106
131		-1.34	1.04	.36	1.41	101
1	3.90	-.26	-.19	.40	.42	50
10		-.19	-.30	.40	.44	50
131		-1.31	.93	.40	1.36	50

CONFIGURATION P.10 RESULTS

ELEMENT	TIME (sec)	CUMULATIVE STRAIN (%) ε_r	ε_θ	ε_z	ε_{eff}	TEMP. (°R)
1	.03	-.068	.041	.092	.095	419
10		-.069	.047	.088	.094	424
131		-.082	.051	.098	.11	412
1	.05	-.12	.066	.15	.16	346
10		-.13	.085	.15	.16	354
131		-.15	.092	.16	.19	333
1	.10	-.16	.059	.21	.21	282
10		-.16	.079	.20	.21	290
131		-.18	.084	.21	.23	272
1	.20	-.17	.007	.26	.25	212
10		-.17	.016	.26	.25	218
131		-.18	.021	.27	.26	206
1	.30	-.17	-.042	.30	.28	165
10		-.17	-.039	.30	.28	168
131		-.19	-.034	.31	.29	160
1	1.65	-.17	-.15	.40	.38	50
10		-.16	-.17	.40	.38	50
131		-.17	-.16	.40	.38	50
1	1.665	-.14	-.17	.35	.34	107
10		-.13	-.19	.35	.34	104
131		-.15	-.17	.36	.35	97
1	1.68	-.028	-.24	.24	.27	244
10		-.007	-.28	.25	.30	235
131		-.072	-.22	.28	.30	196
1	1.685	.066	-.28	.18	.27	315
10		.11	-.34	.19	.33	303
131		.026	-.29	.23	.31	249
1	1.69	.18	-.32	.12	.32	392
10		.24	-.42	.13	.41	376
131		.16	-.38	.18	.36	307

CONFIGURATION P.10 RESULTS (Cont'd)

ELEMENT	TIME (sec)	CUMULATIVE STRAIN (%) ε_r	ε_θ	ε_z	ε_{eff}	TEMP. (°R)
1	1.695	.33	-.39	.032	.41	492
10		.40	-.52	.050	.54	470
131		.30	-.46	.12	.46	383
1	1.70	.48	-.46	-.057	.54	590
10		.57	-.62	-.032	.69	563
131		.45	-.55	.057	.58	461
1	1.706	.67	-.54	-.16	.71	701
10		.78	-.74	-.13	.88	668
131		.65	-.66	-.030	.76	561
1	1.712	.82	-.61	-.25	.86	792
10		.92	-.82	-.21	1.02	755
131		.82	-.76	-.11	.92	645
1	1.725	1.00	-.70	-.37	1.04	917
10		1.09	-.91	-.33	1.19	876
131		.96	-.82	-.22	1.05	764
1	1.738	1.12	-.76	-.41	1.17	1009
10		1.21	-.97	-.42	1.31	967
131		1.06	-.85	-.31	1.13	852
1	1.744	1.16	-.78	-.49	1.21	1039
10		1.25	-.98	-.45	1.34	996
131		1.08	-.85	-.34	1.15	880
1	1.75	1.20	-.79	-.52	1.25	1064
10		1.28	-.99	-.48	1.38	1022
131		1.10	-.85	-.36	1.17	905
1	1.775	1.27	-.81	-.59	1.32	1125
10		1.36	-1.01	-.54	1.45	1080
131		1.15	-.84	-.41	1.21	963
1	1.80	1.34	-.82	-.66	1.39	1184
10		1.44	-1.02	-.61	1.52	1143
131		1.19	-.83	-.47	1.25	1021

CONFIGURATION P.10 RESULTS (Cont'd)

ELEMENT	TIME (sec)	CUMULATIVE STRAIN (%) ε_r	ε_θ	ε_z	ε_{eff}	TEMP. (°R)
1	1.85	1.38	-.79	-.71	1.42	1239
10		1.47	-.98	-.67	1.54	1199
131		1.21	-.78	-.53	1.25	1074
1	1.95	1.39	-.72	-.78	1.43	1299
10		1.48	-.89	-.74	1.53	1263
131		1.20	-.67	-.60	1.23	1133
1	2.50	1.33	-.52	-.91	1.38	1413
10		1.37	-.62	-.81	1.42	1383
131		.99	-.32	-.72	1.04	1244
1	2.85	1.32	-.48	-.93	1.38	1432
10		1.36	-.57	-.90	1.41	1402
131		.96	-.25	-.74	1.01	1262
1	3.20	1.32	-.47	-.94	1.38	1438
10		1.35	-.56	-.90	1.40	1408
131		.94	-.22	-.75	1.00	1267
1	3.205	1.30	-.46	-.91	1.35	1419
10		1.34	-.54	-.88	1.38	1391
131		.92	-.20	-.73	.97	1252
1	3.21	1.28	-.44	-.81	1.33	1400
10		1.32	-.53	-.86	1.36	1372
131		.87	-.16	-.71	.92	1235
1	3.215	1.26	-.43	-.87	1.30	1382
10		1.31	-.54	-.84	1.35	1356
131		.78	-.078	-.69	.86	1220
1	3.22	1.24	-.42	-.85	1.27	1361
10		1.31	-.55	-.82	1.34	1336
131		.67	-.022	-.68	.78	1203
1	3.225	1.21	-.41	-.83	1.24	1344
10		1.30	-.56	-.80	1.33	1320
131		.59	.091	-.66	.73	1189

CONFIGURATION P.10 RESULTS (Cont'd)

ELEMENT	TIME (sec)	CUMULATIVE STRAIN (%) ε_r	ε_θ	ε_z	ε_{eff}	TEMP. (°R)	
1	3.23	1.16	-.39	-.81	1.20	1323	
10		1.28	-.56	-.78	1.31	1300	
131		.50	-.17	-.64	.68	1171	
1	3.24	1.09	-.36	-.76	1.13	1285	
10		1.23	-.54	-.74	1.26	1265	
131		.34	.29	-.60	.62	1139	
1	3.25	1.03	-.33	-.73	1.06	1250	
10		1.18	-.52	-.71	1.20	1232	
131		.22	.38	-.57	.59	1110	
1	3.26	.91	-.28	-.66	.95	1186	
10		1.09	-.49	-.64	1.10	1170	
131		.002	.55	-.51	.61	1053	
1	3.28	.71	-.20	-.52	.74	1068	
10		.95	-.46	-.51	.96	1058	
131		-.38	.82	-.40	.81	950	
1	3.30	.50	-.11	-.40	.54	951	
10		.81	-.42	-.40	.82	946	
131		-.52	.91	-.30	.89	846	
1	3.325	.31	-.046	-.27	.34	814	
10		.66	-.39	-.27	.66	813	
131		-1.03	1.28	-.19	1.35	727	
1	3.35	.12	.023	-.14	.15	679	
10		.50	-.35	-.14	.51	682	
131		-1.34	1.51	.075	1.65	608	
1	3.375	-.031	.068	-.037	.068	569	
10		.37	-.32	-.043	.40	574	
131		-1.54	1.64	.015	1.84	512	
1	3.40	-1.58	.10	.058	.16	460	rev
10		.27	-.31	.052	.34	468	
131		-1.75	1.76	.094	2.03	417	rev

CONFIGURATION P.10 RESULTS (Cont'd)

ELEMENT	TIME (sec)	CUMULATIVE STRAIN (%) ε_r	ε_θ	ε_z	ε_{eff}	TEMP. (°R)
1	3.425	-.24	.11	.13	.24	374
10		.20	-.31	.12	.32	384
131		-1.85	1.81	.16	2.11	343
1	3.45	-.30	.11	.19	.30	298
10		.14	-.32	.18	.32	309
131		-1.92	1.83	.21	2.17	276
1	3.50	-.36	.081	.28	.38	196
10		.094	-.36	.27	.38	206
131		-1.99	1.81	.29	2.21	186
1	3.70	-.32	-.097	.36	.40	104
10		.17	-.61	.35	.59	106
131		-1.94	1.64	.36	2.09	101
1	3.90	-.29	-.19	.40	.43	50
10		.27	-.79	.40	.75	50
131		-1.92	1.56	.40	2.05	50

DISTRIBUTION LIST FOR FINAL REPORT - CR-134823

NAME	NO. OF COPIES
National Aeronautics & Space Administration Lewis Research Center 21000 Brookpark Road Cleveland, OH 44135	
Attn: J. R. Danicic, MS 500-313	1
E. A. Bourke, MS 500-205	5
Technology Utilization Office, MS 3-19	1
Technical Report Control Office, MS 5-5	1
AFSC Liaison Office, MS 501-3	2
Library, MS 60-3	2
Office of Reliability & Quality Assurance, MS 500-211	1
R. J. Quentmeyer, Project Manager, MS 500-204	20
National Aeronautics & Space Administration George C. Marshall Space Flight Center Huntsville, AL 35912	
Attn: Library	1
R. L. Hurford	1
W. B. McPherson	1
N. Schlemmer	1
J. Thomson	1
J. P. Gallagher AFFDL/FBE Wright-Patterson AFB, OH 45433	1
Aerojet Liquid Rocket Company P. O. Box 15847 Sacramento, CA 95813	
Attn: Technical Library 2484-2015A	1
J. Sims	1
Bell Aerosystems, Inc. Box 1 Buffalo, NY 14240	
Attn: Library	1
J. M. Senneff	1
J. Flanagan	1

NAME	NO. OF COPIES
Boeing Company Space Division P. O. Box 868 Seattle, WA 98124	
Attn: Library	1
D. H. Zimmerman	1
Rocketdyne A Division of Rockwell International 6633 Canoga Avenue Canoga Park, CA 91304	
Attn: Library	1
R. J. Burick	1
R. R. Cooper	1
A. Y. Falk	1
R. Campbell	1
N. Bergstresser	1
J. Somerville	1
TRW Systems, Inc. 1 Space Park Redondo Beach, CA 90278	
Attn: Library	1
A. H. Zimmerman	1
W. A. Carter	1
H. Burge	1
United Aircraft Corporation Pratt & Whitney Division Florida Research & Development Center P. O. Box 2691 West Palm Beach, FL 33402	
Attn: Library	1
G. B. Cox	1